2012

Biochemical Studies Of Abce1

Lynn Sims
University of Central Florida

BIOCHEMICAL STUDIES OF ABCE1

by

LYNN M. SIMS
B.S. University of Central Florida, 2003
M.S. University of Central Florida, 2011

A dissertation submitted in partial fulfillment of the requirements
for the degree of Doctor of Philosophy
in the Burnett School of Biomedical Science
in the College of Graduate Studies
at the University of Central Florida
Orlando, Florida

Fall Term
2012

Major Professor: Robert Y. Igarashi

ABSTRACT

The growth and survival of all cells require functional ribosomes that are capable of protein synthesis. The disruption of the steps required for the function of ribosomes represents a potential future target for pharmacological anti-cancer therapy. ABCE1 is an essential Fe-S protein involved in ribosomal function and is vital for protein synthesis and cell survival. Thus, ABCE1 is potentially a great therapeutic target for cancer treatment. Previously, cell biological, genetic, and structural studies uncovered the general importance of ABCE1, although the exact function of the Fe-S clusters was previously unclear, only a simple structural role was suggested. Additionally, due to the essential nature of ABCE1, its function in ribosome biogenesis, ribosome recycling, and the presence of Fe-S within ABCE1, the protein has been hypothesized to be a target for oxidative degradation by ROS and critically impact cellular function. In an effort to better understand the function of ABCE1 and its associated Fe-S cofactors, the goal of this research was to achieve a better biochemical understanding of the Fe-S clusters of ABCE1. The kinetics of the ATPase activity for the *Pyrococcus abyssi* ABCE1 (*Pab*ABCE1) was studied using both *apo*- (without reconstituted Fe-S clusters) and *holo*- (with full complement of Fe-S clusters reconstituted post-purification) forms, and is shown to be jointly regulated by the status of Fe-S clusters and Mg^{2+}. Typically, ATPases require Mg^{2+}, as is true for *Pab*ABCE1, but Mg^{2+} also acts as a unusual negative allosteric effector that modulates ATP affinity of *Pab*ABCE1. Comparative kinetic analysis of Mg^{2+} inhibition shows differences in the degree of allosteric regulation between the *apo*- and *holo-Pab*ABCE1 where the apparent K_m for ATP of *apo*-

*Pab*ABCE1 increases >30 fold from ~30 μM to over 1 mM when in the presence of physiologically relevant concentrations of Mg^{2+}. This effect would significantly convert the ATPase activity of *Pab*ABCE1 from being independent of cellular energy charge (φ) to being dependent on φ with cellular [Mg^{2+}].

The effect of ROS on the Fe-S clusters within ABCE1 from *Saccharomyces cerevisiae* was studied by *in vivo* ^{55}Fe labeling. A dose and time dependent depletion of ABCE1 bound ^{55}Fe after exposure to H_2O_2 was discovered, suggesting the progressive degradation of Fe-S clusters under oxidative stress conditions. Furthermore, our experiments show growth recovery, upon removal of the H_2O_2, reaching a growth rate close to that of untreated cells after ~8 hrs. Additionally, a corresponding increase (~88% recovery) in the ABCE1 bound ^{55}Fe (Fe-S) was demonstrated. Observations presented in this work demonstrate that the majority of growth inhibition, induced by oxidative stress, can be explained by a comparable decrease in ABCE1 bound ^{55}Fe and likely loss of ABCE1 activity that is necessary for normal ribosomal activity.

The regulatory roles of the Fe-S clusters with ABCE1 provide the cell a way to modulate the activity of ABCE1 and effectively regulate translation based on both cellular energy charge and the redox state of the cell. Intricate overlapping effects by both [Mg^{2+}] and the status of Fe-S clusters regulate ABCE1's ATPase activity and suggest a regulatory mechanism, where under oxidative stress conditions, the translational activity of ABCE1 can be inhibited by oxidative degradation of the Fe-S clusters. These findings uncover the regulatory function of the Fe-S clusters with

ABCE1, providing important clues needed for the development of pharmacological agents toward ABCE1 targeted anti-cancer therapy.

ACKNOWLEDGMENTS

First and foremost, I must express my extreme gratitude to my mentor, Dr. Robert Igarashi, for taking me into his laboratory. Being at the University of Central Florida for only four to five months, Dr. Igarashi's lab was still new and in the process of being set up. I remember one of my earliest days there, the very first agarose gel electrophoresis experiment was performed. Dr. Igarashi's unwavering ability to push his students to perform their best has benefited me as a PhD student. I have learned so much both personally and professionally, which will undoubtedly translate to my future success.

Of course, I would have not progressed through these past few years without the constructive input and thought-provoking questions from all my committee members: Dr. Seven Ebert, Dr. Sean Moore, and Dr. William Self. Their ability to help me see the "big picture," as well as address any technical issues by simply asking a couple key questions during annual meetings was invaluable. I will never forget some very wise words of advice given by Dr. Ebert during a transition early in my Ph. D. career.

I also must acknowledge my previous mentor, Dr. John Ballantyne. I began my very first research experience in his laboratory as an undergraduate performing a research internship. I then continued research as a laboratory technician and subsequently began the Doctoral program. I will never forget the research and conference opportunities, as well as some long lasting friendships I have acquired from working in his laboratory.

I am indebted to the many assistants I have had the pleasure of training over the years. Michelle Josey, whom I first met when I was her junior mentor for her undergraduate honors thesis, helped me tremendously when my research studies changed direction. In no time at all, with her assistance, my research was underway and we were working together to solve everyday problems. Also, I will never forget the dedicated support I received from Tayler Croom. She was always willing to perform any task assigned to her, even if it required coming to the lab late at night or in the early morning hours. I was sad to see her leave but not surprised when she moved on to graduate school. Luckily, there is always an endless supply of eager undergraduates who want to obtain research experience, such as Matt Szasz and Nora Vera, who were very willing to help me out even late in the evening. Additionally, I must thank Brian Tish and Shirlynn Chu for aid in protein purifications and the preparation of laboratory protocols. Assistance from Brian Tish was invaluable, especially during a particular two week protein purification marathon we endured. Shirlynn Chu was an excellent protocol writer with great attention to detail. The great deal of motivation that was expressed by all of my assistants was certainly inspiring.

Finally, I thank Karl P. Hopfner and coworkers for kindly providing us with the pET28-N-strep-*Pab*ABCE1∆4 construct. I am thankful for the numerous teaching assistantships assigned to me from the Department of Chemistry and the Department of Molecular Biology and Microbiology. I am also grateful for the funds provided by the University of Central Florida, College of Science, and Office of Research and

Commercialization and the partial support received from the National Science Foundation Grant, NSF-MCB 0920380.

TABLE OF CONTENTS

LIST OF FIGURES xii

LIST OF TABLES xiv

CHAPTER 1: INTRODUCTION 15

ATP Binding Cassette Proteins 15

Structure and Topology of ABC Proteins 15

Mechanism of ATP Hydrolysis 16

ABCE1: The Lone Member of Subfamily E 17

Iron-Sulfur Cluster Biogenesis 19

ABCE1 is Essential for Cell Survival 24

Expression of ABCE1 in Cancer Cells and Tissue 24

Role of ABCE1 in Viral Life Cycle 27

ABCE1: Ribosome Biogenesis, Translation, and Recycling 29

Ribosome Biogenesis 29

Ribosome Maturation and Translation 31

Ribosome Recycling 32

Hypotheses 35

CHAPTER 2: REGULATION OF THE ATPASE ACTIVITY OF ABCE1 FROM *PYROCOCCUS ABYSSI* BY FE-S CLUSTER STATUS AND MG^{2+}: IMPLICATION FOR RIBOSOMAL FUNCTION 37

Introduction 37

Materials and Methods 40

Expression and Purification of *Pab*ABCE1 40

Fe-S Reconstitution 41

RNA Extraction and Purification 42
ATPase Assays 43
Results 44
Temperature Dependence of *Pab*ABCE1 44
Mg^{2+} Dependence of *Pab*ABCE1 ATPase Activity 44
Dependence of ATP Hydrolysis Parameters on Mg^{2+} 49
Effect of Mg^{2+} on Product (ADP) Inhibition 52
Divalent Metal Chelators, EDTA and EGTA, Affect Activity of PabABCE1 56
Effect of Total RNA on Mg^{2+} Inhibition 59
Discussion 62
Mg^{2+} Inhibition of the *Pab*ABCE1 and Other ATPases 63
Mg^{2+} and Fe-S Cluster Status as Possible Component of *Pab*ABCE1 Regulation and Impact on Translation 66
CHAPTER 3: ABCE1 IRON-SULFUR CLUSTERS ARE SENSITIVE TO REACTIVE OXYGEN SPECIES RESULTING IN GROWTH INHIBITION IN *SACCHAROMYCES CEREVISIAE* 70
Introduction 70
Materials and Methods 73
Recombinant Expression of ABCE1 in *S. cerevisiae* 73
Treatment of Cells with H_2O_2 73
In vivo ^{55}Fe Incorporation 74
Immunoprecipitation 74
Results 75
The Stability and Persistence of *Sc*ABCE1 Protein Upon Treatment with H_2O_2 75
ABCE1 Bound Iron is Depleted with Exposure to H_2O_2 77

ABCE1 Bound Iron Declines Due to Continued Exposure to H_2O_2 78
Growth Rate can be Recovered Upon the Removal of H_2O_2 80
Following Exposure to H_2O_2, the Majority of ABCE1 Bound Iron can be Recovered 80
Discussion 83
Effect of ROS on ABCE1 Function in Translation 83
Implications for the Role of ABCE1 During Oxidative Stress 85
CHAPTER 4: SUMMARY 87
Introduction 87
Mg^{2+} Dependence of *Pyrococcus abyssi* ABCE1 88
Role of Fe-S Status and [Mg^{2+}] in the Function of ABCE1 88
Future Perspectives for Studying the Regulatory Roles of Mg^{2+} and Fe-S Cluster Status 89
Effect of Reactive Oxygen Species (ROS) on ABCE1 Fe-S Clusters 91
Impact of Reactive Oxygen Species on the Fe-S Status and Function of ABCE1 . 91
Future Perspectives for Studying the Role of ROS in Regulation of ABCE1 Activity 92
APPENDIX A: COPYRIGHT AGREEMENT 96
LIST OF REFERENCES 101

LIST OF FIGURES

Figure 1. Schematic of ABCE1 protein domains 17

Figure 2. Primary sequence alignment of the Fe-S domain of ABCE1 18

Figure 3. X-Ray diffraction crystallographic structures of ABCE1 for three archeal species 19

Figure 4. Representation of proteins involved in the core Iron Sulfur Cluster (ISC) assembly machinery within the mitochondria 21

Figure 5. A current model for the steps involved in the Cytosolic Iron-sulfur Assembly (CIA) cycle 22

Figure 6. Illustrative description of the iron regulon 23

Figure 7. Schematic of the HIV-1 Gag polyprotein 27

Figure 8. Role of ABCE1 in the HIV viral life cycle. 29

Figure 9. Model for the proposed dual function of *Sc*ABCE1 in translation termination and ribosome recycling. 34

Figure 10. Structure of *Pab*ABCE1, ligands and cofactors. 40

Figure 11. Purification and post purification Fe-S cluster reconstitution scheme 42

Figure 12. Temperature dependence of *Pab*ABCE1 ATPase activity. 44

Figure 13. Mg^{2+} inhibition of *Pab*ABCE1 ATPase activity. 46

Figure 14. Alpha factor increases linearly with [ATP] 48

Figure 15. Activity of *Holo-Pab*ABCE1 in the presence of various anions or divalent metal ions 49

Figure 16. ATP saturation kinetics of *Pab*ABCE1 ATPase activity with varying [Mg^{2+}]. 50

Figure 17. Inhibition by ADP of *holo-Pab*ABCE1 ATPase activity with and without 0.05 mM Mg^{2+}. 54

Figure 18. ATP saturation kinetics of *holo-Pab*ABCE1 ATPase activity with varying ADP and Mg^{2+}. 55

Figure 19. Mg^{2+} bound to *Pab*ABCE1 shown by inhibition of ATPase activity with EDTA or EGTA. 58

Figure 20. Total RNA activates *Pab*ABCE1 ATP hydrolysis in the presence of inhibitory concentrations of Mg^{2+} 61

Figure 21. Model depicting the effect of exposure to to excess H_2O_2 on ABCE1 Fe-S clusters 72

Figure 22. Recombinant expression and detection of ^{55}Fe bound to *Sc*ABCE1-HA in *S. cerevisiae* 75

Figure 23. *Sc*ABCE1 expression analysis following oxidative stress 76

Figure 24. ^{55}Fe depletion from *Sc*ABCE1-HA with increasing [H_2O_2]. 78

Figure 25. ^{55}Fe depletion from *Sc*ABCE1 over time following treatment with 10 mM H_2O_2. 79

Figure 26. Repletion of ABCE1 bound ^{55}Fe in cells subjected to oxidative stress with 10 mM H_2O_2, occurs within 4 hours 82

LIST OF TABLES

Table 1. Kinetic parameters for Mg^{+2} inhibition of *apo*- and *holo*-PabABCE1. 51

Table 2. Kinetic parameters for ADP inhibition of *holo*-*Pab*ABCE1 with and without 0.05 mM $MgCl_2$. 56

CHAPTER 1: INTRODUCTION

ATP Binding Cassette Proteins

Structure and Topology of ABC Proteins

ATP binding cassette (ABC) transporter proteins comprise one of the largest and most ancient protein superfamilies, and are present in all three domains of life [8-11]. In humans, the ABC superfamily of proteins consists of forty-nine functional proteins divided into subfamilies A through G [12]. Most ABC proteins typically have four to six transmembrane domains (TMDs) that span the membrane. The majority of ABC proteins function in transport of a wide variety of solutes, such as sugars, lipids, ions, and drugs, across membranes and are crucial for many processes within the cell [9, 10, 13]. Some ABC transporters, such as the ABC transporters ABCC1 (MRP1), have been implicated in causing multidrug resistance with some cancer treatments, because therapeutic compounds are often transported out of the cell [14].

Proteins are classified as ABC transporters based on their primary sequence and organization of their nucleotide binding domains (NBDs) [8]. ABC proteins contain one or two conserved ATP-binding domains which can exist as a single peptide or more than one peptide that dimerizes with another to form a fully functional transporter [15-17]. The conserved NBDs contain the canonical Walker A ([AG]-x(4)-G-K-[ST]) and Walker B (D-E-x(5-D) motifs, typical of ATP binding proteins, separated by approximately 125 amino acids [18]. ABC proteins also contain an ABC signature sequence (LSGGQ) located between the Walker A and Walker B motifs which sets ABC

proteins apart from other ATPases [19]. The signature sequences within the NBDs are thought to provide some molecular interactions forming dimers in a distinctive head-to-tail orientation.

Mechanism of ATP Hydrolysis

The precise mechanism of ATP hydrolysis is still under debate and may not be universal among wide family of ABC proteins. In general, within the NBD, there are several conserved motifs involved. The formation of the NBD dimers, involves a conserved glutamate residue within the Walker B motif and the D-loop, which likely serves to catalyze ATP hydrolysis via an acid-base mechanism. The Q loop is believed to provide communication between the NBDs and the TMDs. A conserved lysine within the Walker A motif is thought to form hydrogen bonds with the α- and γ-phosphate while a conserved histidine contacts the γ-phosphate. Most ATPases require Mg^{2+} in a complex with ATP in order to neutralize the negative charge of the phosphates. A Mg^{2+} ion coordinates with the oxygen atoms of the β- and γ-phosphates as well as residues within the Q loop, and water molecules [20-23]. The aromatic residue of the A-loop stabilizes the nucleotide by π-π stacking interactions between the aromatic ring of tyrosine and the adenine of ATP [24].

The ATP hydrolysis cycle can vary for each ABC transporter. For instance, the NBDs may be symmetric or asymmetric and may have equal or unequal ATPase activities. Within the p-glycoprotein, ATP hydrolysis occurs at only one of the NBDs per cycle and alternates between the two NBDs [25]. Cooperativity between the NBDs of p-glycoprotein is required. As for CFTR, there is cooperativity between the NBDs,

although the hydrolysis rate may be slower in NBD1 [14]. In general, the ATP hydrolysis cycle is thought to involve first the binding of ATP to one or both NBDs, causing dimerization of the NBDs, resulting in a closed conformation. Once ATP is hydrolyzed, the conformational changes are reversed, opening the channel allowing solutes to flow through, and the enzyme is then ready for the next cycle [14].

ABCE1: The Lone Member of Subfamily E

ABCE1 (also known as Rli1 [26], Pixie [27] or hp68 [28]) is one of the most unique members of the ABC superfamily. To this date, there are only two known subfamilies (E and F) of ABC proteins that do not have TMDs and are not membrane spanning proteins. Subfamily F consists of only three members that are associated with important processes, such as translation initiation and elongation in eukaryotes [29]. There is only one known member of subfamily E, ABCE1 [30] that has essential roles during multiple ribosome related functions from ribosome biogenesis, ribosome recycling and steps of protein synthesis.

Figure 1. Schematic of ABCE1 protein domains
Schematic representation of the domains within *Sc*ABCE1 indicates the relative locations of Fe-S domain and the NBDs.

What distinguishes ABCE1 from the other ABC proteins having no TMDs is that ABCE1 contains a domain having two ferredoxin-like iron-sulfur (Fe-S) clusters (Figure 1). This domain contains the characteristic sequence (CxPxxCxxxCxnKCP) with four

cysteines for binding a Fe_4-S_4 type Fe-S cluster, similar to the sequences (CPxnCx2Cx2C) found in Fe-S cluster containing ferredoxin (Figure 2) [31].

Comparative analysis of ABCE1 primary sequences reveals conservation among diverse organisms, including those from two *Pyrococcal* species. All contain the conserved ATP binding domains and conserved cysteines found in their Fe-S domains [31]. Such conservation suggests these domains must be important for the general function of ABCE1.

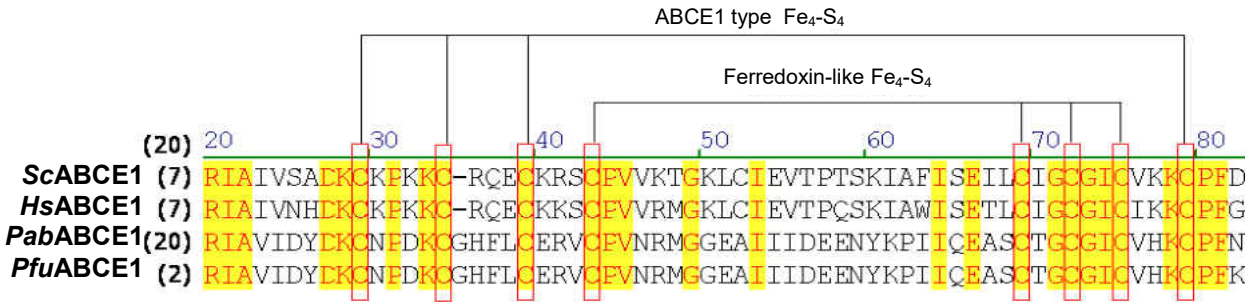

Figure 2. Primary sequence alignment of the Fe-S domain of ABCE1
Partial primary sequence alignment of the Fe-S domain indicates eight conserved cysteine residues, shown with red boxes, as well as other important residues (highlighted) within the indicated species (*S. cerevisiae (Sc)*, *H. sapiens (Hs)*, *P. abyssi (Pab)*, *P. furiosus (Pfu)*).

The X-ray diffraction crystallographic structures (Figure 3) of ABCE1 alone have been determined, with and without the Fe-S cluster domain, from *Pyrococcus furiosus, Pyrococcus abyssi*, and *Sulfolobus solfataricus* [31-34]. The protein has three distinct domains with a hinge region clearly separating the two NBDs. The hypothesis has been presented that the hinge region is involved in mechanical conformational changes between the two NBDs upon ATP hydrolysis [13]. While these three structures are not of the human ABCE1 (*Hs*ABCE1), the availability of these structures that have a high

degree of sequence homology, and structural homology, should aid in understanding of how binding partners, both protein and RNA, may interact with them. The information from the structures of these thermophilic ABCE1s provides a great starting point for biochemical understanding of this important protein.

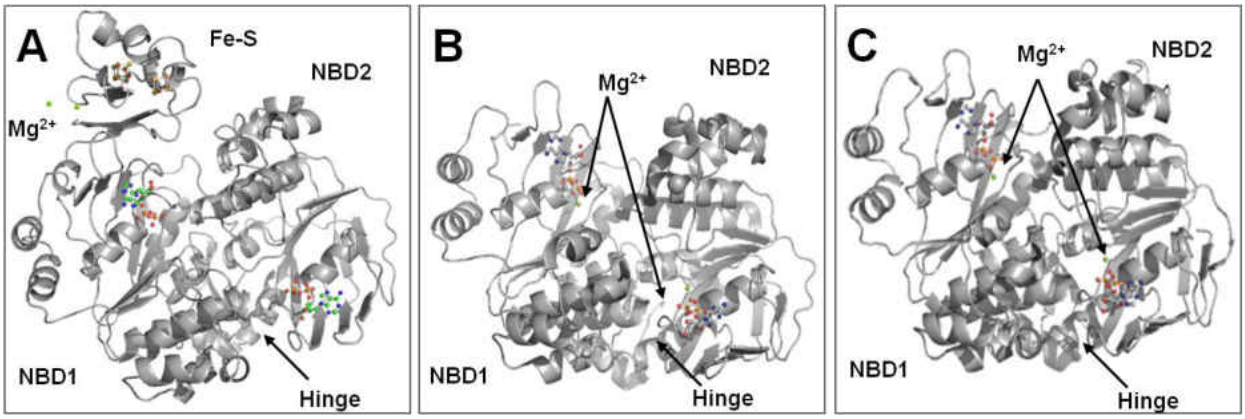

Figure 3. X-Ray diffraction crystallographic structures of ABCE1 for three archeal species
Shown is the (A) X-Ray structure of *Pyrococcus abyssi* (PDB 3BK7 [33]) and (B) *Pyrococcus furiosus*, ΔFe-S (PDB 1YQT [32]), and (C) *Sulfolobus solfataricus* ΔFe-S (PDB 3OZX [31]), as previously published. All three indicate the binding of two ADP molecules within each of the nucleotide binding domains. The two Fe-S clusters are shown in the complete structure of *P. abyssi*.

Iron-Sulfur Cluster Biogenesis

Iron-sulfur clusters are cofactors found in proteins that function in a wide variety of processes and are found in bacteria, plant chloroplasts, and many animal tissues [35] Initially, the primary function of Fe-S clusters was believed to be electron transfer although other functions have been discovered, such as catalysis and radical generation. Some of the well known Fe-S proteins are aconitase [36], Complex I and II of the mitochondrial electron transport chain, and nitrogenase [37]. Fe-S clusters have

now been recognized in a wide range of important cellular processes such as, enzymatic Lewis-acid catalysis, regulation of gene expression, DNA-RNA metabolism, and ribosome biogenesis [1]. Additionally, a role for Fe-S clusters in recognition of damaged bases in DNA base excision repair as in the DNA glycosylases, endonuclease III and MutY [38, 39] has been demonstrated.

Mitochondria play a central role in the metabolism of iron in the Eukaryotic cell, as well as the synthesis of heme, iron regulation, oxidative phosphorylation, and the assembly of Fe-S clusters. Iron-sulfur cluster assembly is performed by the core Iron Sulfur Cluster (ISC) assembly machinery within the mitochondrial matrix. Mitochondria also participate in the assembly of cytosolic and nuclear Fe-S proteins. The key to this function lies in the presence of the Cytosolic Iron-sulfur Assembly (CIA) machinery.

The most current model for Fe-S cluster maturation by the ISC machinery within the mitochondria of *S. cerevisiae* involves at least seventeen proteins and have three major steps [4] (Figure 4). First, after Fe^{+2} is transported into the mitochondria by monothiol glutaredoxins (Grx3/4) [40, 41], the cysteine desulferase complex of Nfs1-Isc11 donates a sulfur, while Yfh1 (frataxin) likely donates iron and interacts with the scaffold protein, IscU. Formation of Fe_2-S_2 cluster on IscU occurs with incorporation of reductive electrons from the electron transport chain involving ferredoxin, ferredoxin reductase, and NAD(P)H. The second major step includes a chaperone system made up of Ssq1, Jac1, and MgeI, which induces the release of the Fe-S cluster from Isu1. Another monothiol glutaredoxin, Grx5, then transfers the Fe-S to *apo*-proteins to form Fe_2-S_2 *holo*-proteins. The third step involves the formation of more complex Fe-S

clusters. This is accomplished by the ISC targeting factors, or several proteins that are each involved in the assembly of specific Fe_4-S_4 proteins.

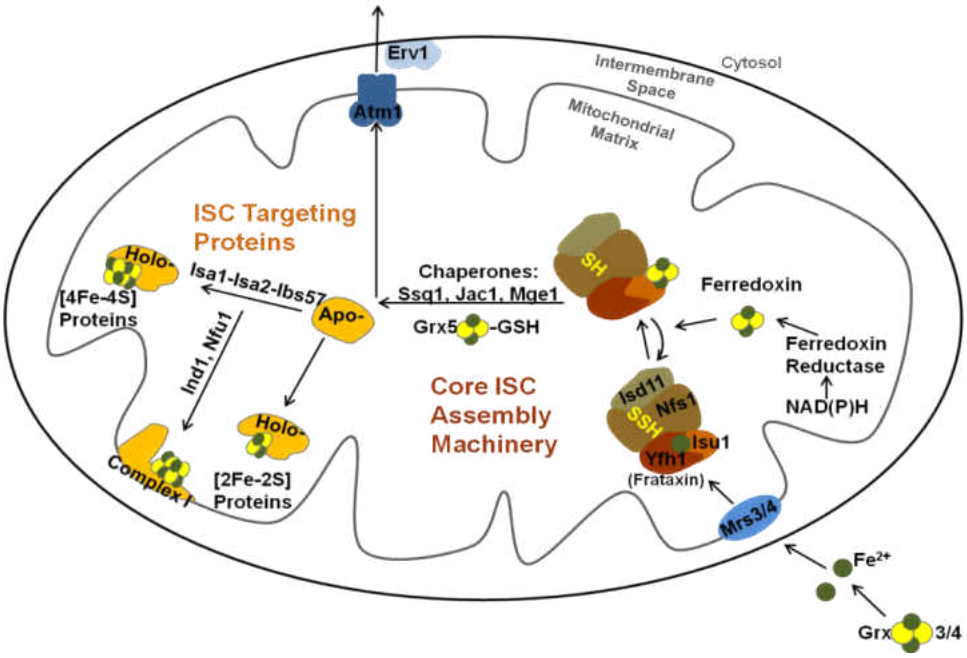

Adapted from [1-3]

Figure 4. Representation of proteins involved in the core Iron Sulfur Cluster (ISC) assembly machinery within the mitochondria

Cytosolic *apo*-proteins receive their Fe-S clusters exported from the mitochondria through, yet another ABC protein, the ABC transporter ABCB7 (Atm1 in yeast) [42] (Figure 4). Following export from the mitochondria, Fe-S clusters are then delivered to cytosolic *apo*-proteins via the CIA machinery in a ATP dependent process [7] (Figure 5). Limited information is available about the transfer reaction, although Dre2 [43] and Erv1, a FAD-linked sulfhydryl oxidase are suspected to be involved [44]. The two P-loop NTPases, Cfd1 and Nbp35 are involved in the initial step of the CIA machinery [45].

The Fe-S clusters are assembled involving the Cft1-Nbp35 complex, Dre2, and an iron and sulfur source. Cft1 binds available iron to promote entry into the CIA machinery [7, 46]. Ultimately, a complex consisting of the Fe-S protein Nar1 and the scaffold protein Cia1 then transiently interact with Cfd1-Nbp35, promoting Fe-S cluster transfer, facilitated by energy from ATP hydrolysis, to cytosolic and nuclear *apo*-proteins (I, Figure 5). Following dissociation of Nar1-Cfd1, *holo*-Nbp35 supports Fe-S assembly of a second subset of cytoplasmic and nuclear *apo*-proteins [7] (II, Figure 5).

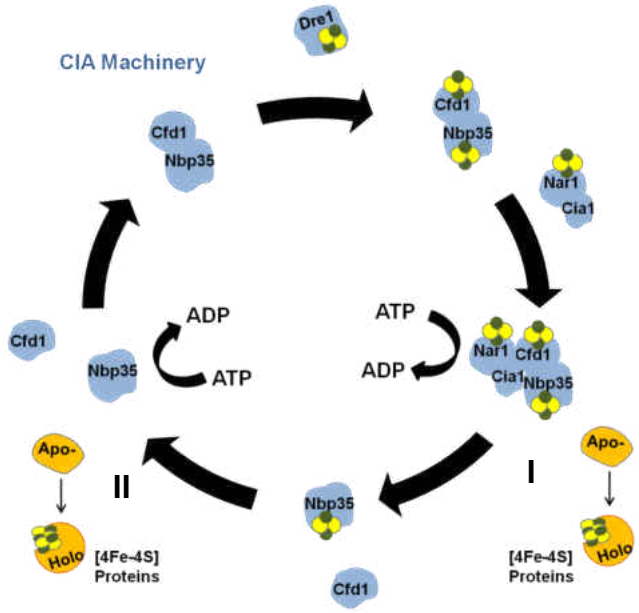

Adapted from [7]

Figure 5. A current model for the steps involved in the Cytosolic Iron-sulfur Assembly (CIA) cycle

Cellular iron regulation is intimately linked to cytosolic Fe-S cluster assembly based on iron availability. In yeast, the genes involved in iron uptake, storage and utilization are controlled transcriptionally and post-transcriptionally by the iron regulon, involving transcription factors Aft1 and Aft2 [7] (Figure 6). Communication between the

mitochondrial Fe-S assembly to Aft, in the iron regulon, is mediated by cytosolic Fe-S proteins, Fra1 and Fra2 [5, 7]. Fra1 and Fra2 bind with Grx3 or Grx4 [47] in a signaling pathway where the presence of bound Fra1 or Fra2 results in the repression of Aft1 activity of the iron regulon, by blocking translocation of Aft1 to the nucleus. The Fra-Grx interaction is thought to function as a signaling intermediate between mitochondrial Fe-S cluster biosynthesis and activation of iron regulon transcription [5].

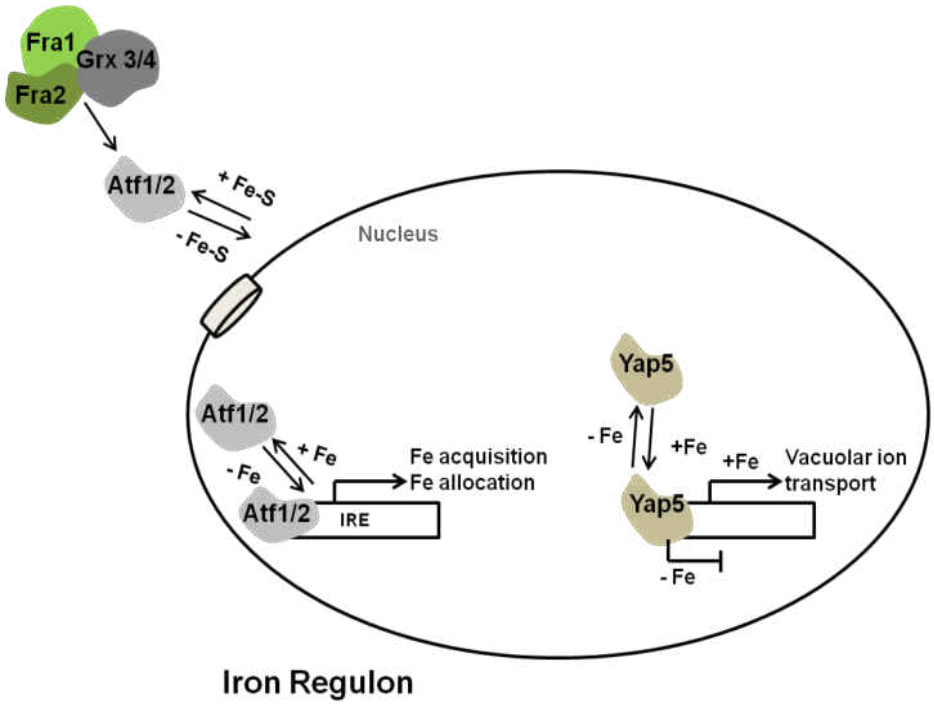

Adapted from [4, 5].

Figure 6. Illustrative description of the iron regulon

ABCE1 and Disease

ABCE1 is Essential for Cell Survival

The importance of ABCE1 in Eukaryotes was first observed when it was found to be one of 356 genes in *S. cerevisiae* that cause a lethal phenotype when deleted as part of a systematic genome-wide deletion analysis [48]. More recent studies have shown that disruption of this cytosolic Fe-S cluster pathway is also lethal since it causes ABCE1 to be devoid of its Fe-S clusters [49]. Importantly, the studies demonstrated the significance of the Fe-S clusters by genetic tetrad analysis of heterozygous site-specific mutations at the key cysteine residues that coordinate the Fe-S clusters [50]. While the function of the Fe-S clusters in ABCE1 was initially elusive, a recent study by Barthelme *et al.* (2011) suggested a structural role. In their study with the *S. solfataricus* ABCE1, the turnover rates and affinity for ATP were not affected by the oxidation state. Furthermore, deletion of the entire Fe-S domain abolished ribosomal binding [34], suggesting that the Fe-S domain or the presence of the Fe-S clusters was required for ribosome binding. While these studies clearly show the essentialness of the Fe-S clusters in ABCE1, the oxidatively sensitive experiments were not conducted in a proper anaerobic environment and thus a role that is more significant than a simple structural component is very possible for the Fe-S clusters of ABCE1.

Expression of ABCE1 in Cancer Cells and Tissue

ABCE1 is a key protein involved in ribosomal function and thus could be hypothesized to be critical for protein synthesis in relation to tumor growth and cancer.

Several studies have investigated the expression levels of multiple ABC transporters in various tissues [51-57], including ABCE1. An earlier report showed that there are two ubiquitously expressed transcripts for ABCE1 (2.4 kb and 3.8 kb in size) in the 15 human tissues examined, albeit that differential expression between tissues is evident [52]. Langmann *et al*. investigated the expression levels of 47 ABC proteins in 20 different human tissues [57]. This study showed ABCE1 was expressed in all tissues, though highly expressed in testis, prostate, and the trachea. Another study, investigating the role of ABC transporters in drug permeability, demonstrated that ABCE1 expression was increased in brain microvessel endothelial cells of five different mammalian species, including human [53].

The precise role that ABCE1 has in tumorigenesis, progression of cancer, or resistance to therapeutics is not clear. Nevertheless, some data show the hyper-expression of ABCE1 in some tumors [58-60]. Investigating the expression levels of 47 ABC transporters in melanoma versus normal melanocytes, Heimerl *et al.* demonstrated that ABCE1 is highly expressed in all cell lines investigated [58]. Additionally, there is a significant increase in expression of ABCE1 in Y79 cells, a chemotherapeutic resistant retinoblastoma cell line [51]. Acquired drug resistance among cancer cell lines could be the result of gene duplication or other genomic alterations of ATP transporter genes. In fact, thirteen ABC transporter genes, including ABCE1, were shown to have multiple gene copies in over 80% of cancer cell lines studied [61].

More recently, the role of ABCE1 has been investigated in specific cancers, such as colon cancer, a very aggressive small cell lung cancer, and hepatocellular carcinoma

[59, 60]. Two peptides derived from ABCE1 are capable of inducing cytotoxic T lymphocytes that react against colon cancer [60] while another study verified the up-regulation of ABCE1 in colon cancer tumors [59]. The proliferation, invasiveness and apoptotic nature of a small cell lung cancer cell line (HCI-H446) was investigated upon the down-regulation of ABCE1 [62]. The knock-down of ABCE1 inhibited proliferation of NCI-H446 cells by 30%. Additionally, an siRNA based knockdown of ABCE1 reduced invasiveness and induced apoptosis as compared to cells that were not transfected with the ABCE1 targeting siRNA [62].

The role of microRNAs (miRNAs) has been investigated for their regulation of ABCE1 in hepatocellular carcinoma [56, 63]. miRNAs are noncoding RNAs that generally repress gene expression and miRNA expression can be deregulated in some cancers. This has been studied in hepatocellular carcinoma cell lines and tumor tissue, where miR-124 and miR-203 have been shown to be epigenetically silenced by methylation. Interestingly, ABCE1 was identified as a possible target of miR-203 in hepatocellular carcinoma cells [56], indicating a possible explanation for high ABCE1 expression levels in some cancers. This was qualitatively confirmed where most of the tumors examined demonstrated high ABCE1 expression levels with a corresponding low expression of miR-203, providing further evidence of the potential role of miR-203 in regulating ABCE1 [63]. There are limited data on the role of ABCE1 in cancer, although this protein is clearly important for cell survival and controlling its activity as a form of cancer treatment could be effective in limiting or eliminating tumor growth.

Role of ABCE1 in Viral Life Cycle

ABCE1 was initially identified as the RNAseL Inhibitor (RLI) that inhibited the binding of RNA and the anti-viral nuclease activity of RNAse L [26], indicating a role for ABCE1 in viral infections. ABCE1 was also introduced as a modulator of a protein-RNA interaction in relation to HIV. RNase L is thought to be the major pathway for interferon mediated antiviral defense and may modulate the stability of both the HIV mRNA transcripts, intended for the expression of the HIV proteins, or the viral genomic RNA that will be inserted into capsids for viral particle production [64, 65]. The capsid protein is translated as part of the Gag polypeptide, which also includes the matrix, nucleocapsid, and three other small peptides. All six peptides are formed following post-translational processing by a HIV-1 protease, resulting in mature functional proteins (Figure 7).

Adapted from [6]

Figure 7. Schematic of the HIV-1 Gag polyprotein

The expression of ABCE1 appears to be upregulated upon HIV infection, which increases the virulence of HIV by decreasing the 2'-5'A/RNAse activity [26, 66]. Additionally, ATP and ABCE1 were shown to be required for late stage capsid assembly which is part of the HIV life cycle (Figure 8) [67]. Lingappa *et al.* narrowed the portion of the GAG polypeptide where ABCE1 binds to the nucleocapsid domain (NC) domain. A

recent study confirmed that the NC domain is required for ABCE1 binding, although it is not binding directly [68]. The data suggest GAG dimerization via the NC domain results in exposure of an ABCE1 binding domain located outside the NC domain [68].

The viral life cycle involves several steps starting from invasion and leading to the maturation within the cell. First a mature viron binds $CD4^+$ cells through a receptor on the surface of the cell. Next, membrane fusion results in the entry of the packaged viral RNA where the coat proteins are then removed exposing the RNA. The RNA is then transcribed to DNA by the viral reverse transcriptase, imported to the nucleus, and integrated into the endogenous DNA. The incorporated viral DNA is then transcribed into the GAG polypeptide, which is then processed to form the proteins required for maturation of viral particles. HIV exploits endogenous ABCE1, requiring its ATPase activity, for use in assembly of the viral capsids at the membrane prior to budding and release of new mature virons (Figure 8). The required use of ABCE1 by HIV capsid assembly intermediates indicates importance of this protein and its potential use as a target for anti-viral therapeutics.

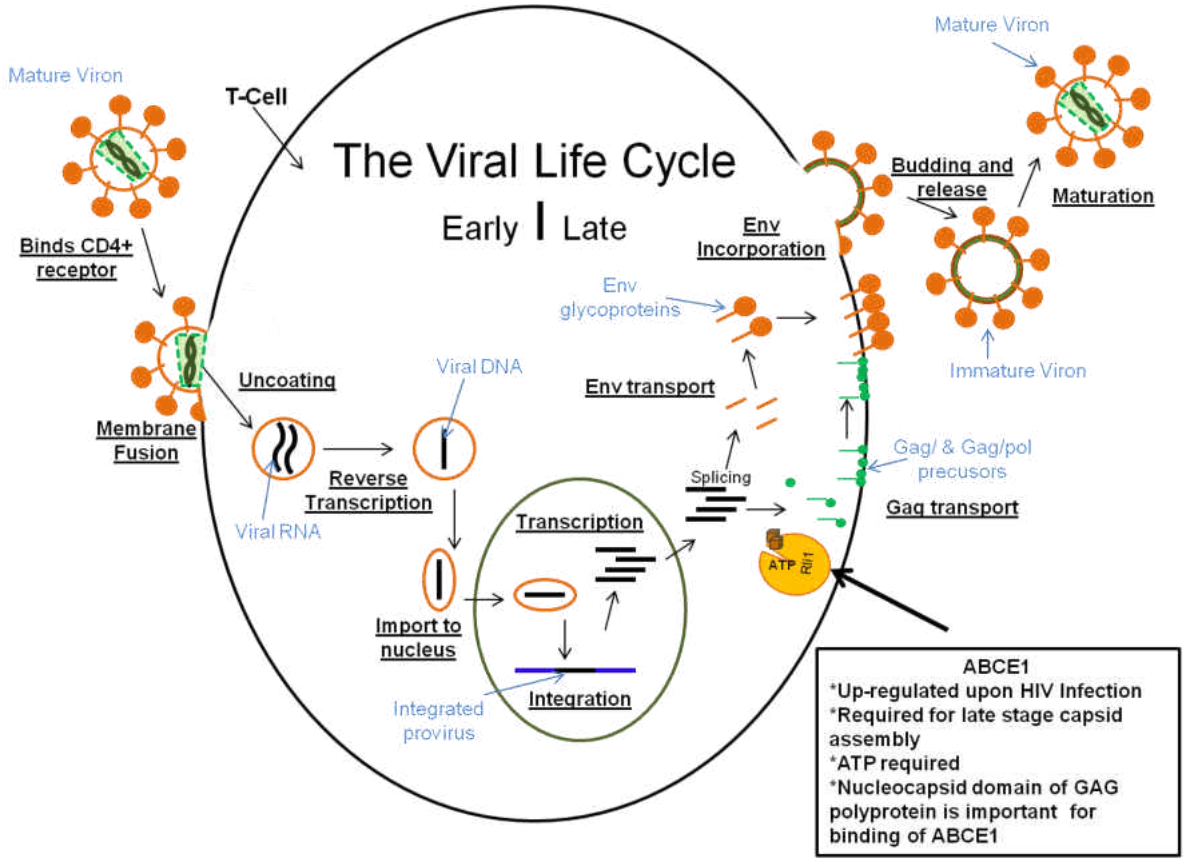

Figure 8. Role of ABCE1 in the HIV viral life cycle.

ABCE1: Ribosome Biogenesis, Translation, and Recycling

Ribosome Biogenesis

The growth and survival of all cells require functional ribosomes that are capable of protein synthesis. Ribosomes are the most complex and most abundant ribozyme in the cell and their production is not merely dependent on the transcription of the ribosomal RNA (rRNA). The ribosome is an intricate protein-RNA complex that has defined folds and sites of interactions for not only the binding of tRNA and mRNA, but

also for numerous factors that regulate the process of translation. Recent structural biology efforts have shed light on structures of both the prokaryotic [69] and eukaryotic [70] ribosomes, but more information needs to be established about how the cell produces such a complex structure. To produce the proper structure of the ribosome, multiple processing events are required in the nucleolus after the transcription of the nascent single ~9.1 Kbase rRNA (80S) [71] . The nascent rRNA is processed by a complex pathway of molecular events involving multiple cleavages to form the respective subunit precursors, trimming by exonucleases, base modifications, structural remodeling to give it the correct fold, followed by their export from the nucleus to the cytoplasm. The sizes of the intermediate rRNA molecules are known, but how the different fragments are produced or how they associate is not well defined. Over 200 non-ribosomal proteins that includes ABCE1, many of which are uncharacterized or undefined, are suspected to be involved in many of these steps [72]. Biochemical understanding of the processing of such RNA molecules to form one of the cell's most important super-structures and learning how small RNA may regulate such a process represents an emerging paradigm in both RNA biology and cancer biology [73, 74]. Undoubtedly, current and future studies will uncover much about the currently unknown processes that are required in ribosome maturation and their impairment leading to cancer. Such processes represent potential molecular targets for the next generation of pharmacological anti-cancer therapies.

Ribosome Maturation and Translation

Among the numerous proteins involved in ribosome biogenesis translation, and recycling, ABCE1 has been identified to play a crucial role in this process. In two simultaneous studies, the importance of the cytosolic Fe-S assembly machinery to both ABCE1 and ribosome biogenesis was demonstrated [49, 50]. The disruption of the cytosolic Fe-S assembly machinery resulted in impaired ABCE1 and nuclear accumulation of pre-ribosomes and ribosomal proteins in *S. cerevisiae*. ABCE1 was shown to co-sediment with 40S, 60S, 80S pre-ribosomes, polysomes, and other ribosomal proteins. Additionally, genetic suppression of ABCE1 causes a similar accumulation of pre-ribosomes in the nuclei [49, 50]. These studies show an important connection between the process of cytosolic iron-sulfur (Fe-S) cluster formation and the function of ABCE1 and the process of ribosome biogenesis. As noted above, ABCE1 interacts with polysomes and it also takes an active role at some stage of protein translation by interacting with eukaryotic initiation factors [75, 76].

The association of *S. solfataricus* ABCE1 with 30S ribosomes occurs when the enzyme is, at least partially, in the closed state where a minimum of one ATP is bound [34]. Wild-type ($ABCE1^{wt}$, with AMPPNP) and several mutants ($ABCE1^{E238/485Q}$, $ABCE1^{E238Q}$, $ABCE1^{E485Q}$, with no AMPPNP required) of ABCE1 bind 30S ribosomal particles, suggesting a conformational switch to the closed state is required for stable association with 30S ribosome particles. In the same study, the Fe-S domain was shown to be required for 30S ribosome association. Upon the deletion of the Fe-S domain, $ABCE1^{\Delta Fe\text{-}S}$, no association with 30S or 50S particles was observed. The

presence of Fe-S clusters was required but the oxidation state of the Fe-S clusters had no effect on 30S binding. In this case, ABCE1^{C54S}, a mutant with one paramagnetic cluster retains binding with 30S particles while the Fe-S defective mutant (ABCE1^{C24S}) does not [34]. These data collectively demonstrate the importance of ABCE1 and its Fe-S clusters in ribosome maturation as well as the connection between Fe-S biogenesis, ribosome biogenesis, and ultimately the survival of the cell.

Ribosome Recycling

A role for *Sc*ABCE1 in ribosome recycling was proposed when ABCE1 was discovered to be involved in the splitting of 40S and 60S ribosomes following translation termination [76-78]. Initially, ABCE1 was demonstrated to physically interact with eukaryotic release factors eRF1/Sup35 and eRF3/Sup45 [78]. Later, the interaction of ABCE1 with Dom34 was shown to be involved in the splitting of 40S and 60S ribosomes following translation termination [76-78].

Interestingly, the concentration of Mg^{2+} seems to affect the dissociation of post-termination complexes into their respective subunits. Ribosomes were found to dissociate in the presence of 1.0 mM Mg^{2+} while dissociation does not occur in the presence of 2.5 mM Mg^{2+} and required release factors. However, ribosomes efficiently dissociated with the addition of ABCE1 at the higher Mg^{2+} concentration. Dissociation (~40%) of ribosomes occurs efficiently below 2.5 mM Mg^{2+} and decreases significantly between Mg^{2+} concentrations of 3.5-10mM. This study reveals that ABCE1 can accelerate ribosome recycling when lower (~1.0 mM) Mg^{2+} concentrations are available.

Also, ABCE1 can still recycle and is required for ribosome recycling in the presence of higher (~2.5 mM) Mg^{2+} concentrations [76].

In the work done by Barthelme *et al*. [36] with ABCE1 isolated from *S. solfataricus*, the interaction between ABCE1 and the peptide release factor aRF1 was found to promote translation post-termination and ribosome recycling. Their structural data suggest that upon ATP binding, ABCE1 undergoes a conformational switch from an open (ADP bound) to a closed (ATP bound) state. Using sucrose gradient centrifugation, they showed that the closed state is required for ABCE1 30S ribosomal particle association. The involvement of aRF1 alone or $ABCE1^{\Delta Fe\text{-}S}$ cannot promote ribosome breakdown indicating that ABCE1 and its Fe-S cluster domain is required for this process to occur. Additionally, ATP hydrolysis by ABCE1 is required for the release of ABCE1 from 30S subunits to begin a new cycle, resulting in continuous ribosomal recycling [34].

Recently, Shoemaker and Green [79] investigated the role of *Sc*ABCE1 in ribosome recycling using an *in vitro* yeast translation system. A stepwise account of the ordered events leading to peptide release and ribosome recycling involving activity of *Sc*ABCE1, Hbs1 and Dom34, was proposed (Figure 9). Shoemaker and Green then investigated whether *Sc*ABCE1 had a role in eRF1/eRF3-mediated peptide release, thus a dual role in translation termination as well as ribosome recycling [77]. The rate of peptide release was measured using elongated ribosome complexes and different combinations of eRF1, eRF3, $eRF3^{H348E}$ (no GTPase activity), and *Sc*ABCE1. Results showed that both *Sc*ABCE1 and $eRF3^{WT}$ can promote peptide release in the presence

of eRF1. Also, a striking increase in peptide release rates (48 fold) in the presence of all three wild-type enzymes was observed, indicating a synergistic effect in the presence of both eRF3^{WT} and *Sc*ABCE1.

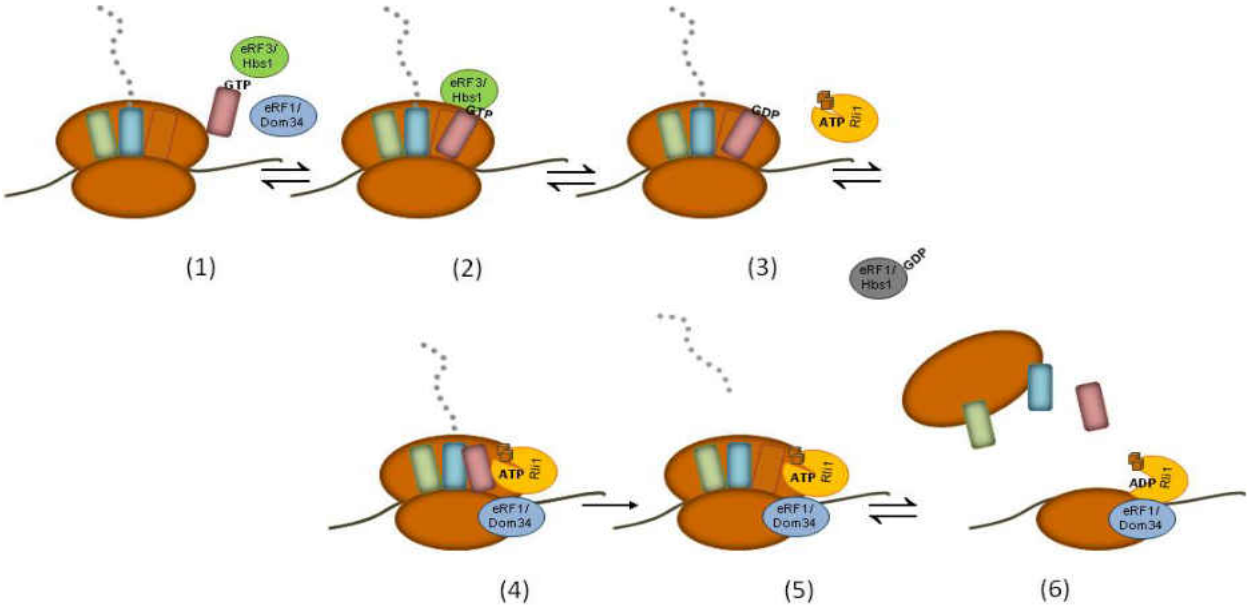

Adapted from [77, 80]

Figure 9. Model for the proposed dual function of *Sc*ABCE1 in translation termination and ribosome recycling.

1.) eRF1:eRF3 or Dom34:Hbs1 bind
2.) GTP hydrolysis by eRF3 or Hbs1 and conformation change in ribosome or eRF3/Dom34
3.) eRF1:GDP or Hbs1:GDP dissociation
4.) Accommodation of eRF1 or Dom34 to the active site, *Sc*ABCE1 association
5.) Peptide release (promoted by *Sc*ABCE1, independent of ATP hydrolysis)
6.) *Sc*ABCE1:eRF1 or *Sc*ABCE1:Dom34, ATP hydrolysis, ribosome splitting

Recently, the interaction between Dom34 and ABCE1 has been confirmed by cryo-electron microscopy reconstructions of eukaryotic and archeal ribosome recycling complexes [80]. Particularly, the Fe-S domain of ABCE1 interacts with CTD of Dom34, stabilizing the complex and inducing a conformational change affecting the central

domain of Dom34. This conformational change results in a direct interaction between Dom34 and the peptidyl transferase center [80], providing an explanation of how ABCE1 could promote peptide release was proposed based on interactions between *Sc*ABCE1 and Dom34 [77].

The dual roles ABCE1 has in translation termination and ribosome biogenesis has been clearly established. Although the studies have identified the function of ABCE1 in translation termination and recycling, a proposal has been made that a similar role likely occurs during ribosome maturation. In this case, evidence suggests ABCE1 splits 80S-like ribosome complexes, resulting in pre-40S ribosomes, during ribosome maturation [81].

Hypotheses

Much remains to be elucidated about the biochemical roles and mechanism of ABCE1 in relation to translation, ribosome recycling, and viral lifecycles. While the previous genetic and cell biological experiments have shown the crucial function of ABCE1 in translation as well as its connection with Fe-S assembly, the precise biochemical role of the Fe-S clusters or the mechanism of ATP hydrolysis is currently unknown.

The work in this dissertation aims to biochemically define the ATPase activity of *Pab*ABCE1, to establish the nature of the requirement of the Fe-S clusters, and to determine what effect ribosomes have on its activity. This study also proposes that oxidative stress affects the Fe-S status of ABCE1 and ultimately affects the function of ABCE1 in relation to protein synthesis and cell growth.

Data generated from this study should provide some intricate clues to the ATPase activity of this unique enzyme, its function in relation to ribosome recycling, and the effects of oxidative stress on the function of ABCE1. There are no known pharmaceuticals developed against Fe-S proteins. Determining the specific biochemical role that ABCE1 has in ribosome biogenesis may lead to the development of a novel anti-cancer pharmaceutical to cause impaired ribosome biosynthesis of uncontrollably dividing cells such as tumor cells.

CHAPTER 2: REGULATION OF THE ATPASE ACTIVITY OF ABCE1 FROM *PYROCOCCUS ABYSSI* BY FE-S CLUSTER STATUS AND MG^{2+}: IMPLICATION FOR RIBOSOMAL FUNCTION

Introduction

Biogenesis and the functions of the ribosome are supported by numerous proteins at various stages. Among these proteins, ABCE1 is essential for ribosome function and for cellular viability in eukaryotic systems. ABCE1 is the lone member of class E in the wide family of ATP Binding Cassette (ABC) proteins [31, 49, 50, 82, 83]. While most members of the ABC protein family have trans-membrane domains (TMDs) and function as transporters of various metabolites, ABCE1 has no TMDs [84]. Instead, ABCE1 has two nucleotide binding domains that are connected by a hinge region and uniquely has a domain containing two Fe_4S_4 clusters (Figure 1). The exact function of these Fe_4S_4 clusters has been somewhat enigmatic.

ABCE1 was initially identified as the RNAseL Inhibitor (RLI) that inhibited the binding of RNA and the anti-viral nuclease activity of RNAse L, which is involved in the pathway for interferon mediated antiviral defense [26]. Later, ABCE1 was also found to be a modulator of a protein-RNA interaction in relation to HIV [64, 65]. The expression of ABCE1 appears to be upregulated upon HIV infection, which increases the virulence of HIV by decreasing the 2'-5' oligoA/RNAse activity [26, 66]. Later, ABCE1 has also been shown to be required for late stage capsid assembly as part of the HIV life cycle [67].

The critical importance of ABCE1 in Eukaryotes was first observed when it was found to be one of 356 genes in *S. cerevsiae* that cause a lethal phenotype when deleted as part of a systematic genome-wide deletion analysis [48]. A later study showed the specific *in vivo* essentiality of the Fe-S clusters of ABCE1 where the cytosolic Fe-S cluster assembly system was disrupted and led to stalling of ribosome maturation [50]. In these studies in cells with disrupted Fe-S cluster assembly, the Fe-S clusterless form of ABCE1 (*apo*-ABCE1) accumulated *in vivo* and was found bound to nucleolar non-functional immature ribosomes and also to cytoplasmic polysomes. Furthermore, tetrad analysis using strains with heterozygous mutations of the Fe-S cluster ligating cysteine residues further showed the specific importance of the Fe-S clusters toward the function of ABCE1 where the homozygous mutated progeny did not grow [50]. These studies showed the essential nature of ABCE1 and its Fe-S clusters in ribosome assembly and maturation.

Recent cell biological studies have shown that ABCE1 and its ATPase activity have roles in translation termination and ribosome recycling. First, it was demonstrated with *Hs*ABCE1 that ATP hydrolysis is required for ribosome dissociation [76]. Studies with the ABCE1 from *Sulfolobus solfataricus* showed that the Fe-S domain is required for association with ribosomes [34]. In a more recent study, the role of *S. cerevisiae* ABCE1 and other recycling factors, Dom34 and Hbs1, in ribosome recycling was investigated and results show the ATPase activity is significantly increased in the presence of Hbs1 and/or Dom34. Additionally, *Sc*ABCE1 can promote recycling prior to the release of the peptide [77].

The structures of ABCE1 from two *Pyrococci* have been determined with (*P. abyssi*) and without (*P. furiosus*) the Fe-S cluster domain [32, 33]. A recent cryo-electron microscopy reconstruction of mixed complexes of *S. cerevisiae* ribosome recycling factors and *P. furiosus* ABCE1 shows interactions with Dom34/Pelota near the peptidyl transferase center on the ribosomes [80]. The structures of these thermophilic ABCE1s are a great starting point for biochemical understanding of this important protein. Much remains to be elucidated about the biochemical roles and mechanism of this protein in relation to ribosome biogenesis, translation and possibly with viral lifecycles. Among the key questions are: how is the energy derived from ATP hydrolysis utilized, what is the role of the Fe-S clusters, and how does it interact with immature and mature ribosomes? Toward the goal of better biochemical understanding for some of these aspects, the hydrolysis of MgATP by the *Pyrococcus abyssi* ABCE1 (*Pab*ABCE1) was studied in the present work. Somewhat unexpectedly, the ATP hydrolysis activity was found to be very sensitive to the concentration of Mg^{2+}, which may possibly be relevant to a mode of regulation *in vivo*.

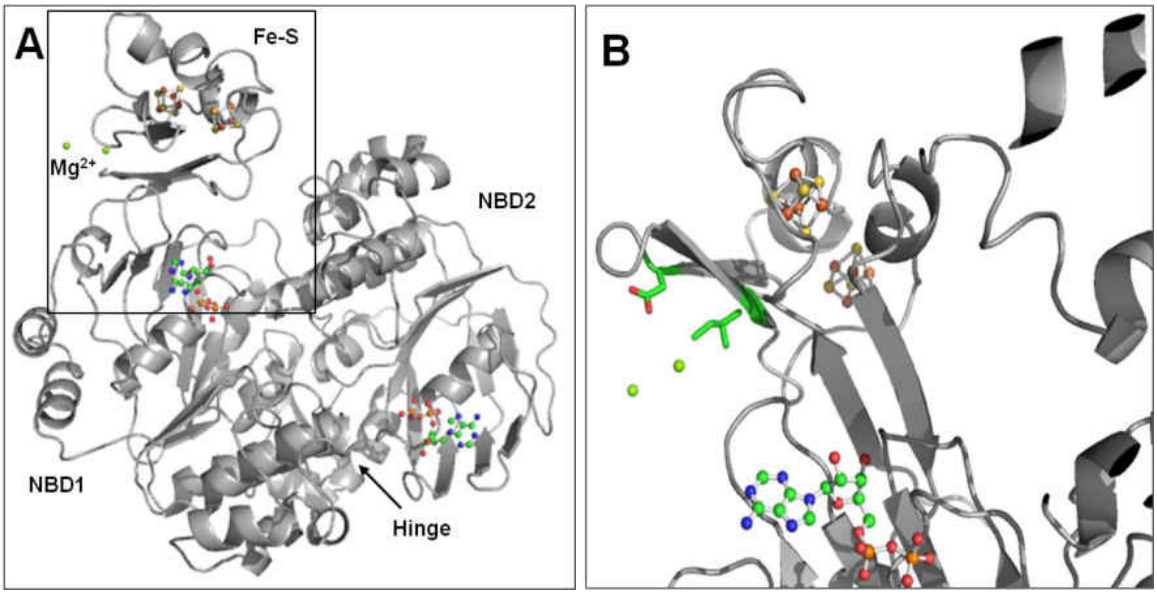

Figure 10. Structure of *Pab*ABCE1, ligands and cofactors.
Shown is the complete crystal structure (A) and Fe-S domain (B) of *Pab*ABCE1 (PDB 3BK7, ([33]). The two Fe-S clusters and both ADP molecules located with each of the nucleotide binding domains are shown in colored ball-and-stick models and green spheres represent two Mg^{2+} ions. Labels refer to different parts of the proteins as described in the Introduction. A box is shown in Panel (A) to indicate the section shown in Panel (B).

Materials and Methods

Expression and Purification of *Pab*ABCE1

Recombinant protein was expressed in *E. coli*, Rosetta2 BL21(DE3)pLysS transformed with plasmid pET28-N-strep-*Pab*ABCE1Δ4 (gift from K.P. Hopfner). Briefly, cells were grown to an optical density of 0.8 followed by induction with 0.5 mM IPTG for 4 hours at 37 ˚C. Purification was performed as described [33] with one modification (Figure 11): Q-sepharose was used for ion exchange chromatography. Following Streptactin affinity chromatography, protein was concentrated to 35 µM using

a Vivaspin 20 concentrator (GE Healthcare). Protein concentration was determined by standard BCA assay with TCA precipitation of purified protein in order to remove reductants [85].

Fe-S Reconstitution

The 'as purified' *Pab*ABCE1, designated the *apo-Pab*ABCE1, typically contained ~0.9 Fe per protein. The *holo-Pab*ABCE1 was prepared by reconstituting the Fe-S cluster after purification. The Fe-S reconstitution procedure was conducted in an anaerobic glove box containing at least 5% H_2 and less than 1 ppm O_2. The buffer for the concentrated protein was exchanged to 50 mM Tris, pH 8.0, 200 mM NaCl, 5 mM DTT simultaneously with the Fe-S cluster reconstitution by dialysis overnight at 4 ˚C. All buffers, protein, and other solutions were degassed and buffers were stored in the glove box for at least 6 hours prior to beginning Fe-S reconstitution. Dialysis was performed using a Slide-A-Lyzer MINI dialysis device, 10K MWCO (Thermo Scientific). $FeCl_2$ was added anaerobically to degassed protein (15:1 Fe:protein ratio) for 5 min prior to dialysis. The protein supplemented with Fe^{2+} was placed into dialysis and equilibrated against 500 fold greater volume of buffer containing 20 μM sodium sulfide. Dialysis/Fe-S reconstitution proceeded overnight at 4 ˚C. The buffer was then thoroughly exchanged to dialysis buffer containing no sodium sulfide. The protein was then removed from dialysis and aliquots in crimp-sealed vials were prepared, frozen on liquid N_2, and stored at -80 ˚C until ready for use. Concentration of bound iron was determined by a colorimetric assay [86] with an additional procedure of modifying DTT by incubating samples with 20 mM iodoacetamide at 37 ˚C for 1 hour, prior to the

colorimetic detection of Fe. The reconstituted *holo-Pab*ABCE1 contained 8.5 ± 0.6 Fe per protein.

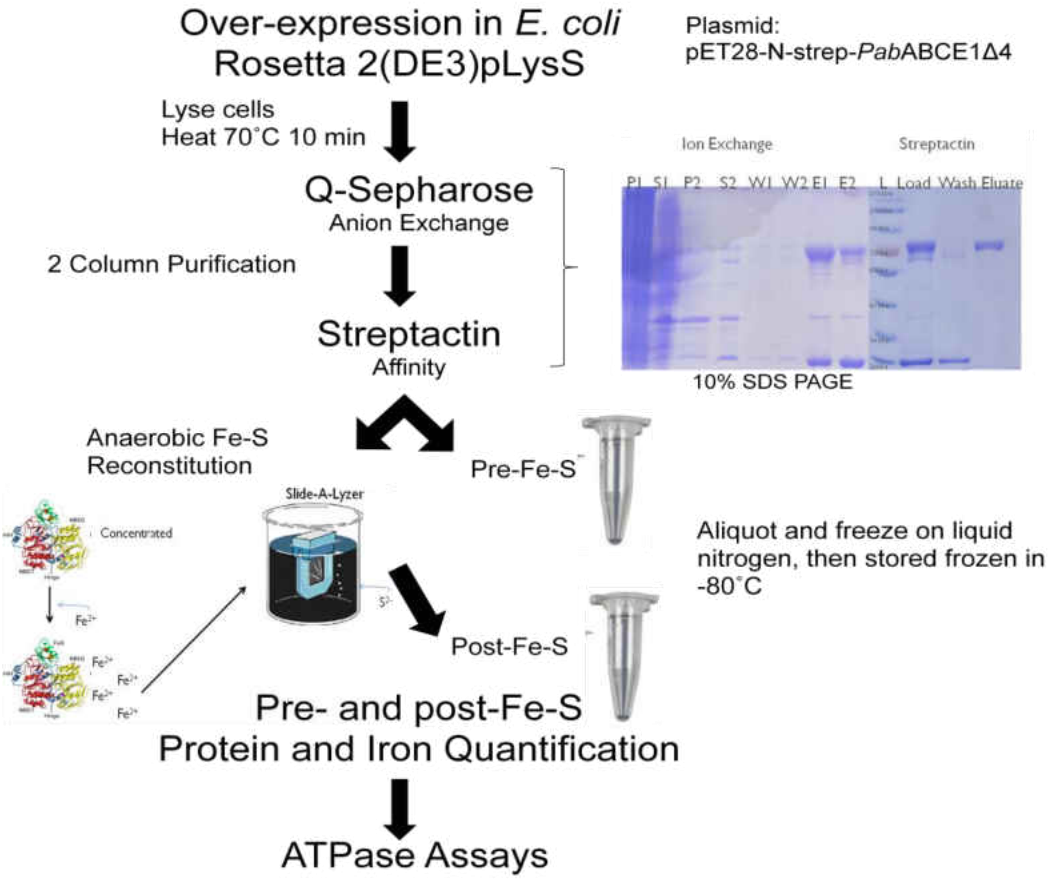

Figure 11. Purification and post purification Fe-S cluster reconstitution scheme

RNA Extraction and Purification

Total RNA was extracted from fresh cultures of *S. cerevisiae*. Yeast cells were disrupted using the BeadBeater (BioSpec) using 0.5 mm beads and shaking 2 min increments for a total of 20 min maintaining a temperature of 4 ˚C. Total RNA was

extracted and purified using Tri-Reagent (Ambion) according to the manufacturer's protocol. Total RNA was quantified using a UV spectrophotometer while its purity and quality was monitored by ensuring the 260:280 nm ratio was close to 2.0.

ATPase Assays

ATPase assays for *Pab*ABCE1 were performed at 70 ˚C for 30 min with 10 pmol *Pab*ABCE1 in 100 mM MOPS, pH 7.5 in a total reaction volume of 200 μL. Anaerobic and reducing conditions were achieved by first degassing all reagents and adding 5mM DTT in an anaerobic chamber for samples that contained *Pab*ABCE1 with its Fe-S clusters (*holo-Pab*ABCE1). Magnesium, ADP, and ATP concentrations are indicated in figure legends for each experimental set. A micro-scale malachite green assay [87-89], with some modifications, was employed for determination of ATPase activity. Briefly, the reaction contained 0.11 mM malachite green, 0.74 N sulfuric acid, 0.31% (w/v) ammonium molybdate, and 0.018% (v/v) Tween-20 in a final volume of 300 μL. Following ten minutes of incubation at room temperature, A_{630nm} measurements were achieved using an Infinite 200 PRO micro plate reader (Tecan). Background correction was achieved with care by performing the same reactions with increasing amounts of ATP with no enzyme present. A standard curve was generated and the amount of background phosphate generated from the corresponding amount of ATP was subtracted from the reactions with enzyme present. Typical measurements at 0.9 fold of V_{max} for a standard ATP titration were about 25 fold above the background.

Results

Temperature Dependence of *Pab*ABCE1

As *Pab*ABCE1 originates from a hyperthermophile that thrives in elevated temperatures, the temperature dependence of its ATPase activity was investigated (Figure 12). Activity is very low below 60 °C, but activity increases with temperature above 65 °C, reaching a plateau around 80 °C. All work described hereafter was performed at 70 °C.

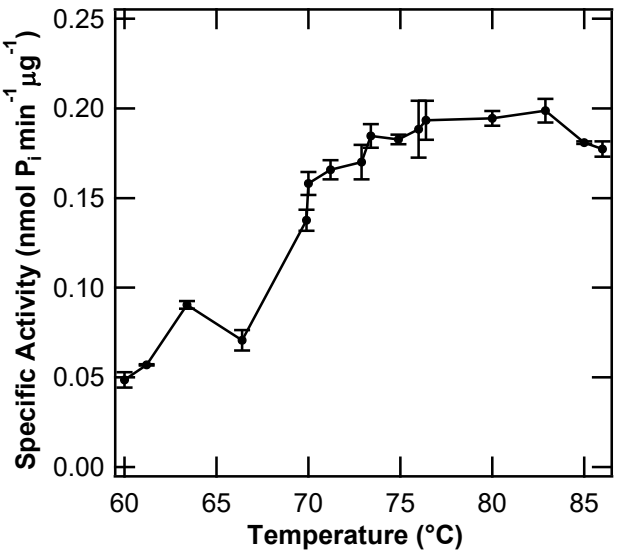

Figure 12. Temperature dependence of *Pab*ABCE1 ATPase activity.
Specific activity of holo-*Pab*ABCE1 was determined over a range of temperatures (60 ˚C - 85 ˚C) in the presence of 1.0 mM ATP and 1.0 mM Mg^{2+} for 1 hour.

Mg^{2+} Dependence of *Pab*ABCE1 ATPase Activity

Most ATPases require Mg^{2+} in the form of a Mg^{2+}-ATP complex to counter the charge on the phosphoesters. This allows ATP to bind in the active site of an ATPase

and facilitate its subsequent hydrolysis. Toward the goal of fully characterizing the ATPase activity of *Pab*ABCE1 and eventually understanding how it relates to ribosomal modification and function, the kinetics for ATPase activity of *Pab*ABCE1 were characterized. Most ATPases have an optimal Mg^{2+} to ATP ratio, and determination of biochemical parameters for ATP are typically performed with a slight excess of Mg^{2+} where $K_d \sim 10^{-5}$ M (p 247 in [90]) and thus nearly all the ATP in solution exists as MgATP. A preliminary determination of the optimal Mg^{2+} concentration was initially performed, and surprisingly an inhibitory sensitivity to Mg^{2+} was found. Two Mg^{2+} ions are observed (Figure 10AB) in the X-ray diffraction structure [33] of *Pab*ABCE1, but are in an odd location in the structure. The assignment of these observed electron densities as Mg^{2+} ions is often difficult to verify and their possible relevance to the apparent Mg^{2+} inhibition properties is difficult to interpret. Inhibition by Mg^{2+} for an ATPase is rare, but has been previously observed for other ATPases [91-96]. For these studies, both the as purified *apo*- form, without *in vitro* Fe-S cluster reconstitution, and the *holo*- form, loaded with full complement of Fe-S cluster by reconstitution after purification, were inspected. ATPase activity was determined with increasing [Mg^{2+}] ($MgCl_2$) in the presence of 1.2, 0.4 and 0.12 mM ATP for both the *apo*- and *holo*-forms of *Pab*ABCE1 (Figure 13AB). *Pab*ABCE1 ATPase activity was the highest without any externally added Mg^{2+} and was apparently inhibited by Mg^{2+}, even at very low concentrations (10 μM) of Mg^{2+}.

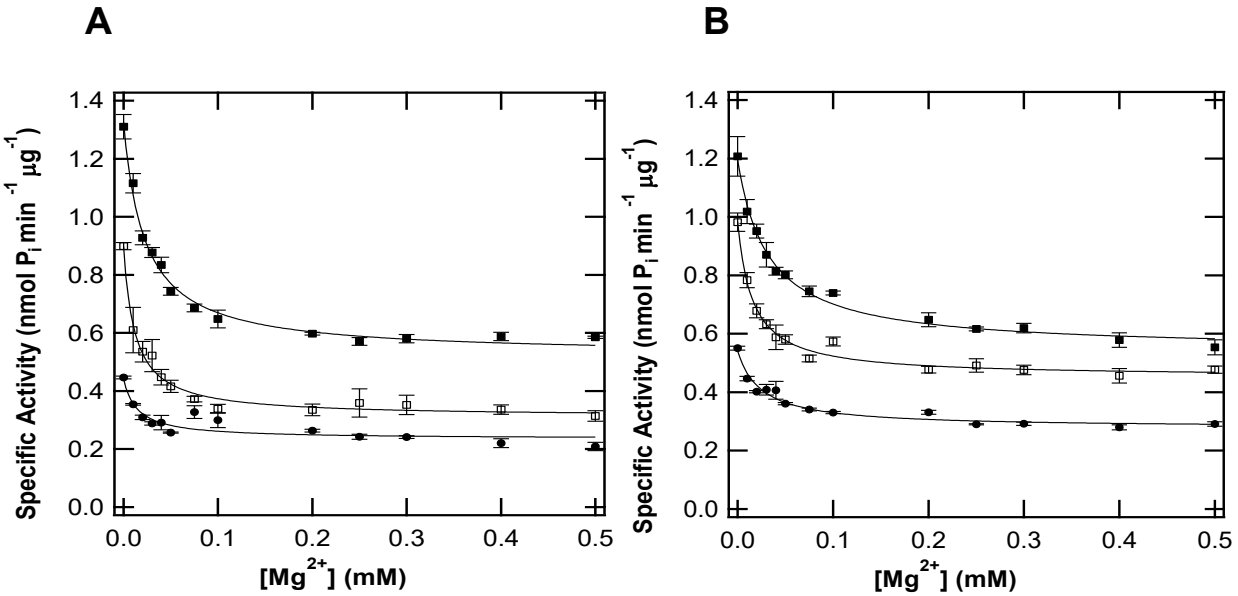

C

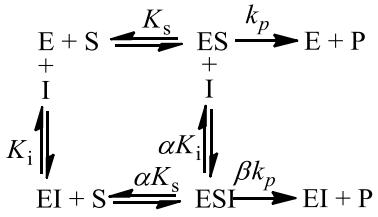

Figure 13. Mg^{2+} inhibition of *Pab*ABCE1 ATPase activity.
ATPase activity in the presence of increasing Mg^{2+} concentrations (0-0.5 mM) for the *apo-Pab*ABCE1 (A) and *holo-Pab* ABCE1 (B). Specific activity was determined in the presence of 1.2 mM ATP (■),0.4 mM ATP (□) and 0.12 mM ATP (●).

The inhibition appears to be non-linear and saturates at ~50-40% of non-inhibited activity without Mg^{2+}. Also, the activity does not approach zero as it would if it were a classical simple inhibition system, as in the case of a pure competitive or pure non-

competitive inhibition. The data were fit to a function that describes partial competitive inhibition:

$$v = \frac{V_{max}[S]}{K_s \frac{\left(1+\frac{[I]}{K_i}\right)}{\left(1+\frac{[I]}{\alpha K_i}\right)} + [S]} \qquad (2.1)$$

where [I] is the total added Mg^{2+} concentration and α is a factor by which K_s changes when I (inhibitor), in this case Mg^{2+}, occupies the enzyme or similarly a factor by which K_i changes when S (substrate) occupies the enzyme. This function describes the rate for system shown in Figure 13C where α > 1 and β = 1 (p 162 in [90]).

The data obtained without Mg^{2+} were initially fitted to a standard Michaelis-Menten equation to estimate V_{max} and K_m. The data with increasing Mg^{2+} were fit to Eq. 2.1 by non-linear fitting both individually for each titration curve and also by global fitting (IGOR Pro, Wavemetrics). Similar values for V_{max} and K_m were obtained, whether Mg^{2+} titrations were fit individually or globally (Table 1).

By a global fitting procedure, linking α among the data does not yield satisfactory fits. Global fits where the values for α were allowed to float yields satisfactory fits where the value for α increases as [ATP] increased with a somewhat linear relationship between the inverse of α and the inverse of [ATP] (Figure 14AB).

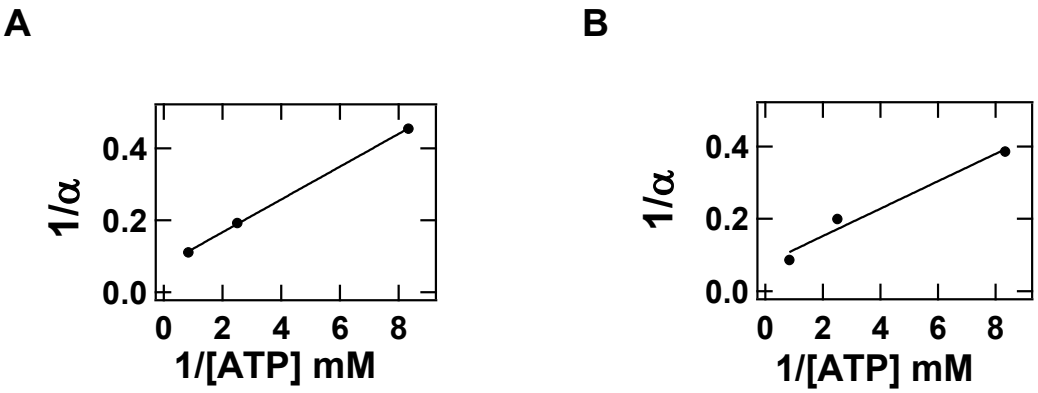

Figure 14. Alpha factor increases linearly with [ATP]
Data from Figure 13 were fitted to equation 1 globally while allowing the α value to vary for *apo-Pab*ABCE1 (A) and *holo-Pab* ABCE1 (B).

Mg^{2+} inhibition was investigated with both *apo*- and *holo*- forms of *Pab*ABCE1 and found to be slightly different. The *apo-Pab*ABCE1 exhibits higher V_{max} and K_m, and values of *α* were larger at higher [ATP] for the *apo*-enzyme. This suggests a complex mechanism of regulation for this enzyme by both the status, *i.e.* the occupancy or oxidation state, of the Fe-S clusters, and effects of Mg^{2+}. To verify the inhibition assigned to Mg^{2+} and not Cl^-, ATPase assays were also performed with MgOAc and $MgSO_4$ or other divalent metal chloride ions, and similar levels of inhibition were observed with corresponding concentrations (Figure 15AB).

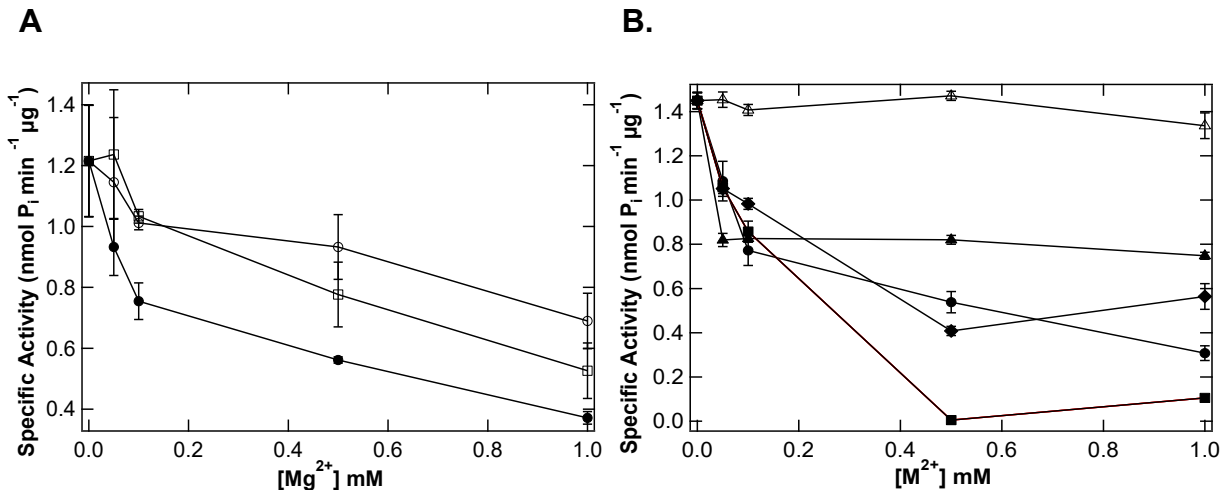

Figure 15. Activity of *Holo-Pab*ABCE1 in the presence of various anions or divalent metal ions
ATPase activity in the presence of increasing Mg^{2+} concentrations (0-1.0 mM) for $MgSO_4$ (□) and Mg ($C_2H_3O_2$) (○) (A) or various divalent metal chloride ions (B).
$FeCl_2$ (■), $MgCl_2$ (●), $MnCl_2$(♦), $ZnCl_2$(▲), $CaCl_2$(Δ).

Dependence of ATP Hydrolysis Parameters on Mg^{2+}

Mg^{2+} clearly has inhibitory effects on the ATPase activity of *Pab*ABCE1, which is peculiar for an ATPase. For the vast majority of ATPases, Mg^{2+} typically affects the K_m of MgATP, V_{max} of ATP hydrolysis, or both. Biochemical parameters with respect to [ATP] were determined in the presence of varying Mg^{2+} concentration for both the *apo*- and *holo-Pab*ABCE1 (Figure 16AD). The rates for each individual data set at the various [Mg^{2+}] concentrations were initially fit to the Hill form of the Michaelis-Menten equation and showed that V_{max} did not significantly change, but showed increasing apparent K_m values with increasing concentration of $MgCl_2$ (Figure 16BE). The data were also fit to the Hill form (*i.e.* [S] raised by n as $[S]^n$) of Eq. 2.1 by global fitting

methods. The data fit well, yielding global V_{max}, K_m and K_i values that were comparable to those determined from the [Mg^{2+}] titrations (Table 1).

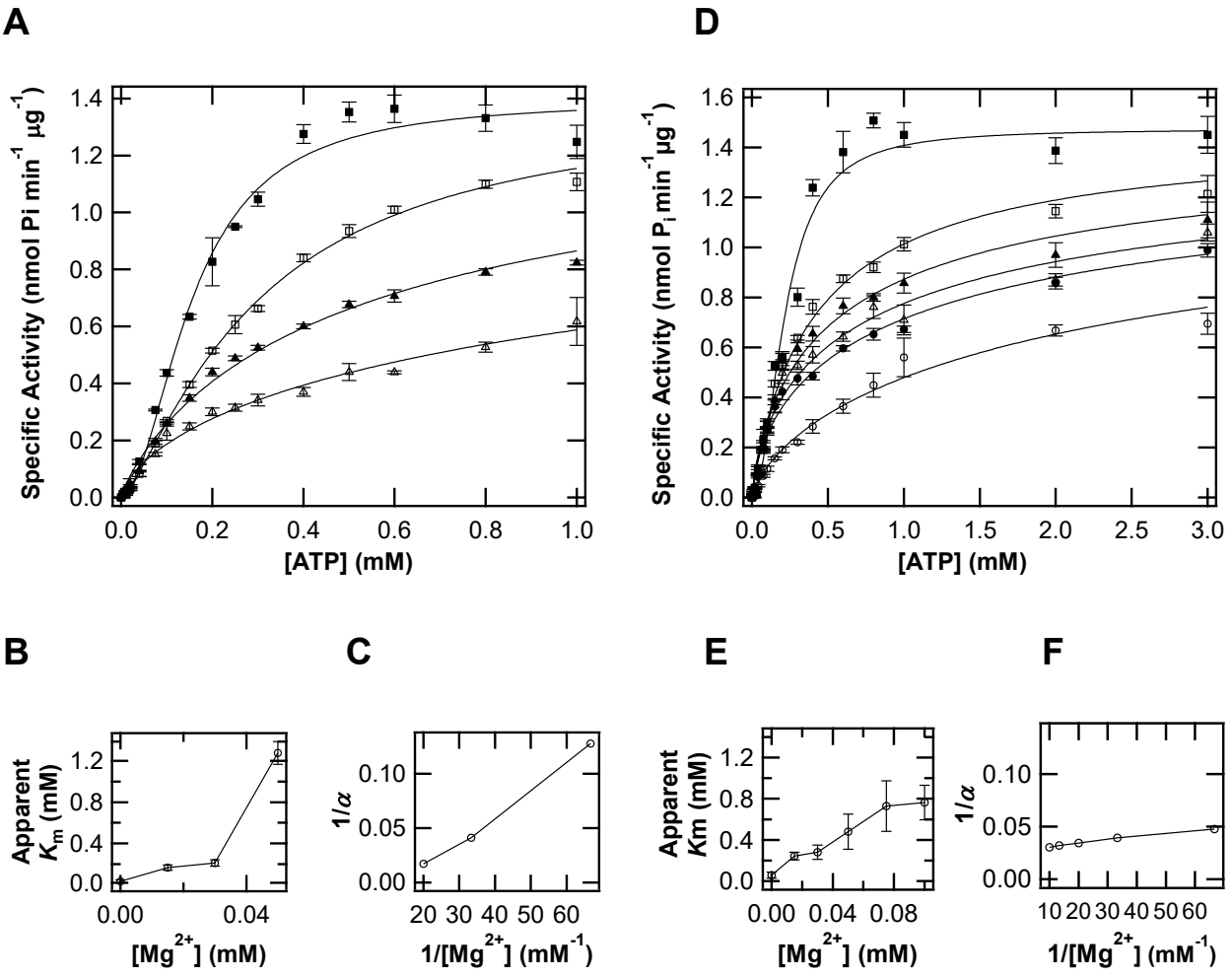

Figure 16. ATP saturation kinetics of *Pab*ABCE1 ATPase activity with varying [Mg^{2+}].

The effects of Mg^{2+} on the ATPase activity and affinity on *Pab*ABCE1 were determined for by titration of ATP in the presence of increasing [Mg^{2+}]. ATPase activity *vs* [ATP] plotted for *apo-Pab*ABCE1 (A) with No Mg^{2+} (■), 0.015 mM Mg^{2+} (□), 0.03 mM Mg^{2+} (▲), and 0.05 mM Mg^{2+} (Δ). ATPase activity *vs* [ATP] plotted for *holo-Pab*ABCE1 (B) with no Mg^{2+} (■),0.015 mM Mg^{2+} (□),0.03 mM Mg^{2+} (▲), 0.05 mM Mg^{2+} (Δ), 0.075 mM Mg^{2+} (●), and 1.0 mM Mg^{2+} (○). Apparent K_m are plotted *vs* [Mg^{2+}] for *apo*- (B) and *holo-Pab*ABCE1 (E). Plots of 1/*α* *vs* 1/[Mg^{2+}] are shown for *apo*- (C) and *holo-Pab*ABCE1 (F).

There appears to be a dependence of n with respect to [Mg^{2+}]. Interestingly, the Hill constant is near 2 in the absence of any added Mg^{2+} for both the *apo*- and *holo*-enzymes and decreases to n = 0.6 as [Mg^{2+}] is increased to 0.1 mM. This apparent cooperativity may be due to cooperative interaction between the two ATPase domains within the enzyme in the absence of Mg^{2+}. Addition of Mg^{2+} appears to disrupt this cooperativity. Also, for both forms of the enzyme in the absence of externally added Mg^{2+}, some product inhibition appears to exist at ATP concentrations greater than ~0.5 mM. Activity peaks at around 0.5 mM ATP and then has a slight decreasing trend toward higher concentrations. Such behavior is observed in some ATPases when there is insufficient Mg^{2+} and the Mg^{2+}: ATP ratio is below optimum. This suggests that ATP itself, not only MgATP, may be binding in an inhibitory fashion at high ATP concentrations and that, while Mg^{2+} is inhibitory, Mg^{2+} is definitely required. This point is further explored below.

Table 1. Kinetic parameters for Mg^{+2} inhibition of *apo*- and *holo*-PabABCE1.

		V_{max} (nmol P_i min^{-1} mg^{-1})	K_m (mM)	K_i (μM)
Globally fitted from Mg^{2+} titrations[a]	*apo-Pab*ABCE1	1.71±0.09	0.35±0.05	7.2±0.3
	*holo-Pab*ABCE1	1.34±0.05	0.16±0.02	6.9±0.2
Globally fitted from ATP titration[b]	*apo-Pab*ABCE1	1.39±0.03	0.029±0.007	0.7±0.5
	*holo-Pab*ABCE1	1.47±0.05	0.047±0.01	0.3±0.1

[a]Kinetic constants were determined by global fitting using Eq. 2.1 applied to data in Figure 13. V_{max}, K_m and K_i were kept linked while α was allowed to vary.
[b]Kinetic constants were determined by global fitting using Eq. 2.1 with [S] raised by *n* as $[S]^n$ and applied to data in Figure 16. V_{max}, K_m and K_i were kept linked while *n* and α were allowed to vary.

As was the case for the [Mg^{2+}] titrations shown in Figure 13, the ATP titration data could only be fit when α was allowed to vary with [Mg^{2+}]. For both the apo- and holo- forms of PabABCE1, there is a linear relationship between the inverse of α with the inverse of [Mg^{2+}]. A significant difference is observed when comparing the slopes for these replots between *apo*- and *holo-Pab*ABCE1 (Figure 16CF). The slope appears to be much steeper for the *apo-Pab*ABCE1 and thus indicates that the *apo-Pab*ABCE1 is more sensitive to Mg^{2+} inhibition. This suggests the involvement of both Fe-S cluster status and Mg^{2+} in a complex regulatory mechanism that is not currently understood for this enzyme.

Effect of Mg^{2+} on Product (ADP) Inhibition

A possible mechanism for the inhibitory effect of Mg^{2+} on this ATPase may be by exacerbating product inhibition. ADP is a product of ATP hydrolysis and often acts as an inhibitor for many ATPases [97]. The *Pab*ABCE1 may be extremely sensitive to product inhibition in conjunction with Mg^{2+}. To probe the effect of Mg^{2+} on product inhibition, reactions of *holo-Pab*ABCE1 with constant concentration of ATP (0.3 mM) were titrated with ADP, with and without inhibitory concentrations of Mg^{2+} (0.05 mM) (Figure 17). The ATPase activity in the presence of 50 μM Mg^{2+}, without ADP, was diminished by about 50% as expected. With increasing [ADP], *Pab*ABCE1 ATPase activity was inhibited in a hyperbolic fashion. However, in contrast to a standard simple inhibitor, the activities do not diminish to zero with increasing [ADP]. Attempts were made to fit the data to standard functions describing simple inhibition kinetics, but were not satisfactory. Since ADP often exhibits mixed inhibition behavior, the data were fit to

the following function describing hyperbolic mixed inhibition or a combination of partial competitive and partial non-competitive inhibition:

$$\boldsymbol{v} = \frac{\boldsymbol{V}_{\mathbf{max}}[\mathbf{S}]^{\boldsymbol{n}}}{\boldsymbol{\alpha K}_{\mathbf{s}}\frac{\left(\mathbf{1}+\frac{[\mathbf{I}]}{\boldsymbol{K}_{\mathbf{i}}}\right)}{\left(\mathbf{1}+\frac{\boldsymbol{\beta}[\mathbf{I}]}{\boldsymbol{\alpha K}_{\mathbf{i}}}\right)}+([\mathbf{S}]^{\boldsymbol{n}})\frac{\left(\mathbf{1}+\frac{[\mathbf{I}]}{\boldsymbol{\alpha K}_{\mathbf{i}}}\right)}{\left(\mathbf{1}+\frac{\boldsymbol{\beta}[\mathbf{I}]}{\boldsymbol{\alpha K}_{\mathbf{i}}}\right)}} \qquad \textbf{(2.2)}$$

where α is a coefficient for K_s as in Eq 2.1, β is a coefficient on the rate constant k_p for product formation and [I] represents the inhibitor concentration of ADP in this case. This function represents the equilibrium model shown in Figure 13C where α > 1 and 0 < β < 1 (p 179 in[90]). Note that α described here is with respect to ADP and is distinct from α for Mg^{2+} inhibition in the previous section. Comparison of the kinetic constants derived from data sets with and without 50 μM $MgCl_2$ shows minimal differences for apparent K_i for ADP (Table 2). While only limited interpretations should be made from fitting only the two curves in Figure 17, it does not appear that Mg^{2+} greatly affects the inhibition by ADP. The experiment does show that Mg^{2+} again decreases the rate by more than 50% and that ADP acts as a partial inhibitor, where β is about 0.17 both with and without Mg^{2+}, indicating that the rate constant for product formation is decreased to 17% with saturating ADP.

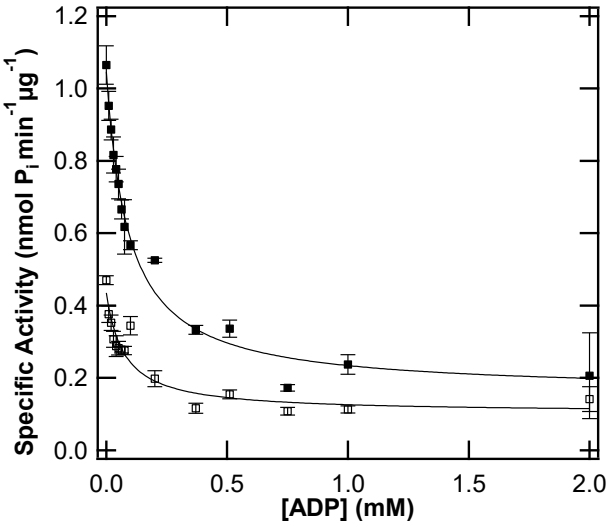

Figure 17. Inhibition by ADP of *holo-Pab*ABCE1 ATPase activity with and without 0.05 mM Mg^{2+}.
ATPase activity of *holo-Pab*ABCE1 is plotted with 0.3 mM ATP and with increasing [ADP] (0-2.0 mM) in the presence of Mg^{2+} (■) and 0.05 mM Mg^{2+} (□).

To further probe the effects of Mg^{2+} on ADP inhibition of *Pab*ABCE1, ATP saturation kinetics were examined in the presence of varying ADP as an inhibitor, both with and without added 0.05 mM Mg^{2+} (Figure 18AC). Initially, the data were fit using standard Hill form of the Michaelis-Menten equation. Replots of the apparent V_{max} in the presence of inhibitor ($V_{\max_i}$) are somewhat linear, but not perfect (Figure 18BD). In the case of a classical intersecting, linear non-competitive inhibitor (mixed inhibition), replots of $1/(V_{\max_i})$ versus [ADP] should be linear, but appear not to be. Attempts were also made to globally fit the data in Figure 18 A and C to functions for a classical mixed inhibitor, but these did not yield satisfactory fits. Given that titrations with ADP at fixed [ATP] do not diminish the ATPase activity to zero, Eq. 2.2 for hyperbolic mixed inhibitor was applied to the data sets in Figure 18A and C by global fitting methods, and

satisfactory fits were obtained. Kinetic constants obtained from this procedure are presented in Table 2.

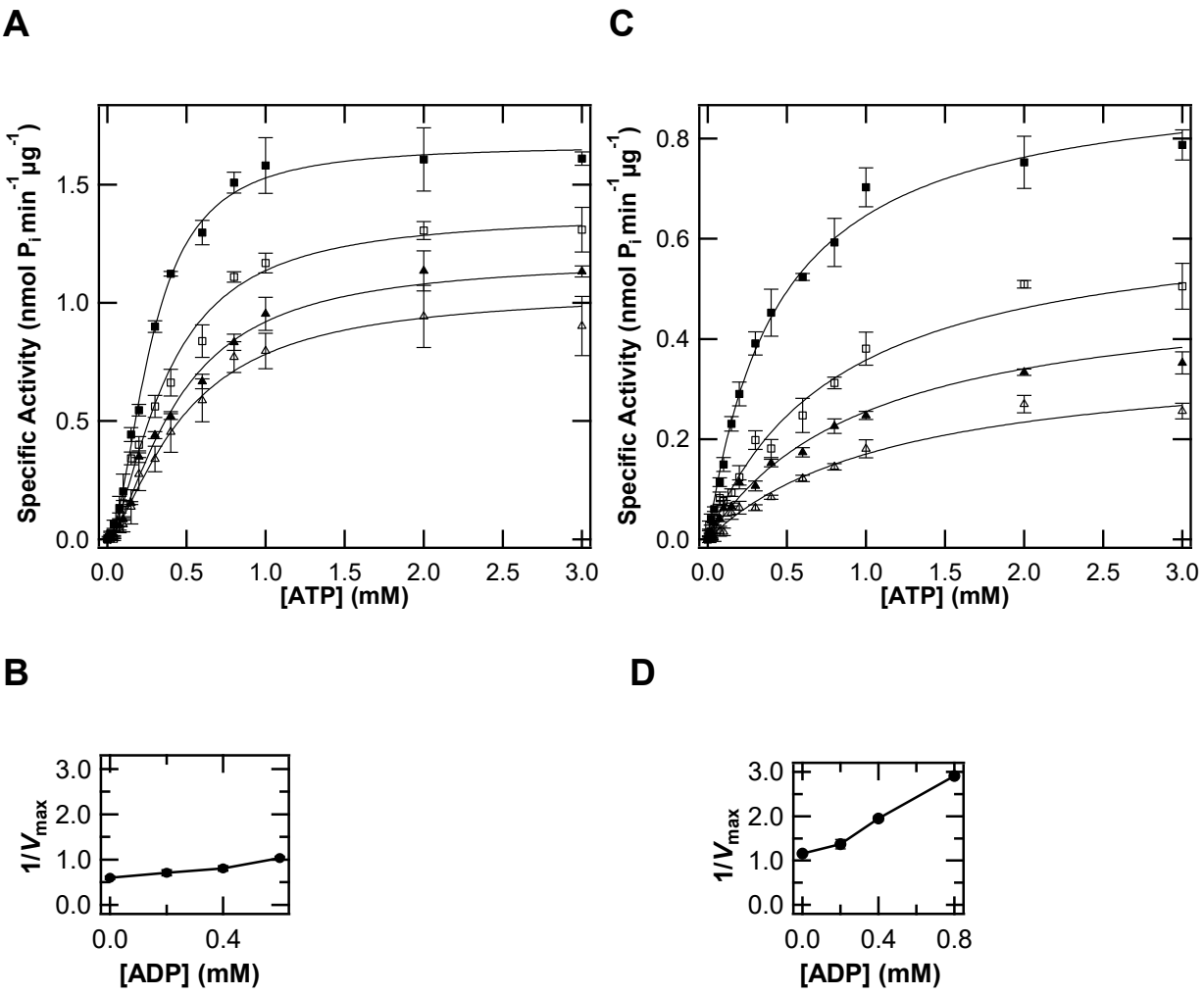

Figure 18. ATP saturation kinetics of *holo-Pab*ABCE1 ATPase activity with varying ADP and Mg^{2+}.
The effects of ADP on the ATPase activity and affinity of *holo-Pab*ABCE1 were determined. ATPase activity *vs* [ATP] is plotted for reactions without any added Mg^{2+} (A) for no ADP (■), 0.2 mM ADP (□), 0.4 mM ADP (▲) and 0.6 mM ADP (∆) or for reaction containing 0.05 mM Mg^{2+} (C) for No ADP (■), 0.2 mM ADP (□), 0.4 mM ADP (▲) and 0.8 mM ADP (∆). Replots of $1/V_{max}$ vs [ADP] are shown for without added Mg (B) and with 0.05 mM Mg^{2+} (D).

The value of V_{max} in the presence of Mg^{2+} decreased by about ~50%, as shown above. The K_m increased in the presence of Mg^{2+} by ~3 fold from 90 μM to 320 μM. The addition of Mg^{2+} only minimally affected the K_i for ADP, changing from 100 μM to 75 μM. Even the α and β parameters with ADP as the inhibitor for conditions with and without Mg^{2+} did not change. As seen before for the ATP titrations with varying Mg^{2+} (Figure 16), the most conspicuous change that occurred with the presence of Mg^{2+} was that it abolished apparent cooperativity where n changes from ~2 to ~1 for all concentrations of ADP. These data taken together suggest that inhibitory effect upon addition of Mg^{2+} was not due to modulation of product inhibition through MgADP.

Table 2. Kinetic parameters for ADP inhibition of *holo-Pab*ABCE1 with and without 0.05 mM $MgCl_2$.

	Mg^{2+} (mM)	V_{max} (nmol P_i min^{-1} mg^{-1})	K_m (mM)	K_i (mM)	α	β
Globally fitted ADP titrations[a]	0.00	1.56±0.02	0.15±0.02	0.07±0.01	1.3±0.1	0.17±0.01
	0.05	0.68±0.02	0.17±0.02	0.36±0.02	0.13±0.02	0.17±0.01
Globally fitted ATP titrations with varying ADP	0.00	1.67±0.02	0.090±0.002	0.102±0.002	7.4±0.4	0.17±0.02
	0.05	0.87±0.01	0.32±0.01	0.074±0.001	7.4±0.7	0.14±0.02

[a]Kinetic constants were determined by global fitting using Eq. 2.2 applied to data in Figure 17. V_{max}, K_m and K_i α and β were kept linked while *n* was allowed to vary.
[b]Kinetic constants were determined by global fitting using Eq. 2.2 applied to data in to data in Figure 18. V_{max}, K_m and K_i α and β were kept linked while *n* was allowed to vary.

Divalent Metal Chelators, EDTA and EGTA, Affect Activity of PabABCE1

The apparent ATPase activity by *Pab*ABCE1 without externally added Mg^{2+} and its inhibition with added Mg^{2+} raises the following question: does ATP hydrolysis by this

enzyme occurs without any Mg^{2+}? Alternatively, does *Pab*ABCE1 indeed require Mg^{2+} as a cofactor, and could there be Mg^{2+} associated with the as-prepared form of *Pab*ABCE1? This was evaluated by adding EDTA or EGTA to chelate the Mg^{2+}, presumably bound to the enzyme, and thus inhibiting the ATPase activity. The addition of EDTA or EGTA to ATPase reactions with 0.3 mM ATP, but no added Mg^{2+}, resulted in a decrease in activity (Figure 19AB). For both EDTA and EGTA, approximately 20 μM was sufficient to decrease ATPase activity. This observation suggests that Mg^{2+} is likely required for ATP hydrolysis, and that the as-purified form of *Pab*ABCE1 probably has some Mg^{2+} bound with high affinity.

A

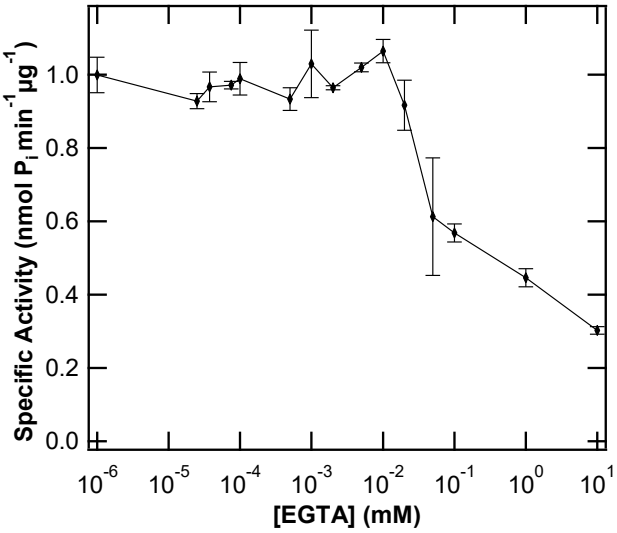

B

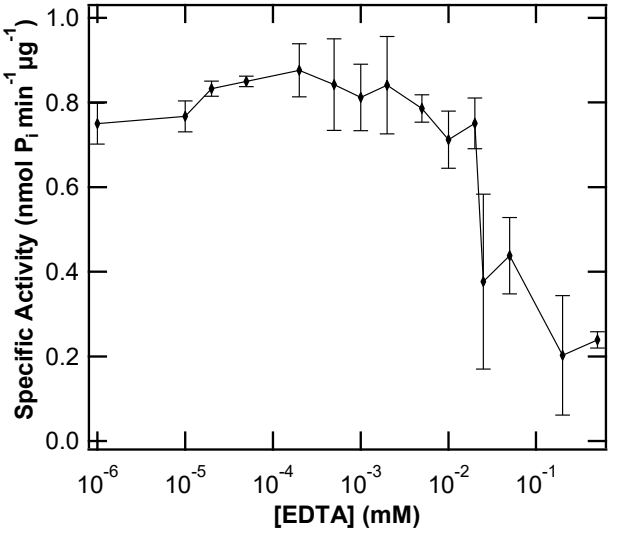

Figure 19. Mg^{2+} bound to *Pab*ABCE1 shown by inhibition of ATPase activity with EDTA or EGTA.

The effect divalent metal chelators on the ATPase activity of *Pab*ABCE1 were observed with increasing concentrations of EDTA (0-0.5 mM) (A) or EGTA (0-10 mM) (B) in the presence of 0.3 mM ATP and without any added Mg^{2+}.

Effect of Total RNA on Mg^{2+} Inhibition

ABCE1 has been shown to be associated with both polysomes and immature nascent ribosomes. ABCE1 has been shown to be functionally essential for both ribosome biogenesis and ribosome recycling [49, 50, 98]. Thus ABCE1 interacts with ribosomes in some sort of intimate way and possibly remodels RNA-RNA or RNA-protein interactions, most likely in an MgATP dependent way. Structural and biochemical analysis of RNA and ribosome structures have shown well the importance of Mg^{2+} in stabilizing structure [99, 100] and also the possible movement of Mg^{2+} upon ribosomal structural changes [101]. Therefore, RNA could have some effect, through Mg^{2+}, to modulate the ATPase activity of *Pab*ABCE1. For the ABCE1 from *S. solfataricus*, addition of ribosomes has been shown to stimulate ATPase activity [34]. Total RNA from yeast, containing 80-85% rRNA [83], was added to *Pab*ABCE1 ATPase reactions to observe possible effects (Figure 20A). Indeed, addition of RNA did have significant effects. Addition of total RNA from *S. cerevisiae* to *Pab*ABCE1 without added Mg^{2+} moderately increased ATPase activity by roughly 1.5 fold. The activity increased up to 20 μg of added total RNA, and then decreased with higher amounts of RNA. Inclusion of 0.5 mM total Mg^{2+} to ABCE1 inhibited its ATPase activity by more than 50% as observed above. Interestingly, addition of total RNA to the Mg^{2+} inhibited reaction increased the ATPase activity by ~4 fold from the Mg^{2+} inhibited activity. While, the binding of *Pab*ABCE1 to the *S. cerevisiae* rRNA, contained in the total RNA, may not be a specific interaction and the high temperature may result in the disruption of rRNA secondary structure, the fact that Mg^{2+} inhibition diminishes is highly significant.

To further confirm the apparent reversal of the Mg^{2+} inhibition of *Pab*ABCE1 ATPase activity by addition of RNA, Mg^{2+} was titrated in the presence of two fixed concentrations of RNA (Figure 20B). In contrast to the Mg^{2+} titration experiment in Figure 13, addition of Mg^{2+} in the presence of 10 or 20 μg of RNA stimulated the ATPase activity of *Pab*ABCE1. The ATPase activity increased as [Mg^{2+}] neared the presumed physiological conditions and then declined at much higher concentrations. The addition of 20 μg RNA had a greater activating effect than 10 μg and maximum activation with respect to Mg^{2+} required about double the concentration of Mg^{2+}. This experiment utilized 0.3 mM ATP and maximal activity required between 0.3 to 0.6 mM Mg^{2+} giving a ratio of 1:1-1:2 between ATP and Mg^{2+}, which is very common for ATPases.

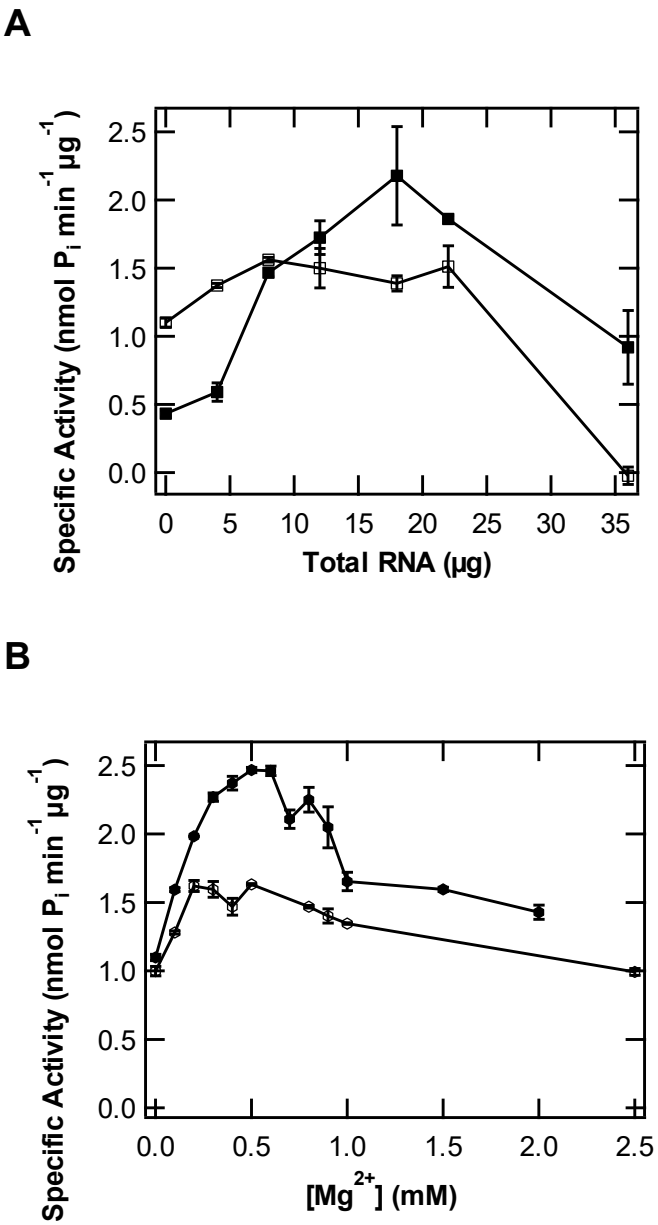

Figure 20. Total RNA activates *Pab*ABCE1 ATP hydrolysis in the presence of inhibitory concentrations of Mg^{2+}.

The affect of total RNA on the inhibition of *Pab*ABCE1 by Mg^{2+} was observed by (A) determining the specific activity in the absence (□) or presence (♦) on 0.5 mM Mg^{2+} and 0.3 mM ATP while increasing the amount of total RNA from 0-35 µg and (B) determining the specific activity in the presence of constant (◊) 10 µg or (♦) 20 µg total RNA and 0.3 mM ATP while increasing the amount of Mg^{2+} from 0-2.0 or 2.5 mM.

The exact mechanism for interaction between the RNA, Mg^{2+} and *Pab*ABCE1 may be complex. An interpretation could be made that the RNA is simply acting as a "sponge" for Mg^{2+}. RNA can definitely bind Mg^{2+} and may possibly counteract the inhibitory effects of Mg^{2+}, but that would not necessarily explain activation of the ATPase activity. The exact biochemical or molecular mechanism for RNA to reverse the inhibitory effects of Mg^{2+} is not possible to interpret from the experiments here. While this investigation used total RNA from *S. cerevisiae*, ribosomes contained in the total RNA are likely to be involved in this effect. However, the data seem to clearly indicate that both Mg^{2+} and some form of RNA positively affect the ATPase activity of *Pab*ABCE1.

Discussion

ABCE1 is an essential protein found in eukaryotic and archaeal organisms that is essential for ribosome biogenesis and ribosome recycling. While recent studies [32, 34, 49, 50, 77, 80] highlight the crucial role of this protein in critical cellular processes, very little is known at the biochemical mechanistic level. Key questions to be answered in the future are 1) how does it interact with ribosomes and what exactly are the transformations that it enacts on ribosomes, 2) what is the role of the Fe-S clusters, and 3) how is the energy from ATP utilized? Toward the goal of elucidating some of these unknowns, this study sought to characterize the ATP hydrolysis activity of *Pab*ABCE1.

Mg^{2+} Inhibition of the *Pab*ABCE1 and Other ATPases

Somewhat unexpectedly, the experiments described in this work clearly show that Mg^{2+} apparently inhibits the ATP hydrolysis activity of ABCE1 from *P. abyssi*. We do not know if Mg^{2+} is involved in regulation of ABCE1 enzymes from other organisms. Such inhibition by Mg^{2+} is definitely unusual for an ATPase, but is not without precedent. For instance, the activity of human GCH I, an enzyme that regulates cellular levels of tetrahydrobiopterin, is inhibited by Mg^{2+} due to the decrease in Mg^{2+}-free GTP [102]. Also, the ATPase activity of CASK, Ca^{2+}/calmodulin-activated Ser-Thr kinase, has been shown to function in an Mg^{2+} independent manner [96]. The ATPase activity of chloroplast coupling factor 1 has complex Mg^{2+} inhibition properties at physiologically relevant concentrations of free Mg^{2+} [93]. Some ATPases are very sensitive to Mg^{2+} mediated product inhibition where Mg^{2+}-ADP binds tightly to such systems as the F_0F_1 ATPase [103-105] or the hRAD51, an enzyme involved in homologous recombination [94, 106]. Such inhibition has been termed ADP-induced Mg^{2+}-dependent inhibition [91, 107-109] where it is likely to be caused by tight binding and slow release of Mg^{2+}-ADP once Pi leaves or the binding of a triple complex of Mg^{2+}-ADP-Pi at the catalytic site [92, 97]. All these examples show the importance of Mg^{2+} having a role in the regulation of enzyme activity.

The data presented here show that *Pab*ABCE1 is evidently inhibited by Mg^{2+}. The Mg^{2+} inhibition did not occur at high concentration, but at physiologically relevant low to mid μM-concentrations of Mg^{2+}. The addition of increasing [Mg^{2+}] decreased the ATPase activity in a saturating fashion, but did not decrease to the limit of no activity as

it would in the case of classical simple inhibition (Figure 13AB). Analysis of the kinetics for ATP hydrolysis, in the presence of varying Mg^{2+}, shows characteristics of complex partial inhibition. The data sets for both Figure 13 and Figure 16 fit well to a function that models partial competitive inhibition [90], where the V_{max} does not change but the apparent K_m increases in the presence of inhibitor. This is demonstrated by the significant increase in K_m, where Mg^{2+} seems to adversely affect the affinity for ATP by *Pab*ABCE1. The α values for this fitting cannot be held constant, but vary linearly between $1/\alpha$ and $1/[Mg^{2+}]$ (Figure 16CF), which may correlate to an additional equilibrium involving Mg^{2+}, perhaps in an allosteric fashion to affect the K_m towards ATP. Magnesium(II) may bind elsewhere on the protein to alter its conformation and shift the enzyme to a state with low affinity toward ATP. For the *apo-Pab*ABCE1, the apparent K_m for ATP increases from ~30 μM to 1.2 mM with the addition of only 50 μM Mg^{2+}, a concentration that is significantly lower than physiological conditions. This effectively alters the *apo-Pab*ABCE1 ATPase activity from essentially not being dependent on the cellular energy charge in the absence of Mg^{2+} to being modulated by cellular energy charge (φ) where intracellular ATP concentrations fluctuate dependent on cellular conditions and metabolism [110].

As noted above, several ATPases have apparent Mg^{2+} inhibition through tight MgADP product binding. ADP product inhibition is typical for most ATPases, and was further examined here with the *Pab*ABCE1 in relation to Mg^{2+}. Addition of increasing [ADP] decreases activity in a saturating way to about 15-18%, with or without added Mg^{2+}. Kinetic analysis of ATPase activity with varying [ADP] and contrasting between

no externally added Mg^{2+} and with 0.05 mM Mg^{2+} shows that Mg^{2+}-dependent inhibition is not due to MgADP. Global fitting of the ADP inhibition data (Figure 17) to a model for complex hyperbolic mixed inhibition [90] shows only a small decrease in K_i for ADP from ~100 μM to ~75 μM, but indicates a significantly altered K_m by 3.5 fold (not the apparent K_m with respect to added ADP) with addition of Mg^{2+}. The values for the α and β parameters for ADP inhibition determined by global fitting analysis are reasonable with α indicating effectively a decreased apparent affinity toward ATP and β indicating an effective decrease in apparent catalytic rate constant. Importantly here with respect to Mg^{2+}, the α and β values determined from both data sets, with and without added Mg^{2+}, are essentially the same. These data, taken together, show that the Mg^{2+}-dependent inhibition of *Pab*ABCE1 ATPase activity is independent of ADP inhibition.

Magnesium(II) ion also appears to alter the cooperativity with respect to [ATP] on *Pab*ABCE1. The Hill coefficient is near n = 2 without added Mg^{2+}, but decreases to around n = 1 when Mg^{2+} is added. Interestingly, there is a difference between the ATP-bound and the Mg^{2+}-ATP bound X-ray structures of the *E. coli* HlyB [21], haemolysin B, a different ABC protein, where there are twice as many water contacts in the ATP-bound form as there are in the Mg^{2+}-ATP-bound structure. Additionally, asymmetry between the two NBDs was discovered in the presence of Mg^{2+} in the HylB ABC protein. The full mechanism of where Mg^{2+} may bind and how it inhibits the *Pab*ABCE1 cannot be fully elucidated from this study and needs further investigation.

Mg^{2+} and Fe-S Cluster Status as Possible Component of *Pab*ABCE1 Regulation and Impact on Translation

Magnesium(II) ions are obviously important for growth and regulation of metabolism. More specifically, intracellular Mg^{2+} concentrations have an effect on protein synthesis [111]. The importance of Mg^{2+} for ribosomal structural integrity and its role in stabilizing, and possibly regulating, ribosomal RNA-RNA and RNA-protein interactions is well appreciated [99, 100, 112-114].

Addition of total RNA (from *S. cerevisiae*) appears to reverse the Mg^{2+} to an apparent activator of ATP hydrolysis. This result is fitting with a model where the *Pab*ABCE1 ATPase activity is inhibited at cellular [Mg^{2+}], but is ready to encounter a ribosome to enact its full activity. Such a model warrants further experiments that are beyond the scope of the current work. Furthermore, current experiments do not show if this would be a general model for all ABCE1 or possibly only specific to *P. abyssi*. In relation specifically to ABCE1 and ribosome recycling in eukaryotes, Mg^{2+} concentration does affect dissociation of ribosomal subunits at post-termination where 1.0 mM Mg^{2+} is permissible, but 2.5 mM Mg^{2+} and higher is inhibitory [98].

This study suggests complex and somewhat opposing dual roles for Mg^{2+} in the mechanism of the *Pab*ABCE1, which may be very appropriate for an enzyme that interacts intimately with ribosomes. First, Mg^{2+} may bind somewhere other than the MgATP sites to allosterically alter the affinity and cooperativity of MgATP binding. Second, as shown by the EDTA chelation experiment (Figure 19) and by the slight ATP substrate inhibition in the absence of added Mg^{2+}, Mg^{2+} is required for ATPase activity,

likely in the form of MgATP. The apparent tight binding of Mg^{2+} and the apparent inhibition at cellular concentrations of Mg^{2+} may be part of a regulatory mechanism for the *Pab*ABCE1 where needless and deleterious ATP hydrolysis is inhibited in the absence of ribosomes. These results correlate with a model where the *Pab*ABCE1 ATPase activity is inhibited at cellular [Mg^{2+}], but is ready to encounter a ribosome to enact its full activity. RNA and ribosomes are well known to chelate Mg^{2+} and binding to a ribosome may remove the bound Mg^{2+} and alleviate the inhibition. Such a model warrants further experiments that are beyond the scope of the current work. Furthermore, current experiments do not show if this would be a general model for all ABCE1 or possibly only specific to *P. abyssi*. In relation, specifically to ABCE1 and ribosome function in eukaryotes, Mg^{2+} concentration does affect dissociation of ribosomal subunits at post-termination where 1.0 mM Mg^{2+} is permissible, but 2.5 mM Mg^{2+} and higher has been observed to be inhibitory [98].

An aspect of ABCE1 that has been rather elusive to define is the role of the Fe-S clusters. The inhibition by Mg^{2+} was probed with both the holo- and Fe-S cluster deficient *apo-Pab*ABCE1. The K_i values for Mg^{2+} determined from global fitting of data in Figure 16 showed a 4-fold increase of the apparent K_m for ATP between the *apo*- and *holo*-forms. Furthermore, the slope for plots of $1/\alpha$ vs. 1/[Mg^{2+}] is steeper (Figure 16CF) for the apo- form. This indicates that the *apo-Pab*ABCE1 without its full complement of Fe-S clusters is more sensitive to Mg^{2+} inhibition and would be more sensitive to overall energy charge. This observed modality for inhibition through Mg^{2+} may be a possible mechanism for regulation of ABCE1 by Fe-S cluster status. A purely structural role for

the Fe-S clusters has been made [34], suggesting that the *apo*- form may just degrade. Studies in yeast clearly show that the *in vivo apo*-ABCE1, produced by inhibiting the Fe-S cluster assembly machinery, does exist both in the nucleolus, bound to immature ribosomes, and in the cytoplasm, bound to stalled polysomes [49]. This may be a basis for regulation of translation with respect to oxidative stress. Recent studies have shown that oxidative stress globally inhibits translation [115, 116]. Previous studies on the *S. solfataricus* ABCE1 by Barthelme *et al*. suggests that its ATPase activity is not affected by mutations of the Fe-S cluster ligands, but do show that ribosome binding is negatively affected by deletion of the Fe-S cluster domain [34]. The *S. solfataricus* ABCE1 may not be affected by Mg^{2+} as the *Pab*ABCE1 or strict anaerobic conditions may not have been maintained where a difference could have been observed. Clearly, more biochemical studies are necessary to truly understand the role(s) of the Fe-S clusters on ABCE1.

Ribosomal modification in either the context of ribosome biogenesis or translation is an extremely complex series of events. This work shows the somewhat unusual Mg^{2+} inhibition of the ATPase activity of *Pab*ABCE1. This inhibition by Mg^{2+} is not through modulation of MgADP product inhibition. The degree of inhibition by Mg^{2+} appears to be different between the *apo*- and *holo*- forms of *Pab*ABCE1. The work taken together supports a model where *Pab*ABCE1 is jointly regulated by Mg^{2+}, Fe-S cluster status, and the likely binding of ribosomes.

A model can be envisioned where resting ABCE1 bound with Mg^{2+} is allosterically inhibited. Binding to active ribosomes, ABCE1, with associated release

factors, performs mechanical work upon ATP hydrolysis, resulting in rearrangement of ribosome, where Mg^{2+} could be moved to a different site upon structural changes of the ribosome.

CHAPTER 3: ABCE1 IRON-SULFUR CLUSTERS ARE SENSITIVE TO REACTIVE OXYGEN SPECIES RESULTING IN GROWTH INHIBITION IN *SACCHAROMYCES CEREVISIAE*

Introduction

Exposure to oxidative stress is a common drawback to all known aerobically respiring organisms [117]. Oxidative stress is most generally caused from the full or partial reduction of oxygen (O_2), forming an endogeneous reactive oxygen species (ROS), such as superoxide ($O_2^{\bullet-}$), hydroxyl radical ($^{\bullet}OH$), hydroxide ion (OH^-) and hydrogen peroxide (H_2O_2) [118]. Additionally, environmental exposure to oxidants, such as ionizing radiation or heavy metals, can also form ROS. Reactive oxygen species are a normal consequence of aerobic metabolism. Therefore, cells have evolved several different antioxidant mechanisms for limiting oxidative stress and damage to macromolecules [117-121]. Oxidative stress occurs when the buildup of ROS overwhelms the cells' natural defense systems that are evolved to fight against oxidative effects.

Oxidative stress defense mechanisms can consist of enzymatic and non-enzymatic systems that are either constitutively present or induced during an adaptive response [117]. Non-enzymatic defense involves antioxidants such as glutathione, thioredoxin, and glutaredoxin [40, 122, 123]. There are several enzymatic antioxidants including catalase, superoxide dismutase, glutathione reductase and peroxidase, as well as thioredoxin reductase [117, 124, 125]. All of these systems work together to maintain the redox state of the cell.

Oxidative stress can result in damage to proteins, DNA, RNA, and lipids as well as the disruption of cellular signalling cascades. Direct oxidation to proteins can result in protein disfunction, degradation, or aggregation [126]. This can have a direct effect on translation, especially if the target is a protein or other component of the translation apparatus. A reversible inhibition of protein synthesis due to ROS has been demonstrated [115, 119]. Cells treated with H_2O_2 resulted in the phosphorylation of eIf2α by Gcn2 kinase, which inhibits translation initiation [12]. Interestingly in the same study, a slower rate of ribosomal runoff in polysome analysis following H_2O_2 treatment was demonstrated, suggesting inhibition of translation downstream of initiation, at elongation and termination. While the inhibition of translation is a clear result of H_2O_2-induced oxidative stress, the precise target of oxidation by H_2O_2 and the mechanism of inactivation is still unknown.

The direct target of oxidation could be the translation complex or it may be a specific components involved in the translation cycle [121, 127]. Some proteins are more sensitive to ROS induced oxidative stress, especially those that contain oxygen sensitive Fe-S clusters. Proteins containing Fe-S clusters can serve as a target or a source of further oxidative damage [128]. As a target of ROS, Fe-S clusters could be converted, by superoxide, to an unstable oxidized state where it loses an Fe^{2+} which also produces H_2O_2. Hydrogen peroxide can react with ferrous iron released during Fe-S degradation, generating a hydroxyl radical in the Fenton reaction, eventually resulting in a chain reaction that forms more ROS species resulting in systemic oxidative stress [118].

ABCE1 could be at the interface between Fe-S biogenesis, protein synthesis, and oxidative stress. In yeast, a defect in the core ISC machinery in the mitochondria due to depletion of yfh1 (frataxin), results in reduced incorporation of ^{55}Fe into ABCE1 [129] and increased sensitivity to oxidative stress. Since ABCE1 functions in such vital cellular processes as ribosome biogenesis, translation initiation, and ribosome recycling, ABCE1 is central to cell growth and survival [34, 49, 50, 76, 82, 130, 131]. The dependence of ABCE1 function on the status of its Fe-S clusters and their essential nature suggests ABCE1 as a likely target for oxidative damage by ROS. This study aims to address whether excess ROS exposure to cells could have an effect on Fe-S clusters of *Sc*ABCE1, a cytosolic Fe-S protein, and also whether the effect correlates with the growth inhibition expected when translation is inhibited (Figure 21).

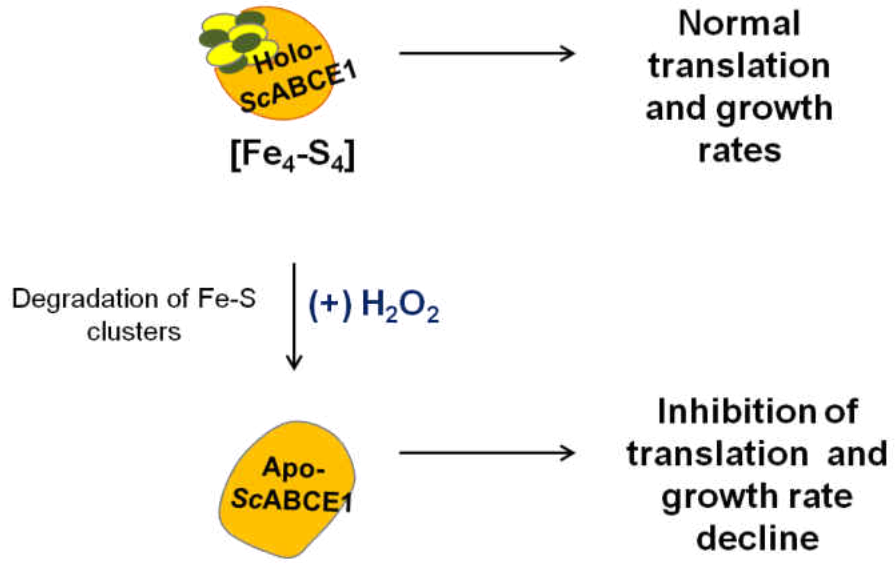

Figure 21. Model depicting the effect of exposure to to excess H_2O_2 on ABCE1 Fe-S clusters

Materials and Methods

Recombinant Expression of ABCE1 in *S. cerevisiae*

The diploid *S. cerevisiae* strain, Y258 (MATa pep4-3, his4-580, ura3-53, leu2-3,112), transformed with BG1805-*Sc*ABCE1-His6-HA-ZZ was used for all experiments (Open Biosystems). The BG1805-*Sc*ABCE1-His6-HA-ZZ vector provides expression of *Sc*ABCE1 with an HA fusion tag on the C-terminus, of under the control of the GAL1 promotor. In all experiments, cells were originally grown in SC medium lacking uracil and containing 2% raffinose with or without 2% galactose unless otherwise noted. Briefly, cells were either induced by the addition of 2% galactose or un-induced for 24 hours. The cells were then pelleted centrifugation (2,000 X *g*, 5 min) and lysed using the bead-beating method. Cell lysate was then subjected to SDS-PAGE, the proteins were transferred to a nitrocellulose membrane and probed with either mouse anti-HA primary antibody (1:5,000) (Covance, MMS-101P) or mouse anti-actin (1:500) (Abcam, ab8224) primary antibody. Colorimetric detection was performed subsequent to the incubation of the membranes with a alkaline phosphatase (AP)-conjugated goat anti-mouse IgG secondary antibody.

Treatment of Cells with H_2O_2

Cells were subjected to oxidative stress by the addition of H_2O_2 (0-20 mM) to the culture media once they reached an optical density of ~1.4. This was followed by a 30 min incubation (unless otherwise noted) at 30 ˚C and shaking (180 RPM). Samples at the indicated H_2O_2 concentration and time intervals were analyzed by pelleting cells by

by centrifugation (2000 x *g*, 8 min), then washed as described previously [132], frozen with liquid nitrogen, and stored at -80˚C.

In vivo ^{55}Fe Incorporation

In vivo labeling of yeast cells was performed following the addition of 1 μCi ^{55}Fe per liter and allowing growth to an optical density of ~1.3-1.5, at 30˚C, shaking at 180 RPM in SC medium lacking uracil, 2% raffinose, 2% galactose. When appropriate, cells were then subjected to oxidative stress by addition of H_2O_2 as described above or in figure legends. Cells were then harvested by centrifugation (2000 x *g,* 8 min) washed as described previously [132].

Immunoprecipitation

All immunoprecipitations were conducted in an anaerobic chamber containing at least 5% H_2 and less than 1 ppm O_2. All buffers were degassed and stored in the anaerobic chamber for at least 12 hours prior to beginning immunoprecipitations. Following growth to the desired optical density, H_2O_2 treatments where indicated, *Sc*ABCE1 was isolated by immunoprecipitation described Pierik *et al* [132] with a slight modification. Briefly, lysates were divided evenly to provide duplicate samples , then were incubated in the presence of α-HA antibody (100 ng) for one hour at 4 ˚C followed by a one hour incubation with 100 μL IgG Sepharose (50% slurry in 50 mM phosphate buffer, pH 7.5). Beads were then washed 4 times with 1 ml TNETG buffer (20 mM Tris pH 7.4, 150 mM NaCl, 2.5 mM EDTA, 0.5% Triton X-100, 10% glycerol), then 2 mL of

scintillation fluid was added. The amount of ^{55}Fe bound to *Sc*ABCE1-HA was measured with a liquid scintillation analyzer.

Results

The Stability and Persistence of *Sc*ABCE1 Protein Upon Treatment with H_2O_2

Since observations for this study must rest solely on the amount of ^{55}Fe specifically associated with ABCE1-HA, the ability to detect the ABCE1-HA bound ^{55}Fe in the absence or presence of H_2O_2 is a necessity. Immunoprecipation performed on lysate from cells not expressing ABCE1-HA reveal negligible detection of ^{55}Fe, while detection in induced cells indicates expression and specific detection of ABCE1-HA by the α-HA antibody (Figure 22 ABC).

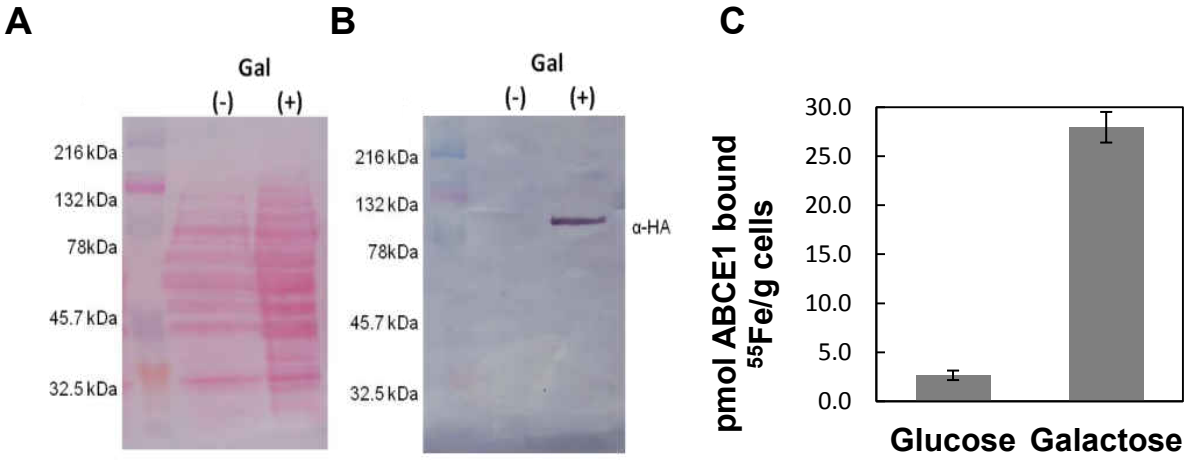

Figure 22. Recombinant expression and detection of ^{55}Fe bound to *Sc*ABCE1-HA in *S. cerevisiae*
Recombinant expression of *Sc*ABCE1-HA was confirmed by polyacrylamide electrophoresis (A) followed by a western blot (B) using an α-HA antibody (C) control ^{55}Fe measurements from immunoprecipitations of uninduced cells (glucose) and induced cells (2%raffinose +2% galactose).

The amount of detectable protein present in the cells should not decrease upon the treatment of H_2O_2, although it is possible that with H_2O_2 treatment, ABCE1-HA could become undetectable due to insolubility or the protein being degraded. This could result in the absence of the protein in the soluble fraction, which would prevent accurate interpretation of results. The ability to detect ABCE1-HA consistently over a wide range of H_2O_2 concentrations, to confirm integrity of ABCE1-HA peptide upon peroxide treatment was important for future experiments. Cells were subjected to 0-20 mM H_2O_2 with fixed amount of antibody, followed by SDS-PAGE and western blot analysis (Figure 23). This allowed the identification of available (soluble) ABCE1-HA so that any distinct differences in the ability to detect ABCE1-HA or any changes in protein amount upon exposure to H_2O_2 could be determined.

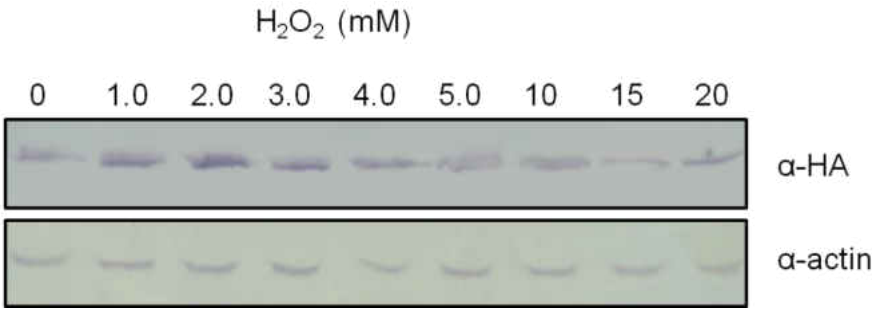

Figure 23. *Sc*ABCE1 expression analysis following oxidative stress
S. cerevisiae expressing BG1805-*Sc*ABCE1 were subjected to oxidative stress by the addition of the indicated [H_2O_2] for 30 minutes. Western blots were probed for α-HA (*Sc*ABCE1) or α-actin.

Western blot analysis demonstrated there was no significant decrease is the amount of ABCE1-HA present in the cells upon treatment with H_2O_2 concentrations up

to 20 mM (Figure 23). In fact, there seems to be a slight increase of ABCE1-HA upon treatment with lower concentrations of H_2O_2 (1-4 mM).

Next, the experimental strategy for immunoprecipitation was to determine an optimal fixed amount of ABCE1-HA but still limiting the amount of ABCE1-HA being detected to a fraction of the available ABCE1-HA. This ensures that even if there were any changes in the amount of protein in future experiments, the depletion of ^{55}Fe bound ABCE1-HA due to the effects of H_2O_2 could be accurately detected rather than just a decrease in the availability of ABCE1-HA. An optimal limiting amount of α-HA antibody and IgG sepharose was determined and described in the methods section.

ABCE1 Bound Iron is Depleted with Exposure to H_2O_2

To explore whether exposure to the prooxidant H_2O_2 has an effect on the occupancy of Fe-S clusters within ABCE1, cells were treated with increasing amounts of H_2O_2. Overexpression of ABCE1 has been shown to provide resistance to prooxidants, including H_2O_2 (0.25mM), in a *tet*-regulatable system [133].

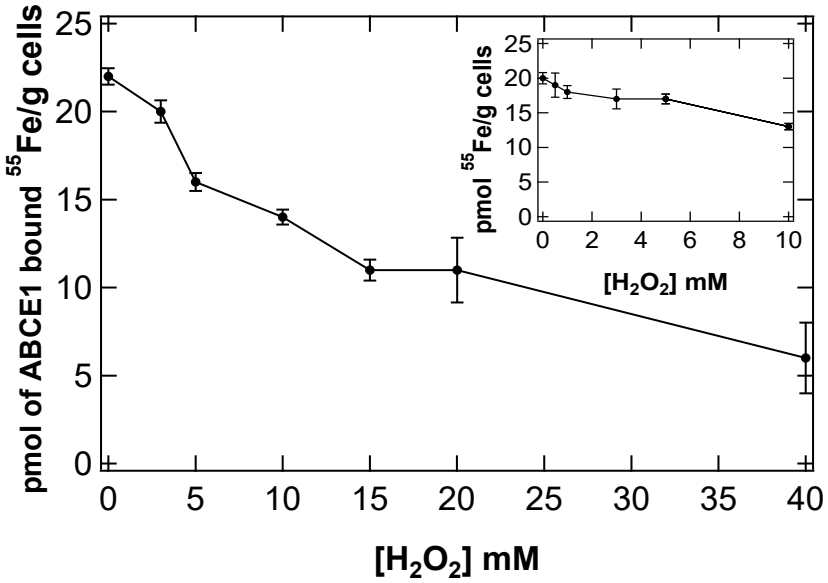

Figure 24. ^{55}Fe depletion from *Sc*ABCE1-HA with increasing [H_2O_2].
S. cerevisiae Y258 transformed with BG1805-*Sc*ABCE1-HA, were subjected to oxidative stress by the addition of increasing H_2O_2 concentration (0-40 mM H_2O_2) for 30 min, in 1.5% raffinose/2%galactose.

At H_2O_2 concentrations under 5 mM, a minimal decrease in ABCE1 bound ^{55}Fe was observed, suggesting some resistance to oxidative stress in the presence of lower H_2O_2 concentrations (Figure 24, inset). At higher concentrations of H_2O_2, there was a dose dependent decrease in the amount of ABCE1 bound ^{55}Fe with exposure to H_2O_2. The depletion of ^{55}Fe reached ~75% with the addition of 40 mM H_2O_2. These data suggest that ROS generated from H_2O_2 or H_2O_2 itself affects the Fe-S cofactors bound to ABCE1-HA.

ABCE1 Bound Iron Declines Due to Continued Exposure to H_2O_2

To support the conclusion that H_2O_2 caused the reduction in the amount of ABCE1 bound ^{55}Fe, cells were subjected to oxidative stress over time with a constant

amount of H_2O_2. The effect on ABCE1 bound ^{55}Fe due to H_2O_2 induced oxidative stress were consistent between experiments, where there was a ~40% decreased of ABCE1 bound ^{55}Fe (Figure 24) after 30 min of H_2O_2 exposure. Continued exposure to 10 mM H_2O_2 resulted in a gradual decline in the amount of ABCE1 bound ^{55}Fe where after 2.5 hours ABCE1 bound ^{55}Fe decreased by ~62% (Figure 25).

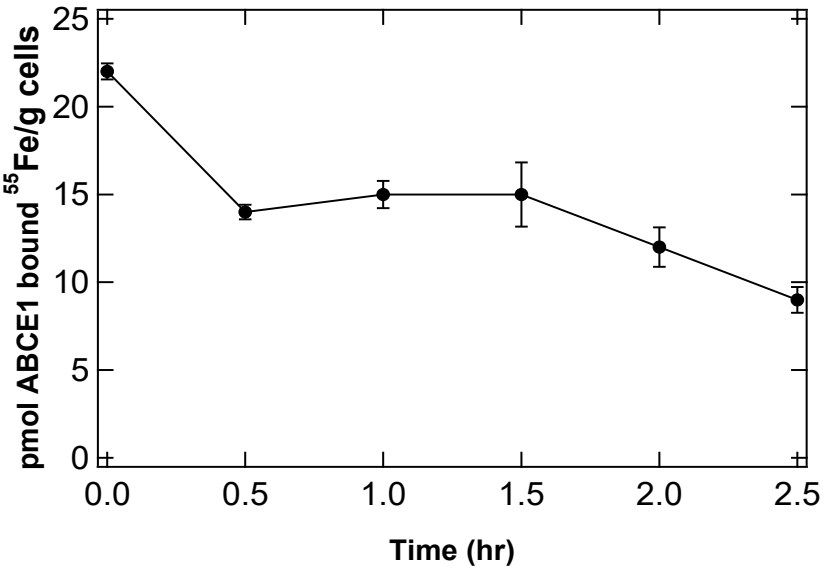

Figure 25. ^{55}Fe depletion from *Sc*ABCE1 over time following treatment with 10 mM H_2O_2.
S. cerevisiae, Y258 transformed with BG1805-*Sc*ABCE1-HA, were subjected to oxidative stress by the addition of 10 mM H_2O_2 for 30 min. Aliquots of cells were harvested, washed, and weighed, every 30 min. for up to 2.5 hours.

There appears to a lag in the time between 0.5 and 1.5 hours of exposure, possibly due to resistance or some other adaptive response (Figure 25). This suggests there may be sufficient antioxidant resistance to maintain a level of functional (or ^{55}Fe bound) ABCE1. After 1.5 hours, the balance between antioxidant resistance and

oxidative stress could have been shifted, perhaps due to the build-up of ROS. These data provide additional support for the hypothesis that exposure to H_2O_2 affects the Fe-S status of ABCE1. Here, the effects of H_2O_2 are likely partial or total degradation of the Fe-S clusters, since the Fe-S clusters (^{55}Fe) were already incorporated into ABCE1-HA. In addition, the possible negative impact of H_2O_2 on ^{55}Fe incorporation over time is also very possible.

Growth Rate can be Recovered Upon the Removal of H_2O_2

If the decrease in growth is the result of the presence of H_2O_2, then the growth rate should recover after the removal of H_2O_2. Upon media exchange and removal of H_2O_2, the growth rate began to increase gradually to ~6 hrs/doubling, almost completely recovered from the toxic effects of H_2O_2 (Figure 26A). Meanwhile, the growth rate remained very low for cells with continuous exposure to H_2O_2 where there was only slightly increasing and the doubling time extended to ~12 hrs. Thus, the growth rate of the stressed cells is ~50% lower than that of the recovering cells. The 40% reduction in ABCE1 bound ^{55}Fe described above can be the source of almost all the growth inhibition observed upon continued exposure to H_2O_2. These data suggest that, during conditions of oxidative stress, the key mediator between growth and growth inhibition could be the Fe-S status of ABCE1.

Following Exposure to H_2O_2, the Majority of ABCE1 Bound Iron can be Recovered

Results from the growth recovery experiment suggest the removal of H_2O_2 allows the restoration of function of ABCE1-HA. If the ABCE1-HA bound ^{55}Fe show a

corresponding increase over time, upon the removal of H_2O_2, then the Fe-S cluster and function of ABCE1-HA has likely been restored. Following removal of the H_2O_2, the amount of ABCE1 bound ^{55}Fe began to increase within the first 2 hours of recovery, where in comparison the amount ABCE1 bound ^{55}Fe did not increase in the cells subjected to continued exposure to H_2O_2 (Figure 26B). After ~8 hrs, the amount of ^{55}Fe bound to ABCE1 reached a maximum where it stayed through 12 hrs. The amount of ABCE1 bound ^{55}Fe following recovery was within 12% of the original amount prior to H_2O_2 treatment. The original, untreated cells contained ~26 pmol ^{55}Fe/g cells whereas at 12 hrs post-recovery, there were ~23 pmol ^{55}Fe/g cells. Following media exchange, the amount of ABCE1 bound ^{55}Fe detected cells that were subjected to, continued exposure to H_2O_2 continued to decline to ~56%. What is most notable is that the initiation of increase of growth rate corresponds to the same time that the ABCE1 bound ^{55}Fe started to increase (Figure 26AB). Combined, these data further support that the Fe-S clusters of ABCE1 are degraded upon oxidative stress and its activity is likely negatively modulated by loss of its Fe-S clusters. In turn, translation may be affected with decreased ABCE1 activity upon Fe-S cluster degradation and likely affects overall cellular growth rate.

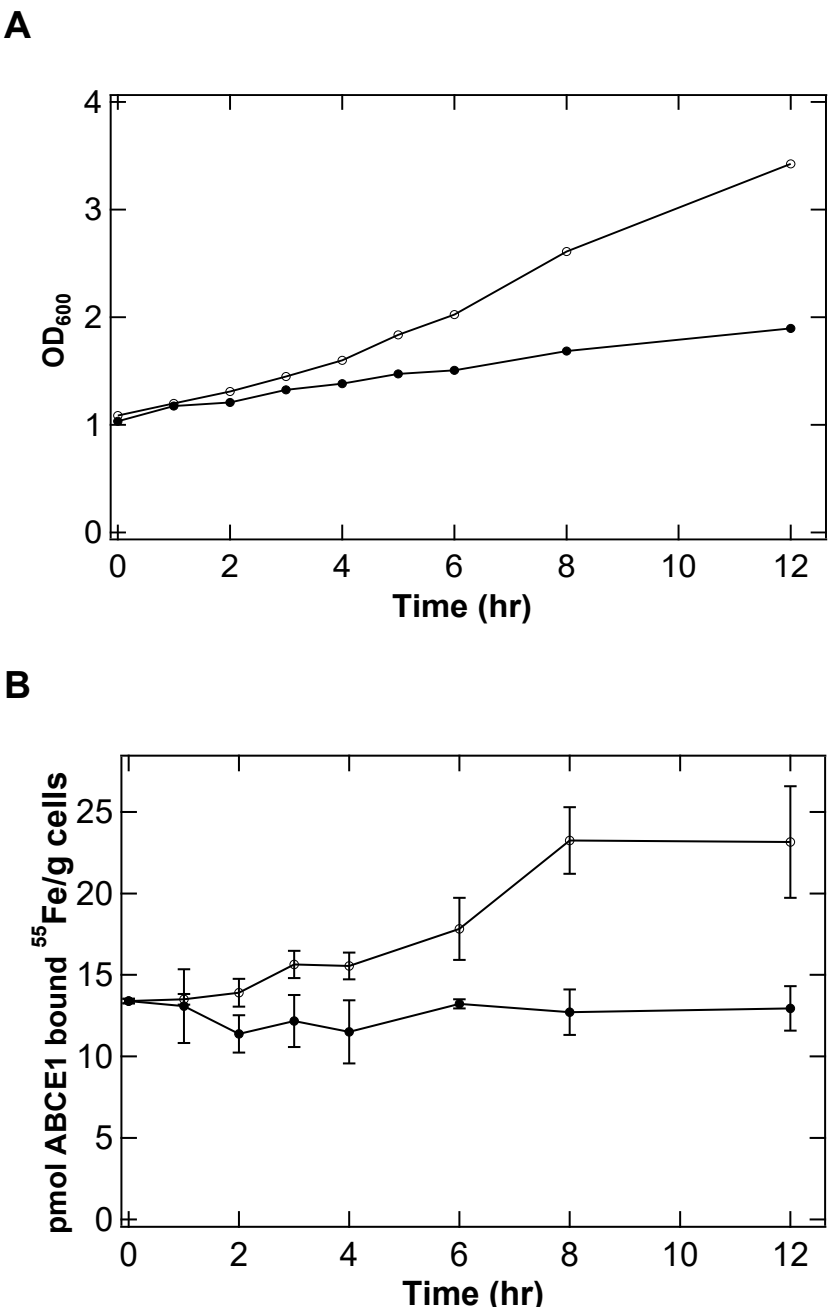

Figure 26. Repletion of ABCE1 bound ^{55}Fe in cells subjected to oxidative stress with 10 mM H_2O_2, occurs within 4 hours

S. cerevisiae, Y258 transformed with BG1805-*Sc*ABCE1-HA, were grown to an OD_{600} of 1.0, subjected to oxidative stress for 30 min by the addition of 10 mM H_2O_2. Cells were then harvested and resuspended in fresh media containing ^{55}Fe, consisting of (○) No H_2O_2 and (●) 10 mM H_2O_2. The OD_{600} was monitored (A) in conjunction with the amount of ^{55}Fe determined from immunoprecipitations (B).

Discussion

Effect of ROS on ABCE1 Function in Translation

This study aimed to address the proposed effect of ROS on the Fe-S clusters within the the cytosolic Fe-S protein, *Sc*ABCE1 (Figure 21). The global effect that H_2O_2 has on translation in yeast has been previously shown where protein synthesis declines with even mild oxidative stress [115, 119]. In *S. cerevisiae*, H_2O_2 has been shown to cause global translation inhibition and a corresponding dose-dependent decrease in growth rate, which can be reversed [115, 134]. The effects of oxidative stress have been observed at all stages of translation, including initiation, elongation, and termination [115]. Previously, in yeast, a defect in the core ISC machinery, by deletion of Yfh1 (frataxin), in the mitochondria demonstrated diminished incorporation of ^{55}Fe into ABCE1 [129]. In the same study, deletion of Yfh1 caused a considerable decrease in growth rates, demonstrating increased sensitivity to oxidative stress induced by H_2O_2, which was attributed to a defect in activities of mitochondrial Fe-S proteins. What exactly caused the global translation inhibition, growth rate decline, and ultimate toxicity demonstrated in wild-type cells was unknown. Due to the essential nature of ABCE1, its function in ribosome biogenesis, ribosome recycling, and the presence of Fe-S within ABCE1, the protein has been deemed a target for ROS, accounting for the growth inhibition typically observed under oxidative stress conditions [133].

The work presented here investigates the specific role of ABCE1 in response to oxidative stress in yeast. Our results demonstrate a 30 min of treatment with [H_2O_2] >5mM was required to see a marked decrease in ABCE1 bound ^{55}Fe (Figure 24),

suggesting overexpression of ABCE1 could confer resistance to oxidative stress. Resistance to the effects of oxidative stress, due to overexpression of ABCE1-HA, was demonstrated in a Fe-S defective strain (mxrΔ), and an antioxidant defective strain (sod2Δ), which are normally sensitive to prooxidants [133]. This may explain the high concentrations of H_2O_2 required in our system, where the endogenous ABCE1 is supplemented by the recombinant ABCE1-HA. ABCE1 may be up-regulated as a defense mechanism, upon exposure to low levels of H_2O_2, although this warrants further investigation.

The data shown in this work also shows a slight increase in ABCE1 bound ^{55}Fe between 30 min and 1.5hrs following H_2O_2 (Figure 25). It could be resistance caused by H_2O_2-induced expression of antioxidant defense systems, including possible up-regulation of ABCE1, which may have been able to fight against the toxic effects of H_2O_2 for a short period of time until they were overwhelmed. An alternative is that at the H_2O_2 concentration used in the experiment, a limit for direct Fe-S degradation could have been reached after 30 minutes. Over time, the buildup of additional H_2O_2 induced ROS can occur, overwhelming the cellular anti-oxidant defense systems where Fe-S degradation can continue.

Our initial experiments were principally restricted to the measurement of the amount ABCE1 bound ^{55}Fe depleted from Fe-S clusters pre-incorporated into ABCE1. A dose and time dependent depletion of ABCE1 bound ^{55}Fe under oxidative stress conditions induced by H_2O_2 was observed. While our experiments primarily measured the degradation of pre-incorporated ^{55}Fe (Fe-S) upon H_2O_2 treatment, experiments

conducted by others have shown the disruption of incorporation of ^{55}Fe to ABCE1 upon treatment with $Cu(NO_3)_2$ and paraquat [133]. The results presented here show the damaging effects the buildup of H_2O_2 can have on cell survival, through the likely degradation of the essential Fe-S clusters.

Implications for the Role of ABCE1 During Oxidative Stress

Although ABCE1 has been considered a credible target for ROS, the effects of oxidation *in vivo* were not investigated until recently. Here we have shown that H_2O_2 exposure results in a diminishment of the ABCE1 bound ^{55}Fe amount, suggesting direct oxidative degradation of the Fe-S clusters. Observations presented in this work demonstrate that the majority of growth inhibition, induced by oxidative stress, can be explained by a comparable decrease in ABCE1 bound ^{55}Fe (Figure 26AB) and likely loss of ABCE1 activity to facilitate ribosomal activity [49, 50]. Interestingly, our experiments show growth recovery upon removal of the H_2O_2, reaching a growth rate close to that of untreated cells after ~8 hrs. Additionally, a corresponding increase (~88% recovery) in the ABCE1 bound ^{55}Fe (Fe-S) was demonstrated. The results suggest a regulatory mechanism, where under oxidative stress conditions, the activity of ABCE1 supporting protein synthesis can be inhibited temporarily by oxidative degradation of the Fe-S clusters. In agreement with our data, the nuclear accumulation of Rps2-GFP was observed when yeast was exposed to various oxidants, which was subsequently rescued by overexpression of ABCE1 [133]. In our case, the cause of reduced growth and a decrease of ABCE1bound ^{55}Fe is very likely caused by oxidative damage to the Fe-S, decreasing the amount of ^{55}Fe (Fe-S) bound to ABCE1 and

causing a growth rate decline, although a decrease in ^{55}Fe incorporation could contribute over time.

A model can be envisioned where, under periods of stress, translation could be repressed by means of temporarily suppressing the function of ABCE1 via its oxidatively sensitive Fe-S clusters. Once the cause of the oxidative stress is removed (H_2O_2), normal cellular processes can be eventually restored. These data reveal that ABCE1 is likely to be at the center of an intricate balance between translation, cell growth, and cellular redox status.

CHAPTER 4: SUMMARY

Introduction

ABCE1 is an essential Fe-S protein involved in ribosomal function and vital for protein synthesis and cell survival, and thus has strong potential as a therapeutic target for cancer treatment. The function of ABCE1 in tumorigenesis, progression of cancer, or resistance to therapeutics is unclear, but nevertheless is likely to be significant. Additionally, the essential role of ABCE1 in viral infections, such as HIV/AIDS, could be important chemotherapeutic target toward the control of one of the most widespread pandemics. Previously, cell biological, genetic, and structural studies uncovered the cellular importance of ABCE1. The function of the Fe-S clusters of ABCE1 has been unclear until recently, where only a simple structural role was previously suggested. In an effort to better understand the function of ABCE1 and its associated Fe-S cofactors, the goal of this research was to elucidate the function of the Fe-S clusters of ABCE1 from a biochemical standpoint.

Upon biochemical analysis of *Pab*ABCE1, the ATPase activity was found to be regulated by its Fe-S cluster status and [Mg^{2+}], while total RNA had a positive effect on the regulation. Additionally, the Fe-S clusters were determined to regulate the function of ABCE1 based on the redox state of the cell. The oxidatively labile Fe-S clusters of

ABCE1 are lost under oxidative stress, resulting in a decrease in growth rate. This oxidative effect was reversible where an increase in ABCE1 bound Fe content

coincided with an increase in growth rate. The two major studies described here uncovered a more likely regulatory role for the Fe-S clusters of ABCE1.

Mg^{2+} Dependence of *Pyrococcus abyssi* ABCE1

Role of Fe-S Status and [Mg^{2+}] in the Function of ABCE1

The ATPase activity of the *Pab*ABCE1 was studied using both *apo*- and *holo*-forms, and was shown to be regulated by both Fe-S cluster status and Mg^{2+}. The rates were determined at the various [Mg^{2+}] concentrations and the data were fit to the Hill form of the Michaelis-Menten equation which determined that the apparent K_m values for ATP hydrolysis increased with increasing concentration of Mg^{2+} while the V_{max} did not change significantly. Physiological [Mg^{2+}] inhibits the *Pab*ABCE1 ATPase for both *apo*- and *holo*-*Pab*ABCE1, although the *apo*-*Pab*ABCE1 is more sensitive to Mg^{2+} inhibition. This is demonstrated by at least a 30 fold increase in the apparent ATP K_m of *apo*-*Pab*ABCE1, which is above the typical metabolic concentration of ATP.

*Pab*ABCE1 does require Mg^{2+}, like most ATPases, but Mg^{2+} also acts as a negative allosteric effector that controls the ATP affinity of *Pab*ABCE1, and does not inhibit by exacerbating product inhibition. Interestingly, an apparent cooperativity was seen in the absence of added Mg^{2+}, where the Hill constant is near 2 for both the *apo*- and *holo*- enzymes and decreases as [Mg^{2+}] is increased. A cooperative interaction between the two ATPase domains within the enzyme in the absence of Mg^2 may occur, where the addition of Mg^{2+} appears to disrupt the cooperativity. This suggests some

type of allosteric effect of Mg^{2+} binding to induce conformational change upon Mg^{2+} binding.

ABCE1 requires its Fe-S clusters for proper function in ribosome biogenesis and recycling. The inhibitory effect of Mg^{2+} could be alleviated and slightly activated by the presence of total RNA. All these data combined suggest that the function of *Pab*ABCE1 can be regulated by not only Fe-S status but also cellular energy charge (φ) in the presence of cellular [Mg^{2+}].

Future Perspectives for Studying the Regulatory Roles of Mg^{2+} and Fe-S Cluster Status

The main goal of this study was investigate the function of the Fe-S clusters associated with ABCE1 from a biochemical perspective. Comparative analysis of ABCE1 primary sequences reveals conservation among diverse organisms, from the archeal *Pyrococcus abyssi* ABCE1 to the human ABCE1, and suggests an important cellular function. Even with the high degree of sequence homology of ABCE1 and presumed structural homology between the ABCE1 from these organisms, the conclusions drawn from the studies with *Pab*ABCE1 may still not be directly extended to *Hs*ABCE1 or even *Sc*ABCE1. Once these proteins are able to be purified in sufficient quantity and appropriate quality for biochemical analysis, and kinetic analysis, then the question of Mg^{2+} sensitivity can be addressed.

The abolished cooperativity seen in *Pab*ABCE1 with added Mg^{2+} could be a consequence of NBDs that differ in activity or sensitivity to the inhibitory [Mg^{2+}]. In this case, the Mg^{2+} could bind in a fashion that inhibits one of the NBDs, while the other is still active, which can explain the Mg^{2+} titration curves that never reached an activity of

zero. To address this possibility, construction of point mutations at one or both of the catalytic amino acids (glutamate and/or aspartate) within each of the NBDs would be necessary to inactivate one NBD while allowing the activity of the other to be discretely studied.

The interpretation of the influence of RNA presented in this work should be interpreted with some caution, but may be significant. The work here suggests that Mg^{2+} may be bound to an inhibitory site on ABCE1 until it comes into contact with a binding partner such as, the ribosome, Dom34, of eRF3 [80]. Once associated with the translation apparatus, the inhibitory Mg^{2+} is released or relocated, resulting in ABCE1 activity. This hypothesis could be addressed using a reconstituted *in vitro* yeast translation system to address how Mg^{2+} could regulate the function of ABCE1 in ribosomal subunit splitting [77].

The *in vivo* effects of excess Mg^{2+} in relation to ribosome recycling are not yet clear. Since the RNA experiments in this work show a 2 fold increase in activity at a maximum of 0.5 mM Mg^{2+} followed by a decline in activity, the Mg^{2+} associated with pabABCE1 activity could have declined due to excess RNA. To test this hypothesis, experiments involving the addition of increasing amount of Mg^{2+} could be performed. In this case, an increased amount of available Mg^{2+} could result in a more dramatic activation of *Pab*ABCE1 in the presence of RNA as opposed to the condition without added Mg^{2+}.

Sensitivity to Mg^{2+} by either *Sc*ABCE1 or *Hs*ABCE1 has not yet been demonstrated. It may be specific only to hyperthermophiles. In fact, some

hyperthermophiles are known to have high intracellular salt concentrations and studies on DNA polymerase demonstrate that high salt concentrations protects the DNA from heat-induced cleavage, by preventing depurination [135, 136]. *Hs*ABCE1 is particularly important, mainly because it directly applies to a function in humans where cancer is prevalent. Depletion of *Hs*ABCE1 in the small cell lung cancer cell line, affects the proliferation of the cancer, suggesting a direct role for ABCE1 in cancer invasiveness [62]. The link between magnesium and cancer is somewhat complicated due to the fact that magnesium deficiency can either help prevent or promote tumor development [137]. Additionally, the alteration in the expression of magnesium channels has been demonstrated. If the ATPase activity of *Hs*ABCE1 is sensitive to magnesium as in *Pab*ABCE1, then magnesium deficiency could promote tumor development. The hypothesis could be tested using a cell line overexpressing a Mg^{2+} transporter, such as SLC41A1, which is associated with magnesium deficiency in some tissues [138, 139]. Here, a deficiency of Mg^{2+} in the cell would be expected to allow cells to proliferate due to increased activity of *Hs*ABCE1.

Effect of Reactive Oxygen Species (ROS) on ABCE1 Fe-S Clusters

Impact of Reactive Oxygen Species on the Fe-S Status and Function of ABCE1

The data presented in this work support the hypothesis that, during conditions of oxidative stress, one of the key mediators between growth and growth inhibition could be the Fe-S status of ABCE1. The oxidatively labile Fe-S clusters of ABCE1 can be degraded upon oxidative stress, and ABCE1 and/or its Fe-S cluster activity decreased

due to the partial or total degradation of the Fe-S clusters. In turn, translation is affected with decreased ABCE1 activity resulting in a decrease in cellular growth rate.

Some resistance to oxidative stress was discovered, in the presence of relatively low H_2O_2 while at higher concentrations of H_2O_2 (>5mM) there was a dose dependent decrease in the amount of ABCE1 bound ^{55}Fe with exposure to H_2O_2. Most (~75%) of the ^{55}Fe was depleted with the addition of 40 mM H_2O_2. The dose dependent decrease in ABCE1-HA bound ^{55}Fe suggests degradation of the ABCE1-HA bound Fe-S clusters due to ROS generated from H_2O_2 or H_2O_2 itself. Additionally, continued exposure to 10 mM H_2O_2 resulted in a progressive decline in ABCE1-HA bound ^{55}Fe, supporting the conclusion obtained with the dose dependent data.

Our results suggest a regulatory mechanism, where under oxidative stress conditions, the translational activity of ABCE1 can be inhibited temporarily by oxidative degradation of the Fe-S clusters. This was demonstrated when a growth recovery and concurrent increase in ABCE1 bound ^{55}Fe, upon removal of the H_2O_2, occurred reaching a growth rate (~88% recovery) close to that of untreated cells after ~8 hrs. Combined, these data further support that the Fe-S clusters of ABCE1 are degraded upon oxidative stress and ABCE1 activity is likely negatively modulated by loss of its Fe-S clusters.

Future Perspectives for Studying the Role of ROS in Regulation of ABCE1 Activity

The main goal in this study was to investigate the effects of ROS on the function of *Sc*ABCE1 in *S. cerevisiae*. Translation repression due to the effects of ROS has

been documented [115, 119]. Since *Sc*ABCE1 has an essential function in ribosome biogenesis and recycling, the protein is ultimately linked to translation and cell survival. The work here suggests that exposure to ROS such as H_2O_2 itself can affect the function of *Sc*ABCE1, due to the likely degradation of its Fe-S cofactors. A structural role has been suggested for the Fe-S domain, where *Sc*ABCE1 Fe-S clusters are required to interact with Dom34 during ribosome recycling and/or the rescue of stalled ribosomes [77, 80, 140]. A defect in the export of ribosomes from the nucleus during oxidative stress has been demonstrated [133]. In our system, a decrease in translation would be expected to follow degradation of ABCE1 associated Fe-S clusters following treatment with H_2O_2. This hypothesis could be addressed by monitoring the depletion of ABCE1 bound ^{55}Fe while simultaneously monitoring the progress of global translation using ^{35}S cysteine/methionine. Upon recovery, or removal of H_2O_2, a likewise increase in ABCE1 bound ^{55}Fe as well as an increase in the amount of protein bound ^{35}S cysteine/methionine, providing a direct link to oxidative stress and translational output.

A few additional questions could be presented: Does exposure to H_2O_2 result in a defect in ribosome recycling or only the export of ribosomes from the nucleus? Does oxidative stress abolish the binding of ABCE1 to partners such as, the ribosome, Dom34, or eRF3, during ribosome biogenesis or recycling? Additionally, does *Sc*ABCE1 become sequestered to stress granules during oxidative stress and then released upon recovery? One preliminary experiment could be to investigate the apparent K_d for ribosome binding in the presence of ROS. Some of these other questions could be answered using the reconstituted *in vitro* yeast translation system

described previously [77] or utilizing a GFP-*Sc*ABCE1 fusion protein to determine the location of *Sc*ABCE1 during oxidative stress. In this case, ribosome splitting would decline in the presence of a prooxidant and possibly co-localize with proteins associated with stress granules such as Tia-1 or Tiar [141]. If the effects of oxidative stress result in abolished interactions with recycling factors, then co-immunoprecipitation experiments would show the absence of Dom34, in cells exposed to a prooxidant as well as a decrease in growth rate.

The work presented here investigated the effect of H_2O_2 on Fe-S clusters already loaded into *Sc*ABCE1. Treatment with $Cu(NO_3)$ or paraquat has shown a decrease in ABCE1 bound ^{55}Fe, indicative of disruption of Fe-S incorporation into ABCE1 [133]. The effect of H_2O_2 on the incorporation of Fe-S clusters has not been determined and could be addressed in our system by simply adding H_2O_2 and ^{55}Fe simultaneously. If ROS affects the incorporation of Fe-S into *Sc*ABCE1, at what step does ROS affect the Fe-S clusters in the cytosolic machinery? This could be addressed by monitoring the presence of ^{55}Fe in each of the proteins involved in the CIA complex, possibly answering the question of whether the Fe-S are more labile during the transfer to ABCE1 or at some point prior to that.

The effect of ROS on ABCE1 in relation to cancer is not quite clear. Metabolism in cancer cells is known to vary and overproduction of ROS is common in many cancers [142]. If this is so, and ABCE1 function is regulated by ROS resulting in translation inhibition, how do cancer cells continue to proliferate? This suggests there may be

other factors involved in the progression of cancer due to the effects of ROS and further research in the area is needed.

The studies described in this dissertation point to a regulatory role for the Fe-S clusters of ABCE1, where the ATPase activity and likely ribosome binding is modulated based on redox and occupancy status of the Fe-S cluster. The ATPase activity of *Pab*ABCE1 is regulated by its Fe-S status and cellular charge, in terms of [Mg^{2+}] and the *in vivo* work in *S. cerevisiae* show the Fe-S clusters of *Sc*ABCE1 can be regulated by the physiological state of the cell, in this case oxidative stress. Both of these concepts have implications in cancer progression or tumorigenesis and provide clues needed for a future research for the development of cancer or viral therapeutics to target ABCE1.

APPENDIX A: COPYRIGHT AGREEMENT

Order reference number	
Title of your thesis/dissertation	REGULATION OF THE ATPASE ACTIVITY OF ABCE1 FROM PYROCOCCUS ABYSSI BY FE-S CLUSTER STATUS AND MG2+: IMPLICATION FOR RIBOSOMAL FUNCTION & ABCE1 IRON-SULFUR CLUSTERS ARE SENSITIVE TO REACTIVE OXYGEN SPECIES RESULTING IN GROWTH INHIBITION IN SACCHAROMYCES CEREVISIAE
Expected completion date	Dec 2012
Estimated size (number of pages)	200
Elsevier VAT number	GB 494 6272 12
Permissions price	0.00 USD
VAT/Local Sales Tax	0.0 USD / 0.0 GBP
Total	0.00 USD

Terms and Conditions

INTRODUCTION

1. The publisher for this copyrighted material is Elsevier. By clicking "accept" in connection with completing this licensing transaction, you agree that the following terms and conditions apply to this transaction (along with the Billing and Payment terms and conditions established by Copyright Clearance Center, Inc. ("CCC"), at the time that you opened your Rightslink account and that are available at any time at http://myaccount.copyright.com).

GENERAL TERMS

2. Elsevier hereby grants you permission to reproduce the aforementioned material subject to the terms and conditions indicated.

3. Acknowledgement: If any part of the material to be used (for example, figures) has appeared in our publication with credit or acknowledgement to another source, permission must also be sought from that source. If such permission is not obtained then that material may not be included in your publication/copies. Suitable acknowledgement to the source must be made, either as a footnote or in a reference list at the end of your publication, as follows:

"Reprinted from Publication title, Vol /edition number, Author(s), Title of article / title of chapter, Pages No., Copyright (Year), with permission from Elsevier [OR APPLICABLE SOCIETY COPYRIGHT OWNER]." Also Lancet special credit - "Reprinted from The Lancet, Vol. number, Author(s), Title of article, Pages No., Copyright (Year), with permission from Elsevier."

4. Reproduction of this material is confined to the purpose and/or media for which permission is hereby given.

5. Altering/Modifying Material: Not Permitted. However figures and illustrations may be altered/adapted minimally to serve your work. Any other abbreviations, additions, deletions and/or any other alterations shall be made only with prior written authorization of Elsevier Ltd. (Please contact Elsevier at permissions@elsevier.com)

6. If the permission fee for the requested use of our material is waived in this instance, please be advised that your future requests for Elsevier materials may attract a fee.

7. Reservation of Rights: Publisher reserves all rights not specifically granted in the combination of (i) the license details provided by you and accepted in the course of this licensing transaction, (ii) these terms and conditions and (iii) CCC's Billing and Payment terms and conditions.

8. License Contingent Upon Payment: While you may exercise the rights licensed immediately upon issuance of the license at the end of the licensing process for the transaction, provided that you have disclosed complete and accurate details of your proposed use, no license is finally effective unless and until full payment is received from you (either by publisher or by CCC) as provided in CCC's Billing and Payment terms and conditions. If full payment is not received on a timely basis, then any license preliminarily granted shall be deemed automatically revoked and shall be void as if never granted. Further, in the event that you breach any of these terms and conditions or any of CCC's Billing and Payment terms and conditions, the license is automatically revoked and shall be void as if never granted. Use of materials as described in a revoked license, as well as any use of the materials beyond the scope of an unrevoked license, may constitute copyright infringement and publisher reserves the right to take any and all action to protect its copyright in the materials.

9. Warranties: Publisher makes no representations or warranties with respect to the licensed material.

10. Indemnity: You hereby indemnify and agree to hold harmless publisher and CCC, and their respective officers, directors, employees and agents, from and against any and all claims arising out of your use of the licensed material other than as specifically authorized pursuant to this license.

11. No Transfer of License: This license is personal to you and may not be sublicensed, assigned, or transferred by you to any other person without publisher's written permission.

12. No Amendment Except in Writing: This license may not be amended except in a writing signed by both parties (or, in the case of publisher, by CCC on publisher's behalf).

13. Objection to Contrary Terms: Publisher hereby objects to any terms contained in any purchase order, acknowledgment, check endorsement or other writing prepared by you, which terms are inconsistent with these terms and conditions or CCC's Billing and Payment terms and conditions. These terms and conditions, together with CCC's Billing and Payment terms and conditions (which are incorporated herein), comprise the entire agreement between you and publisher (and CCC) concerning this licensing transaction. In the event of any conflict between your obligations established by these terms and conditions and those established by CCC's Billing and Payment terms and conditions, these terms and conditions shall control.

14. Revocation: Elsevier or Copyright Clearance Center may deny the permissions described in this License at their sole discretion, for any reason or no reason, with a full refund payable to you. Notice of such denial will be made using the contact information provided by you. Failure to receive such notice will not alter or invalidate the denial. In no event will Elsevier or Copyright Clearance Center be responsible or liable for any costs, expenses or damage incurred by you as a result of a denial of your permission request, other than a refund of the amount(s) paid by you to

Elsevier and/or Copyright Clearance Center for denied permissions.

LIMITED LICENSE

The following terms and conditions apply only to specific license types:

15. **Translation**: This permission is granted for non-exclusive world **English** rights only unless your license was granted for translation rights. If you licensed translation rights you may only translate this content into the languages you requested. A professional translator must perform all translations and reproduce the content word for word preserving the integrity of the article. If this license is to re-use 1 or 2 figures then permission is granted for non-exclusive world rights in all languages.

16. **Website**: The following terms and conditions apply to electronic reserve and author websites:
Electronic reserve: If licensed material is to be posted to website, the web site is to be password-protected and made available only to bona fide students registered on a relevant course if:
This license was made in connection with a course,
This permission is granted for 1 year only. You may obtain a license for future website posting,
All content posted to the web site must maintain the copyright information line on the bottom of each image,
A hyper-text must be included to the Homepage of the journal from which you are licensing at http://www.sciencedirect.com/science/journal/xxxxx or the Elsevier homepage for books at http://www.elsevier.com , and
Central Storage: This license does not include permission for a scanned version of the material to be stored in a central repository such as that provided by Heron/XanEdu.

17. **Author website** for journals with the following additional clauses:

All content posted to the web site must maintain the copyright information line on the bottom of each image, and the permission granted is limited to the personal version of your paper. You are not allowed to download and post the published electronic version of your article (whether PDF or HTML, proof or final version), nor may you scan the printed edition to create an electronic version.
A hyper-text must be included to the Homepage of the journal from which you are licensing at http://www.sciencedirect.com/science/journal/xxxxx . As part of our normal production process, you will receive an e-mail notice when your article appears on Elsevier's online service ScienceDirect (www.sciencedirect.com). That e-mail will include the article's Digital Object Identifier (DOI). This number provides the electronic link to the published article and should be included in the posting of your personal version. We ask that you wait until you receive this e-mail and have the DOI to do any posting.

Central Storage: This license does not include permission for a scanned version of the material to be stored in a central repository such as that provided by Heron/XanEdu.

18. **Author website** for books with the following additional clauses:
Authors are permitted to place a brief summary of their work online only.
A hyper-text must be included to the Elsevier homepage at http://www.elsevier.com . All content

posted to the web site must maintain the copyright information line on the bottom of each image. You are not allowed to download and post the published electronic version of your chapter, nor may you scan the printed edition to create an electronic version.

Central Storage: This license does not include permission for a scanned version of the material to be stored in a central repository such as that provided by Heron/XanEdu.

19. **Website** (regular and for author): A hyper-text must be included to the Homepage of the journal from which you are licensing at http://www.sciencedirect.com/science/journal/xxxxx. or for books to the Elsevier homepage at http://www.elsevier.com

20. **Thesis/Dissertation**: If your license is for use in a thesis/dissertation your thesis may be submitted to your institution in either print or electronic form. Should your thesis be published commercially, please reapply for permission. These requirements include permission for the Library and Archives of Canada to supply single copies, on demand, of the complete thesis and include permission for UMI to supply single copies, on demand, of the complete thesis. Should your thesis be published commercially, please reapply for permission.

21. **Other Conditions**:

v1.6

If you would like to pay for this license now, please remit this license along with your payment made payable to "COPYRIGHT CLEARANCE CENTER" otherwise you will be invoiced within 48 hours of the license date. Payment should be in the form of a check or money order referencing your account number and this invoice number RLNK500871561. Once you receive your invoice for this order, you may pay your invoice by credit card. Please follow instructions provided at that time.

Make Payment To:
Copyright Clearance Center
Dept 001
P.O. Box 843006
Boston, MA 02284-3006

For suggestions or comments regarding this order, contact RightsLink Customer Support: customercare@copyright.com or +1-877-622-5543 (toll free in the US) or +1-978-646-2777.

Gratis licenses (referencing $0 in the Total field) are free. Please retain this printable license for your reference. No payment is required.

LIST OF REFERENCES

(1) Lill, R., and Muhlenhoff, U. (2008) Maturation of iron-sulfur proteins in eukaryotes: mechanisms, connected processes, and diseases, *Annu. Rev. Biochem. 77*, 669-700.

(2) Lill, R., and Muhlenhoff, U. (2006) Iron-sulfur protein biogenesis in eukaryotes: components and mechanisms, *Annu. Rev. Cell. Dev. Biol. 22*, 457-486.

(3) Lill, R., Dutkiewicz, R., Elsasser, H. P., Hausmann, A., Netz, D. J., Pierik, A. J., Stehling, O., Urzica, E., and Muhlenhoff, U. (2006) Mechanisms of iron-sulfur protein maturation in mitochondria, cytosol and nucleus of eukaryotes, *Biochim. Biophys. Acta. 1763*, 652-667.

(4) Lill, R., Hoffmann, B., Molik, S., Pierik, A. J., Rietzschel, N., Stehling, O., Uzarska, M. A., Webert, H., Wilbrecht, C., and Muhlenhoff, U. (2012) The role of mitochondria in cellular iron-sulfur protein biogenesis and iron metabolism, *Biochim. Biophys. Acta. 1823*, 1491-1508.

(5) Kumanovics, A., Chen, O. S., Li, L., Bagley, D., Adkins, E. M., Lin, H., Dingra, N. N., Outten, C. E., Keller, G., Winge, D., Ward, D. M., and Kaplan, J. (2008) Identification of FRA1 and FRA2 as genes involved in regulating the yeast iron regulon in response to decreased mitochondrial iron-sulfur cluster synthesis, *J. Biol. Chem. 283*, 10276-10286.

(6) Balasubramaniam, M., and Freed, E. O. (2011) New insights into HIV assembly and trafficking, *Physiology (Bethesda). 26*, 236-251.

(7) Sharma, A. K., Pallesen, L. J., Spang, R. J., and Walden, W. E. (2010) Cytosolic iron-sulfur cluster assembly (CIA) system: factors, mechanism, and relevance to cellular iron regulation, *J. Biol. Chem. 285*, 26745-26751.

(8) Dean, M. (2002) The Human ATP-Binding Cassette (ABC) Transporter Superfamily. National Center for Biotechnology Information (US), Bethesda, MD.

(9) Dean, M., and Allikmets, R. (2001) Complete characterization of the human ABC gene family, *J. Bioenerg. Biomembr. 33*, 475-479.

(10) Dean, M., Hamon, Y., and Chimini, G. (2001) The human ATP-binding cassette (ABC) transporter superfamily, *J. Lipid Res. 42*, 1007-1017.

(11) Dean, M., Rzhetsky, A., and Allikmets, R. (2001) The human ATP-binding cassette (ABC) transporter superfamily, *Genome Res. 11*, 1156-1166.

(12) Barbet, R., Peiffer, I., Hutchins, J. R., Hatzfeld, A., Garrido, E., and Hatzfeld, J. A. (2012) Expression of the 49 human ATP binding cassette (ABC) genes in pluripotent embryonic stem cells and in early- and late-stage multipotent mesenchymal stem cells: possible role of ABC plasma membrane transporters in maintaining human stem cell pluripotency, *Cell Cycle. 11*, 1611-1620.

(13) van der Does, C., and Tampe, R. (2004) How do ABC transporters drive transport?, *Biol. Chem. 385*, 927-933.

(14) Altenberg, G. A. (2003) The engine of ABC proteins, *News Physiol. Sci. 18*, 191-195.

(15) Bauer, B. E., Wolfger, H., and Kuchler, K. (1999) Inventory and function of yeast ABC proteins: about sex, stress, pleiotropic drug and heavy metal resistance, *Biochim Biophys Acta. 1461*, 217-236.

(16) Decottignies, A., and Goffeau, A. (1997) Complete inventory of the yeast ABC proteins, *Nat Genet. 15*, 137-145.

(17) Schuller, H. J. (2003) Transcriptional control of nonfermentative metabolism in the yeast *Saccharomyces cerevisiae*, *Curr Genet. 43*, 139-160.

(18) Walker, J. E., Eberle, A., Gay, N. J., Runswick, M. J., and Saraste, M. (1982) Conservation of structure in proton-translocating ATPases of *Escherichia coli* and mitochondria, *Biochem Soc Trans. 10*, 203-206.

(19) Schmees, G., Stein, A., Hunke, S., Landmesser, H., and Schneider, E. (1999) Functional consequences of mutations in the conserved 'signature sequence' of the ATP-binding-cassette protein MalK, *Eur J Biochem. 266*, 420-430.

(20) Davidson, A. L., Dassa, E., Orelle, C., and Chen, J. (2008) Structure, Function, and Evolution of Bacterial ATP-Binding Cassette Systems, *Microbiol. Mol. Biol. Rev. 72*, 317-364.

(21) Zaitseva, J., Oswald, C., Jumpertz, T., Jenewein, S., Wiedenmann, A., Holland, I. B., and Schmitt, L. (2006) A structural analysis of asymmetry required for catalytic activity of an ABC-ATPase domain dimer, *EMBO J. 25*, 3432-3443.

(22) Verdon, G., Albers, S. V., Dijkstra, B. W., Driessen, A. J. M., and Thunnissen, A.-M. W. H. (2003) Crystal Structures of the ATPase Subunit of the Glucose ABC Transporter from *Sulfolobus solfataricus*: Nucleotide-free and Nucleotide-bound Conformations, *J. Mol. Biol. 330*, 343-358.

(23) Oldham, M. L., and Chen, J. (2011) Snapshots of the maltose transporter during ATP hydrolysis, *Proc. Natl. Acad. Sci. U. S. A. 108*, 15152-15156.

(24) Procko, E., O'Mara, M. L., Bennett, W. F., Tieleman, D. P., and Gaudet, R. (2009) The mechanism of ABC transporters: general lessons from structural and functional studies of an antigenic peptide transporter, *FASEB J. 23*, 1287-1302.

(25) Senior, A. E., and Gadsby, D. C. (1997) ATP hydrolysis cycles and mechanism in P-glycoprotein and CFTR, *Semin. Cancer Biol. 8*, 143-150.

(26) Bisbal, C., Martinand, C., Silhol, M., Lebleu, B., and Salehzada, T. (1995) Cloning and characterization of a RNAse L inhibitor. A new component of the interferon-regulated 2'-5'A pathway, *J. Biol. Chem. 270*, 13308-13317.

(27) Coelho, C. M., Kolevski, B., Bunn, C., Walker, C., Dahanukar, A., and Leevers, S. J. (2005) Growth and cell survival are unevenly impaired in pixie mutant wing discs, *Development. 132*, 5411-5424.

(28) Zimmerman, C., Klein, K. C., Kiser, P. K., Singh, A. R., Firestein, B. L., Riba, S. C., and Lingappa, J. R. (2002) Identification of a host protein essential for assembly of immature HIV-1 capsids, *Nature. 415*, 88-92.

(29) Kerr, I. D. (2004) Sequence analysis of twin ATP binding cassette proteins involved in translational control, antibiotic resistance, and ribonuclease L inhibition, *Biochem. Biophys. Res. Commun. 315*, 166-173.

(30) Dassa, E., and Bouige, P. (2001) The ABC of ABCS: a phylogenetic and functional classification of ABC systems in living organisms, *Res Microbiol. 152*, 211-229.

(31) Barthelme, D., Scheele, U., Dinkelaker, S., Janoschka, A., Macmillan, F., Albers, S. V., Driessen, A. J., Stagni, M. S., Bill, E., Meyer-Klaucke, W., Schunemann, V., and Tampe, R. (2007) Structural organization of essential iron-sulfur clusters in the evolutionarily highly conserved ATP-binding cassette protein ABCE1, *J. Biol. Chem. 282*, 14598-14607.

(32) Karcher, A., Buttner, K., Martens, B., Jansen, R. P., and Hopfner, K. P. (2005) X-ray structure of RLI, an essential twin cassette ABC ATPase involved in ribosome biogenesis and HIV capsid assembly, *Structure. 13*, 649-659.

(33) Karcher, A., Schele, A., and Hopfner, K. P. (2008) X-ray structure of the complete ABC enzyme ABCE1 from *Pyrococcus abyssi*, *J. Biol. Chem. 283*, 7962-7971.

(34) Barthelme, D., Dinkelaker, S., Albers, S. V., Londei, P., Ermler, U., and Tampe, R. (2011) Ribosome recycling depends on a mechanistic link between the FeS cluster domain and a conformational switch of the twin-ATPase ABCE1, *Proc. Natl. Acad. Sci. U. S. A. 108*, 3228-3233.

(35) Brzoska, K., Meczynska, S., and Kruszewski, M. (2006) Iron-sulfur cluster proteins: electron transfer and beyond, *Acta Biochim Pol. 53*, 685-691.

(36) Flint, D. H., and Allen, R. M. (1996) Iron-Sulfur Proteins with Nonredox Functions, *Chem Rev. 96*, 2315-2334.

(37) Chan, J. M., Ryle, M. J., and Seefeldt, L. C. (1999) Evidence that MgATP accelerates primary electron transfer in a *Clostridium pasteurianum* Fe protein-*Azotobacter vinelandii* MoFe protein nitrogenase tight complex, *J Biol Chem. 274*, 17593-17598.

(38) Boal, A. K., Yavin, E., Lukianova, O. A., O'Shea, V. L., David, S. S., and Barton, J. K. (2005) DNA-bound redox activity of DNA repair glycosylases containing [4Fe-4S] clusters, *Biochemistry. 44*, 8397-8407.

(39) Lukianova, O. A., and David, S. S. (2005) A role for iron-sulfur clusters in DNA repair, *Curr Opin Chem Biol. 9*, 145-151.

(40) Muhlenhoff, U., Molik, S., Godoy, J. R., Uzarska, M. A., Richter, N., Seubert, A., Zhang, Y., Stubbe, J., Pierrel, F., Herrero, E., Lillig, C. H., and Lill, R. (2010) Cytosolic monothiol glutaredoxins function in intracellular iron sensing and trafficking via their bound iron-sulfur cluster, *Cell. Metab. 12*, 373-385.

(41) Li, H., and Outten, C. E. (2012) Monothiol CGFS Glutaredoxins and BolA-like Proteins: [2Fe-2S] Binding Partners in Iron Homeostasis, *Biochemistry. 51*, 4377-4389.

(42) Pondarre, C., Antiochos, B. B., Campagna, D. R., Clarke, S. L., Greer, E. L., Deck, K. M., McDonald, A., Han, A. P., Medlock, A., Kutok, J. L., Anderson, S. A., Eisenstein, R. S., and Fleming, M. D. (2006) The mitochondrial ATP-binding cassette transporter Abcb7 is essential in mice and participates in cytosolic iron-sulfur cluster biogenesis, *Hum. Mol. Genet. 15*, 953-964.

(43) Zhang, Y., Lyver, E. R., Nakamaru-Ogiso, E., Yoon, H., Amutha, B., Lee, D. W., Bi, E., Ohnishi, T., Daldal, F., Pain, D., and Dancis, A. (2008) Dre2, a conserved eukaryotic Fe/S cluster protein, functions in cytosolic Fe/S protein biogenesis, *Mol. Cell. Biol. 28*, 5569-5582.

(44) Lange, H., Lisowsky, T., Gerber, J., Muhlenhoff, U., Kispal, G., and Lill, R. (2001) An essential function of the mitochondrial sulfhydryl oxidase Erv1p/ALR in the maturation of cytosolic Fe/S proteins, *EMBO Rep. 2*, 715-720.

(45) Leipe, D. D., Wolf, Y. I., Koonin, E. V., and Aravind, L. (2002) Classification and evolution of P-loop GTPases and related ATPases, *J Mol Biol. 317*, 41-72.

(46) Lill, R. (2009) Function and biogenesis of iron-sulphur proteins, *Nature. 460*, 831-838.

(47) Ho, Y., Gruhler, A., Heilbut, A., Bader, G. D., Moore, L., Adams, S. L., Millar, A., Taylor, P., Bennett, K., Boutilier, K., Yang, L., Wolting, C., Donaldson, I., Schandorff, S., Shewnarane, J., Vo, M., Taggart, J., Goudreault, M., Muskat, B., Alfarano, C., Dewar, D., Lin, Z., Michalickova, K., Willems, A. R., Sassi, H., Nielsen, P. A., Rasmussen, K. J., Andersen, J. R., Johansen, L. E., Hansen, L. H., Jespersen, H., Podtelejnikov, A., Nielsen, E., Crawford, J., Poulsen, V., Sorensen, B. D., Matthiesen, J., Hendrickson, R. C., Gleeson, F., Pawson, T., Moran, M. F., Durocher, D., Mann, M., Hogue, C. W., Figeys, D., and Tyers, M. (2002) Systematic identification of protein complexes in *Saccharomyces cerevisiae* by mass spectrometry, *Nature. 415*, 180-183.

(48) Winzeler, E. A., Shoemaker, D. D., Astromoff, A., Liang, H., Anderson, K., Andre, B., Bangham, R., Benito, R., Boeke, J. D., Bussey, H., Chu, A. M., Connelly, C., Davis, K., Dietrich, F., Dow, S. W., El Bakkoury, M., Foury, F., Friend, S. H., Gentalen, E., Giaever, G., Hegemann, J. H., Jones, T., Laub, M., Liao, H., Liebundguth, N., Lockhart, D. J., Lucau-Danila, A., Lussier, M., M'Rabet, N., Menard, P., Mittmann, M., Pai, C., Rebischung, C., Revuelta, J. L., Riles, L., Roberts, C. J., Ross-MacDonald, P., Scherens, B., Snyder, M., Sookhai-Mahadeo, S., Storms, R. K., Veronneau, S., Voet, M., Volckaert, G., Ward, T. R., Wysocki, R., Yen, G. S., Yu, K., Zimmermann, K., Philippsen, P., Johnston, M., and Davis, R. W. (1999) Functional characterization of the *S. cerevisiae* genome by gene deletion and parallel analysis, *Science. 285*, 901-906.

(49) Yarunin, A., Panse, V. G., Petfalski, E., Dez, C., Tollervey, D., and Hurt, E. C. (2005) Functional link between ribosome formation and biogenesis of iron-sulfur proteins, *EMBO J. 24*, 580-588.

(50) Kispal, G., Sipos, K., Lange, H., Fekete, Z., Bedekovics, T., Janaky, T., Bassler, J., Aguilar Netz, D. J., Balk, J., Rotte, C., and Lill, R. (2005) Biogenesis of cytosolic ribosomes requires the essential iron-sulphur protein Rli1p and mitochondria, *EMBO J. 24*, 589-598.

(51) Hendig, D., Langmann, T., Zarbock, R., Schmitz, G., Kleesiek, K., and Gotting, C. (2009) Characterization of the ATP-binding cassette transporter gene expression profile in Y79: a retinoblastoma cell line, *Mol. Cell. Biochem. 328*, 85-92.

(52) Aubry, F., Mattei, M. G., Barque, J. P., and Galibert, F. (1996) Chromosomal localization and expression pattern of the RNase L inhibitor gene, *FEBS Lett. 381*, 135-139.

(53) Warren, M. S., Zerangue, N., Woodford, K., Roberts, L. M., Tate, E. H., Feng, B., Li, C., Feuerstein, T. J., Gibbs, J., Smith, B., de Morais, S. M., Dower, W. J., and Koller, K. J. (2009) Comparative gene expression profiles of ABC transporters in brain microvessel endothelial cells and brain in five species including human, *Pharmacol. Res. 59*, 404-413.

(54) Liu, D. Z., Tian, D. L., and Ren, Y. (2008) [Expression and clinical significance of ABCE1 in human lung adenocarcinoma], *Zhonghua Zhong Liu Za Zhi. 30*, 296-297.

(55) Chloupkova, M., Pickert, A., Lee, J. Y., Souza, S., Trinh, Y. T., Connelly, S. M., Dumont, M. E., Dean, M., and Urbatsch, I. L. (2007) Expression of 25 human ABC transporters in the yeast *Pichia pastoris* and characterization of the purified ABCC3 ATPase activity, *Biochemistry. 46*, 7992-8003.

(56) Furuta, M., Kozaki, K. I., Tanaka, S., Arii, S., Imoto, I., and Inazawa, J. (2010) miR-124 and miR-203 are epigenetically silenced tumor-suppressive microRNAs in hepatocellular carcinoma, *Carcinogenesis. 31*, 766-776.

(57) Langmann, T., Mauerer, R., Zahn, A., Moehle, C., Probst, M., Stremmel, W., and Schmitz, G. (2003) Real-time reverse transcription-PCR expression profiling of the complete human ATP-binding cassette transporter superfamily in various tissues, *Clin. Chem. 49*, 230-238.

(58) Heimerl, S., Bosserhoff, A. K., Langmann, T., Ecker, J., and Schmitz, G. (2007) Mapping ATP-binding cassette transporter gene expression profiles in melanocytes and melanoma cells, *Melanoma Res. 17*, 265-273.

(59) Hlavata, I., Mohelnikova-Duchonova, B., Vaclavikova, R., Liska, V., Pitule, P., Novak, P., Bruha, J., Vycital, O., Holubec, L., Treska, V., Vodicka, P., and Soucek, P. (2012) The role of ABC transporters in progression and clinical outcome of colorectal cancer, *Mutagenesis. 27*, 187-196.

(60) Shichijo, S., Ishihara, Y., Azuma, K., Komatsu, N., Higashimoto, N., Ito, M., Nakamura, T., Ueno, T., Harada, M., and Itoh, K. (2005) ABCE1, a member of ATP-binding cassette transporter gene, encodes peptides capable of inducing

HLA-A2-restricted and tumor-reactive cytotoxic T lymphocytes in colon cancer patients, *Oncol. Rep. 13*, 907-913.

(61) Yasui, K., Mihara, S., Zhao, C., Okamoto, H., Saito-Ohara, F., Tomida, A., Funato, T., Yokomizo, A., Naito, S., Imoto, I., Tsuruo, T., and Inazawa, J. (2004) Alteration in copy numbers of genes as a mechanism for acquired drug resistance, *Cancer Res. 64*, 1403-1410.

(62) Huang, B., Gao, Y., Tian, D., and Zheng, M. (2010) A small interfering ABCE1-targeting RNA inhibits the proliferation and invasiveness of small cell lung cancer, *Int. J. Mol. Med. 25*, 687-693.

(63) Borel, F., Han, R., Visser, A., Petry, H., van Deventer, S. J., Jansen, P. L., Konstantinova, P., and Reseau Centre de Ressources Biologiques Foie, F. (2012) Adenosine triphosphate-binding cassette transporter genes up-regulation in untreated hepatocellular carcinoma is mediated by cellular microRNAs, *Hepatology. 55*, 821-832.

(64) Martinand, C., Salehzada, T., Silhol, M., Lebleu, B., and Bisbal, C. (1998) The RNase L inhibitor (RLI) is induced by double-stranded RNA, *J. Interferon Cytokine Res. 18*, 1031-1038.

(65) Martinand, C., Salehzada, T., Silhol, M., Lebleu, B., and Bisbal, C. (1998) RNase L inhibitor (RLI) antisense constructions block partially the down regulation of the 2-5A/RNase L pathway in encephalomyocarditis-virus-(EMCV)-infected cells, *Eur. J. Biochem. 254*, 248-255.

(66) Martinand, C., Montavon, C., Salehzada, T., Silhol, M., Lebleu, B., and Bisbal, C. (1999) RNase L inhibitor is induced during human immunodeficiency virus type 1 infection and down regulates the 2-5A/RNase L pathway in human T cells, *J. Virol. 73*, 290-296.

(67) Lingappa, J. R., Dooher, J. E., Newman, M. A., Kiser, P. K., and Klein, K. C. (2006) Basic residues in the nucleocapsid domain of Gag are required for interaction of HIV-1 gag with ABCE1 (HP68), a cellular protein important for HIV-1 capsid assembly, *J. Biol. Chem. 281*, 3773-3784.

(68) Klein, K. C., Reed, J. C., Tanaka, M., Nguyen, V. T., Giri, S., and Lingappa, J. R. (2011) HIV Gag-Leucine Zipper Chimeras Form ABCE1-Containing Intermediates and RNase-Resistant Immature Capsids Similar to Those Formed by Wild-Type HIV-1 Gag, *J. Virol. 85*, 7419-7435.

(69) Berk, V., and Cate, J. H. (2007) Insights into protein biosynthesis from structures of bacterial ribosomes, *Curr Opin Struct Biol. 17*, 302-309.

(70) Chandramouli, P., Topf, M., Menetret, J. F., Eswar, N., Cannone, J. J., Gutell, R. R., Sali, A., and Akey, C. W. (2008) Structure of the mammalian 80S ribosome at 8.7 A resolution, *Structure. 16*, 535-548.

(71) Venema, J., and Tollervey, D. (1999) Ribosome synthesis in *Saccharomyces cerevisiae*, *Annu Rev Genet. 33*, 261-311.

(72) Granneman, S., and Tollervey, D. (2007) Building ribosomes: even more expensive than expected?, *Curr Biol. 17*, R415-417.

(73) Lempiainen, H., and Shore, D. (2009) Growth control and ribosome biogenesis, *Curr Opin Cell Biol. 21*, 855-863.

(74) Lindstrom, M. S. (2009) Emerging functions of ribosomal proteins in gene-specific transcription and translation, *Biochem Biophys Res Commun. 379*, 167-170.

(75) Chen, Z. Q., Dong, J., Ishimura, A., Daar, I., Hinnebusch, A. G., and Dean, M. (2006) The essential vertebrate ABCE1 protein interacts with eukaryotic initiation factors, *J. Biol. Chem. 281*, 7452-7457.

(76) Pisarev, A. V., Skabkin, M. A., Pisareva, V. P., Skabkina, O. V., Rakotondrafara, A. M., Hentze, M. W., Hellen, C. U., and Pestova, T. V. (2010) The role of ABCE1 in eukaryotic posttermination ribosomal recycling, *Mol. Cell. 37*, 196-210.

(77) Shoemaker, C. J., and Green, R. (2011) Kinetic analysis reveals the ordered coupling of translation termination and ribosome recycling in yeast, *Proc. Natl. Acad. Sci. U. S. A. 108*, 1392-1398.

(78) Khoshnevis, S., Gross, T., Rotte, C., Baierlein, C., Ficner, R., and Krebber, H. (2010) The iron-sulphur protein RNase L inhibitor functions in translation termination, *EMBO Rep. 11*, 214-219.

(79) Shoemaker, C. J., and Green, R. (2011) Kinetic analysis reveals the ordered coupling of translation termination and ribosome recycling in yeast, *Proc Natl Acad Sci U S A. 108*, E1392-1398.

(80) Becker, T., Franckenberg, S., Wickles, S., Shoemaker, C. J., Anger, A. M., Armache, J. P., Sieber, H., Ungewickell, C., Berninghausen, O., Daberkow, I., Karcher, A., Thomm, M., Hopfner, K. P., Green, R., and Beckmann, R. (2012) Structural basis of highly conserved ribosome recycling in eukaryotes and archaea, *Nature. 482*, 501-506.

(81) Strunk, B. S., Novak, M. N., Young, C. L., and Karbstein, K. (2012) A Translation-Like Cycle Is a Quality Control Checkpoint for Maturing 40S Ribosome Subunits, *Cell. 150*, 111-121.

(82) Dong, J., Lai, R., Nielsen, K., Fekete, C. A., Qiu, H., and Hinnebusch, A. G. (2004) The essential ATP-binding cassette protein RLI1 functions in translation by promoting preinitiation complex assembly, *J. Biol. Chem. 279*, 42157-42168.

(83) Warner, J. R. (1999) The economics of ribosome biosynthesis in yeast, *Trends Biochem. Sci. 24*, 437-440.

(84) Decottignies, A., and Goffeau, A. (1997) Complete inventory of the yeast ABC proteins, *Nature Genet. 15*, 137-145.

(85) Lovrien, R., and Matulis, D. (2005) Assays for total protein, *Curr. Protoc. Microbiol.*, Appendix 3A.

(86) Zachariades, C., and McGavock, W. C. (1971) Spectrophotometric determination of Fe(II), Fe(III), and total Fe, *J. Pharm. Sci. 60*, 918-919.

(87) Baykov, A. A., Evtushenko, O. A., and Avaeva, S. M. (1988) A malachite green procedure for orthophosphate determination and its use in alkaline phosphatase-based enzyme immunoassay, *Anal. Biochem. 171*, 266-270.

(88) Geladopoulos, T. P., Sotiroudis, T. G., and Evangelopoulos, A. E. (1991) A malachite green colorimetric assay for protein phosphatase activity, *Anal. Biochem. 192*, 112-116.

(89) Henkel, R. D., VandeBerg, J. L., and Walsh, R. A. (1988) A microassay for ATPase, *Anal. Biochem. 169*, 312-318.

(90) Segel, I. H. (1993) *Enzyme kinetics : behavior and analysis of rapid equilibrium and steady state enzyme systems*, Wiley Classics Library ed., Wiley, New York :.

(91) Minkov, I. B., Fitin, A. F., Vasilyeva, E. A., and Vinogradov, A. D. (1979) Mg^{2+}-induced ADP-dependent inhibition of the ATPase activity of beef heart mitochondrial coupling factor F1, *Biochem. Biophys. Res. Commun. 89*, 1300-1306.

(92) Feldman, R. I., and Boyer, P. D. (1985) The role of tightly bound ADP on chloroplast ATPase, *J. Biol. Chem. 260*, 13088-13094.

(93) Digel, J. G., Moore, N. D., and McCarty, R. E. (1998) Influence of divalent cations on nucleotide exchange and ATPase activity of chloroplast coupling factor 1, *Biochemistry. 37*, 17209-17215.

(94) Shim, K.-S., Tombline, G., Heinen, C. D., Charbonneau, N., Schmutte, C., and Fishel, R. (2006) Magnesium influences the discrimination and release of ADP by human RAD51, *DNA Repair. 5*, 704-717.

(95) Mukherjee, K., Sharma, M., Jahn, R., Wahl, M. C., and Sudhof, T. C. (2010) Evolution of CASK into a Mg^{2+}-sensitive kinase, *Sci. Signal. 3*, ra33.

(96) Mukherjee, K., Sharma, M., Urlaub, H., Bourenkov, G. P., Jahn, R., Sudhof, T. C., and Wahl, M. C. (2008) CASK Functions as a Mg^{2+}-independent neurexin kinase, *Cell. 133*, 328-339.

(97) Drobinskaya, I. Y., Kozlov, I. A., Murataliev, M. B., and Vulfson, E. N. (1985) Tightly bound adenosine diphosphate, which inhibits the activity of mitochondrial F_1-ATPase, is located at the catalytic site of the enzyme, *FEBS Lett. 182*, 419-424.

(98) Pisarev, A. V., Skabkin, M. A., Pisareva, V. P., Skabkina, O. V., Rakotondrafara, A. M., Hentze, M. W., Hellen, C. U., and Pestova, T. V. The role of ABCE1 in eukaryotic post-termination ribosomal recycling, *Mol. Cell. 37*, 196-210.

(99) Yamamoto, T., Shimizu, Y., Ueda, T., and Shiro, Y. (2010) Mg^{2+} dependence of 70 S ribosomal protein flexibility revealed by hydrogen/deuterium exchange and mass spectrometry, *J. Biol. Chem. 285*, 5646-5652.

(100) Zitomer, R. S., and Flaks, J. G. (1972) Magnesium dependence and equilibrium of the *Escherichia coli* ribosomal subunit association, *J. Mol. Biol. 71*, 263-279.

(101) Ivanov, D. A., and Lerman, M. I. (1976) Loosening and unfolding of *E. coli* 50 S ribosomal subunits: dependence on magnesium content and temperature, *Mol. Biol. Rep. 3*, 39-46.

(102) Suzuki, T., Kurita, H., and Ichinose, H. (2004) GTP cyclohydrolase I utilizes metal-free GTP as its substrate, *Eur. J. Biochem. 271*, 349-355.

(103) Fleury, B., Di Pietro, A., Godinot, C., and Gautheron, D. C. (1980) Role of magnesium on kinetic parameters of soluble F_1-ATPase from pig heart mitochondria, *Biochimie. 62*, 733-737.

(104) Bulygin, V. V., and Vinogradov, A. D. (1991) Interaction of Mg^{2+} with F_0-F_1 mitochondrial ATPase as related to its slow active/inactive transition, *Biochem. J. 276 (Pt 1)*, 149-156.

(105) Allison, W. S., Ren, H., and Dou, C. (2000) Inhibitory Mg-ADP—Fluoroaluminate Complexes Bound to Catalytic Sites of F_1-ATPases: Are They Ground-State or Transition-State Analogs?, *J. Bioenerg. Biomembr. 32*, 531-538.

(106) Baumann, P., and West, S. C. (1997) The human Rad51 protein: polarity of strand transfer and stimulation by hRP-A, *EMBO J. 16*, 5198-5206.

(107) Fitin, A. F., Vasilyeva, E. A., and Vinogradov, A. D. (1979) An inhibitory high affinity binding site for ADP in the oligomycin-sensitive ATPase of beef heart submitochondrial particles, *Biochem. Biophys. Res. Commun. 86*, 434-439.

(108) Vasilyeva, E. A., Fitin, A. F., Minkov, I. B., and Vinogradov, A. D. (1980) Kinetics of interaction of adenosine diphosphate and adenosine triphosphate with adenosine triphosphatase of bovine heart submitochondrial particles, *Biochem. J. 188*, 807-815.

(109) Vasilyeva, E. A., Minkov, I. B., Fitin, A. F., and Vinogradov, A. D. (1982) Kinetic mechanism of mitochondrial adenosine triphosphatase. ADP-specific inhibition as revealed by the steady-state kinetics, *Biochem. J. 202*, 9-14.

(110) Ataullakhanov, F. I., and Vitvitsky, V. M. (2002) What determines the intracellular ATP concentration, *Biosci. Rep. 22*, 501-511.

(111) Terasaki, M., and Rubin, H. (1985) Evidence that intracellular magnesium is present in cells at a regulatory concentration for protein synthesis, *Proc. Natl. Acad. Sci. U. S. A. 82*, 7324-7326.

(112) Blaha, G., Burkhardt, N., and Nierhaus, K. H. (2002) Formation of 70S ribosomes: large activation energy is required for the adaptation of exclusively the small ribosomal subunit, *Biophys. Chem. 96*, 153-161.

(113) Lucas-Lenard, J., and Lipmann, F. (1967) Initiation of polyphenylalanine synthesis by N-acetylphenylalanyl-SRNA, *Proc. Natl. Acad. Sci. U. S. A. 57*, 1050-1057.

(114) Schilling-Bartetzko, S., Bartetzko, A., and Nierhaus, K. H. (1992) Kinetic and thermodynamic parameters for tRNA binding to the ribosome and for the translocation reaction, *J. Biol. Chem. 267*, 4703-4712.

(115) Shenton, D., Smirnova, J. B., Selley, J. N., Carroll, K., Hubbard, S. J., Pavitt, G. D., Ashe, M. P., and Grant, C. M. (2006) Global Translational Responses to Oxidative Stress Impact upon Multiple Levels of Protein Synthesis, *J. Biol. Chem. 281*, 29011-29021.

(116) Grant, C. M. (2011) Regulation of translation by hydrogen peroxide, *Antioxidants & Redox Signaling. 15*, 191-203.

(117) Jamieson, D. J. (1998) Oxidative stress responses of the yeast *Saccharomyces cerevisiae*, *Yeast. 14*, 1511-1527.

(118) Lushchak, V. I. (2011) Adaptive response to oxidative stress: Bacteria, fungi, plants and animals, *Comp. Biochem. Physiol. C. Toxicol. Pharmacol. 153*, 175-190.

(119) Grant, C. M. (2011) Regulation of translation by hydrogen peroxide, *Antioxid. Redox Signal. 15*, 191-203.

(120) Faulkner, M. J., and Helmann, J. D. (2011) Peroxide stress elicits adaptive changes in bacterial metal ion homeostasis, *Antioxid. Redox Signal. 15*, 175-189.

(121) Thorpe, G. W., Fong, C. S., Alic, N., Higgins, V. J., and Dawes, I. W. (2004) Cells have distinct mechanisms to maintain protection against different reactive oxygen species: oxidative-stress-response genes, *Proc. Natl. Acad. Sci. U. S. A. 101*, 6564-6569.

(122) Zechmann, B., Liou, L. C., Koffler, B. E., Horvat, L., Tomasic, A., Fulgosi, H., and Zhang, Z. (2011) Subcellular distribution of glutathione and its dynamic changes under oxidative stress in the yeast *Saccharomyces cerevisiae*, *FEMS Yeast Res. 11*, 631-642.

(123) Rouhier, N., Couturier, J., Johnson, M. K., and Jacquot, J. P. (2010) Glutaredoxins: roles in iron homeostasis, *Trends Biochem. Sci. 35*, 43-52.

(124) Yang, M., Cobine, P. A., Molik, S., Naranuntarat, A., Lill, R., Winge, D. R., and Culotta, V. C. (2006) The effects of mitochondrial iron homeostasis on cofactor specificity of superoxide dismutase 2, *EMBO J. 25*, 1775-1783.

(125) Fomenko, D. E., and Gladyshev, V. N. (2012) Comparative genomics of thiol oxidoreductases reveals widespread and essential functions of thiol-based redox control of cellular processes, *Antioxid. Redox Signal. 16*, 193-201.

(126) Sohal, R. S. (2002) Role of oxidative stress and protein oxidation in the aging process, *Free Radic. Biol. Med. 33*, 37-44.

(127) Avery, S. V. (2011) Molecular targets of oxidative stress, *Biochem. J. 434*, 201-210.

(128) Py, B., Moreau, P. L., and Barras, F. (2011) Fe-S clusters, fragile sentinels of the cell, *Curr. Opin. Microbiol. 14*, 218-223.

(129) Muhlenhoff, U., Richhardt, N., Ristow, M., Kispal, G., and Lill, R. (2002) The yeast frataxin homolog Yfh1p plays a specific role in the maturation of cellular Fe/S proteins, *Hum. Mol. Genet. 11*, 2025-2036.

(130) Tian, Y., Han, X., and Tian, D. L. (2012) The biological regulation of ABCE1, *IUBMB Life. 64*, 795-800.

(131) Rodnina, M. V. (2010) Protein synthesis meets ABC ATPases: new roles for Rli1/ABCE1, *EMBO Rep. 11*, 143-144.

(132) Pierik, A. J., Netz, D. J., and Lill, R. (2009) Analysis of iron-sulfur protein maturation in eukaryotes, *Nat. Protoc. 4*, 753-766.

(133) Alhebshi, A., Sideri, T. C., Holland, S. L., and Avery, S. V. (2012) The essential iron-sulfur protein Rli1 is an important target accounting for inhibition of cell growth by reactive oxygen species, *Mol. Biol. Cell. 23*, 3582-3590.

(134) Shenton, D., and Grant, C. M. (2003) Protein S-thiolation targets glycolysis and protein synthesis in response to oxidative stress in the yeast *Saccharomyces cerevisiae*, *Biochem. J. 374*, 513-519.

(135) Marguet, E., and Forterre, P. (1998) Protection of DNA by salts against thermodegradation at temperatures typical for hyperthermophiles, *Extremophiles. 2*, 115-122.

(136) Scholz, S., Sonnenbichler, J., Schafer, W., and Hensel, R. (1992) Di-myo-inositol-1,1'-phosphate: a new inositol phosphate isolated from *Pyrococcus woesei*, *FEBS Lett. 306*, 239-242.

(137) Wolf, F. I., and Trapani, V. (2012) Magnesium and its transporters in cancer: a novel paradigm in tumour development, *Clin. Sci. (Lond). 123*, 417-427.

(138) Goytain, A., and Quamme, G. A. (2005) Functional characterization of human SLC41A1, a Mg^{2+} transporter with similarity to prokaryotic MgtE Mg^{2+} transporters, *Physiol. Genomics. 21*, 337-342.

(139) Goytain, A., and Quamme, G. A. (2005) Identification and characterization of a novel mammalian Mg^{2+} transporter with channel-like properties, *BMC Genomics. 6*, 48.

(140) Franckenberg, S., Becker, T., and Beckmann, R. (2012) Structural view on recycling of archaeal and eukaryotic ribosomes after canonical termination and ribosome rescue, *Curr. Opin. Struct. Biol.*

(141) Emara, M. M., Fujimura, K., Sciaranghella, D., Ivanova, V., Ivanov, P., and Anderson, P. (2012) Hydrogen peroxide induces stress granule formation independent of eIF2alpha phosphorylation, *Biochem. Biophys. Res. Commun. 423*, 763-769.

(142) Kobayashi, C. I., and Suda, T. (2012) Regulation of reactive oxygen species in stem cells and cancer stem cells, *J. Cell. Physiol. 227*, 421-430.